

AD-A218 607

WHOI-89-17

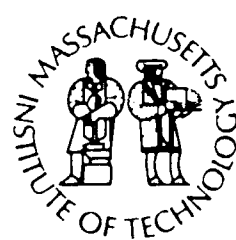
DTIC FILE COPY

0

# Woods Hole Oceanographic Institution Massachusetts Institute of Technology



Joint Program  
in Oceanography  
and  
Oceanographic Engineering



## DOCTORAL DISSERTATION

### Trace Metal Sources for the Atlantic Inflow to the Mediterranean Sea

by

Alexander F.M.J. van Geen

June 1989

DTIC  
ELECTED  
MARCH 2 1990  
S B D

90 03 01 220

DISTRIBUTION STATEMENT A

Approved for public release;  
Distribution Unlimited

**Trace Metal Sources for the Atlantic Inflow  
to the Mediterranean Sea**

by

Alexander F.M.J. van Geen

Woods Hole Oceanographic Institution  
Woods Hole, Massachusetts 02543

and

The Massachusetts Institute of Technology  
Cambridge, Massachusetts 02139

June 1989

**Doctoral Dissertation**

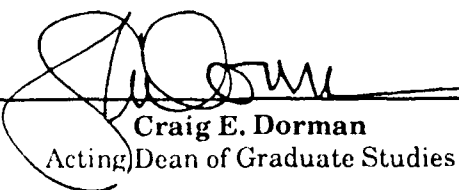
Funding was provided by the Office of Naval Research through the  
Massachusetts Institute of Technology.

Reproduction in whole or in part is permitted for any purpose of the  
United States Government. This thesis should be cited as:  
Alexander F.M.J. van Geen, 1989. Trace Metal Sources for the Atlantic Inflow  
to the Mediterranean Sea. Ph.D. Thesis. MIT/WHOI, WHOI-89-17.

Approved for publication; distribution unlimited.

**Approved for Distribution:**

  
\_\_\_\_\_  
**Frederick L. Sayles, Chairman**  
Department of Chemistry

  
\_\_\_\_\_  
**Craig E. Dorman**  
Acting Dean of Graduate Studies

TRACE METAL SOURCES FOR THE ATLANTIC INFLOW  
TO THE MEDITERRANEAN SEA

by

Alexander F.M.J. van Geen

B.S., University of Washington

(1982)

SUBMITTED IN PARTIAL FULFILLMENT  
OF THE REQUIREMENTS FOR THE DEGREE OF  
DOCTOR OF PHILOSOPHY

at the

MASSACHUSETTS INSTITUTE OF TECHNOLOGY

and the

WOODS HOLE OCEANOGRAPHIC INSTITUTION

MAY, 1989

© Massachusetts Institute of Technology 1989

Signature of Author..... *Alexander F.M.J. van Geen*.....  
Department of Earth, Atmospheric, and Planetary Sciences,  
Massachusetts Institute of Technology and the Joint Program in  
Oceanography, Massachusetts Institute of Technology/Woods Hole  
Oceanographic Institution, March 1989

Certified by..... *H. Boyle*.....  
Edward A. Boyle, Thesis Supervisor

Accepted by..... *P. M. Gschwend*.....  
Philip M. Gschwend, Chairman, Joint Committee for Chemical  
Oceanography, Massachusetts Institute of Technology/Woods Hole  
Oceanographic Institution

TRACE METAL SOURCES FOR THE ATLANTIC INFLOW  
TO THE MEDITERRANEAN SEA

by

Alexander F.M.J. van Geen

Submitted to the Department of Earth, Atmospheric and Planetary Sciences  
on May 5th, 1989 in partial fulfillment of the requirements for  
the Degree of Doctor of Philosophy in Oceanography

ABSTRACT

Cu, Cd and Zn concentrations over a 40 km long portion of the Spanish continental shelf are an order of magnitude higher than enrichments generally found in coastal water. All samples were analyzed with a simple device which automates the pre-concentration of Cu, Ni, Cd, Zn and from seawater and fresh water by bis (2-hydroxyethyl)- dithiocarbamate-metal complex retention on a hydrophobic column. Enrichments observed over the Spanish shelf are sufficient to influence the composition of the Mediterranean because Spanish coastal water is entrained in the inflow to the Alboran Sea. Trace metal and ancillary data for 172 samples from the Gulf of Cadiz collected in April and October'86 confirm that Spanish shelf water dominates Cu, Cd and Zn fluxes through the Strait of Gibraltar. Following a review of alternative explanations, a shelf "metal-trap" mechanism is presented in order to reconcile the magnitude of observed metal enrichments with their geographical distribution and seasonal variability. A simple box model of the metal-trap indicates this mechanism must be operating over the whole length of the Iberian Atlantic coast (rather than the Gulf of Cadiz only) in order to support the important metal sink through the Strait of Gibraltar.

The three water masses originating in the Atlantic and entering the Alboran Sea through the Strait of Gibraltar are (1) Atlantic surface water, (2) North Atlantic Central Water and (3) Spanish shelf water, based on salinity and Cu, Ni, Cd and Zn concentrations. A conservative mixing model of these end-members is solved by weighted least-squares and shown to be consistent

with tracer data for 43 surface stations in the Strait of Gibraltar. Spanish shelf water is restricted to the northern half of the Strait and can be traced as a plume in the Alboran Sea. On three occasions (April'86, June'82 and October'86), salinity, Cu, Ni, Cd and Zn distributions in the surface Alboran Sea are consistent in most cases with conservative mixing of the three previously defined end-members with Mediterranean water. A metal enriched plume originating from the Spanish shelf was present in the Alboran Sea during all three sampling periods, but was significantly stronger in June'82.

Cu, Cd and Zn flux estimates at the Strait of Gibraltar for the Atlantic inflow and the saline outflow confirm that Spanish shelf water influences the composition of a basin as large as the Mediterranean. In- and outflow are roughly in balance for these elements. In contrast to Cu, Cd and Zn, Ni concentrations for the inflow are a factor of two lower than the Mediterranean outflow. Estimates of metal sources within the basin indicate the difference may be due to river input. Estimates of atmospheric input of Cu, Cd, Ni and Zn are an order of magnitude higher than either the uncertainty in the difference between in- and outflow concentrations, or the east-west gradient in surface water concentrations of the Mediterranean. This is true when aerosol input of these elements is scaled to the observed change in dissolved Al concentration in the water column and enrichment factors in aerosols relative to the crust from either the remote Pacific ocean, the Atlantic ocean or the Mediterranean Sea. The discrepancy may indicate either significant scavenging of trace elements in the Mediterranean, or that enrichment factors measured in aerosols are not representative of the composition of the dust input which dissolves in the water column.

<b>Accession For</b>	
NTIS GRA&I	<input checked="" type="checkbox"/>
DTIC TAB	<input type="checkbox"/>
Unannounced	<input type="checkbox"/>
<b>Justification</b>	
<b>By</b>	
<b>Distribution/</b>	
<b>Availability Codes</b>	
<b>Dist</b>	<b>Avail and/or Special</b>
A-1	

#### ACKNOWLEDGMENTS

A freshman at the University of Washington, I was given a first glimpse of oceanography in the laboratory of John Hedges. My return to graduate school a few years later was, for a large part, due to what I remembered from discussions with John, and with John Ertel.

Through a combination of openness and (at times) suspicion, Ed Boyle has strongly stimulated me throughout these years at MIT. Ed has been an incomparable example of energy and thoroughness. May the years to come show that he has not wasted his time with me.

I thank the members of my Committee, Bill Jenkins, John Bullister and Jorge Sarmiento for thoughtfull comments at my thesis defense.

Art Spivack provided much encouragement when I arrived in Cambridge. I thank Art in particular for help during our two trips to acid lakes in the Adirondacks. During these first years I was also lucky to have Benno Blumenthal as a roommate. I owe to discussions with Benno, among other things, my initiation to linear regression.

Rob Sherrell and I have now shared an office for most of these five years, and I am very glad we have. I have learned a lot from Rob - not only in oceanography - and will no doubt miss him.

I thank my fellow students, in particular Glen Shen, Kelly Kennison Falkner, David Lea, Debbie Colodner and Erik Brown for their stimulating curiosity about the ocean. I particularly regret not to have overlapped at MIT for a longer period of time with Yair Rosenthal. Chris Measures has always been open to questions and willing to give advice. Paula Rosener has kept the lab running so well, despite considerable space constraints, that we are now all spoiled for ever.

Finally, I wish to thank my father who trusted my decision to come to the US ten years ago. I was particularly happy that we were together again for my thesis defense, the final leg of a voyage he has supported all along. I have missed my mother, Francesca, and Jacques and Christine during the long separations and hope we will be together more often in the future.

This work was supported by the Office of Naval Research under grant # N0001486-K-0325.

Ad Alessandra

## TABLE OF CONTENTS

Abstract.....	2
Acknowledgements.....	4
Table of contents.....	6
List of figures.....	8
List of tables.....	11
 CHAPTER 1. INTRODUCTION.....	13
 CHAPTER 2. AUTOMATED PRE-CONCENTRATION OF TRACE METALS FROM SEA WATER AND FRESH WATER	
2.1 Introduction.....	19
2.2 Experimental Section.....	20
2.2.1 Apparatus.....	20
2.2.2 Reagents.....	24
2.2.3 Procedure.....	26
2.3 Results and Discussion.....	30
2.4 Conclusion.....	34
 CHAPTER 3. CU, NI, CD AND ZN ENRICHMENTS IN THE GULF OF CADIZ	
3.1 Introduction.....	38
3.2 Sampling and Analysis.....	38
3.3 Results.....	40
3.4 Discussion.....	51
3.4.1 Riverine metal source.....	52
3.4.2 Anthropogenic discharges.....	54
3.4.3 Shelf sediments.....	55
3.4.4 Box model for metal enrichments.....	61
3.4.5 Composition of water masses entering the Strait of Gibraltar	71
3.5 Conclusion.....	74
 CHAPTER 4. VARIABILITY OF TRACE METAL FLUXES THROUGH THE STRAIT OF GIBRALTAR	
4.1 Introduction.....	87
4.2 Sampling and Analysis.....	88
4.3 The conservative mixing model.....	88
4.4 How robust are the solutions ?.....	96
4.5 Distribution of end-members in the Strait of Gibraltar.....	107
4.5 Conclusion.....	111

CHAPTER 5. VARIABILITY OF CU, NI, CD AND ZN DISTRIBUTIONS IN SURFACE WATERS  
OF THE ALBORAN SEA

5.1	Introduction.....	116
5.2	Analysis.....	117
5.3	Results.....	118
5.4	Discussion.....	126
5.5	Conclusion.....	151
CHAPTER 6. CONCLUSIONS.....		160
APPENDIX	End-member regression program.....	173
Biographical note.....		179

## LIST OF FIGURES

Fig. 2.1 Components of automated pre-concentration device.....	21
Fig. 2.2 Flow paths for four configurations of pre-concentration device.....	27
Fig. 3.1a Salinity and phosphate in Gulf of Cadiz surface water.....	41
Fig. 3.1b Zn in Gulf of Cadiz surface water.....	42
Fig. 3.2 Zn vs. Cu, Ni and Cd for April and October'86 surface samples....	44
Fig. 3.3 Salinity vs. Cu, Ni, Cd and Zn in surface samples.....	45
Fig. 3.4 Chemical profiles in the Gulf of Cadiz.....	47
Fig. 3.5 Salinity vs phosphate, Cd and Ni for profiles unaffected by shelf processes.....	48
Fig. 3.6 Zn in western approaches to the Strait of Gibraltar, April and October '86.....	49
Fig. 3.7a $^{228}\text{Ra}/^{226}\text{Ra}$ activity ratio in Gulf of Cadiz surface water.....	58
Fig. 3.7b Salinity vs. $^{228}\text{Ra}/^{226}\text{Ra}$ activity ratio.....	58
Fig. 3.8 Metal-trap box model with water transport fluxes.....	62
Fig. 4.1 End-member distributions in the Strait of Gibraltar for April 11th, and 16-18th.....	80
Fig. 4.2 Range for tracer composition of end-members.....	94

Fig. 4.3 Observed vs. model-predicted data, Strait of Gibraltar.....	105
Fig. 5.1a Surface Alboran Sea salinity, April'86.....	119
Fig. 5.1b Surface Alboran Sea salinity, June '82.....	120
Fig. 5.1c Surface Alboran Sea salinity, October'86.....	121
Fig. 5.2a Surface Alboran Sea Zn concentration, April'86.....	122
Fig. 5.2b Surface Alboran Sea Zn concentration, June '82.....	123
Fig. 5.2c Surface Alboran Sea Zn concentration, October '86.....	124
Fig. 5.3 Zn vs. Cu for surface Alboran Sea.....	127
Fig. 5.4 Zn vs. Cd for surface Alboran Sea.....	128
Fig. 5.5 Salinity vs. Ni for surface Alboran Sea.....	129
Fig. 5.6 Observed vs. model derived data, Alboran Sea.....	132
Fig. 5.7a Surface Atlantic end-member in western Alboran Sea, April '86.....	136
Fig. 5.7b Surface Atlantic end-member in western Alboran Sea, June '82.....	137
Fig. 5.7c Surface Atlantic end-member in western Alboran Sea, October'86..	138
Fig. 5.8a Spanish shelf end-member in western Alboran Sea, April '86.....	139
Fig. 5.8b Spanish shelf end-member in western Alboran Sea, June '82.....	140
Fig. 5.8c Spanish shelf end-member in western Alboran Sea, October'86.....	141
Fig. 5.9a NACW end-member in western Alboran Sea, April '86.....	142

Fig. 5.9b NACW end-member in western Alboran Sea, June '82.....	143
Fig. 5.9c NACW Atlantic end-member in western Alboran Sea, October'86....	144
Fig. 5.10a Mediterranean end-member in western Alboran Sea, April '86....	145
Fig. 5.10b Mediterranean end-member in western Alboran Sea, June '82.....	146
Fig. 5.10c Mediterranean end-member in western Alboran Sea, October'86....	147
Fig. 5.11 Salinity-property plots for Station 4, June'82.....	150
Fig. 6.1 Cu, Ni, Cd and Zn in Mediterranean surface water.....	168

## LIST OF TABLES

Table 2.1 Solenoid channel functions.....	23
Table 2.2 Timer program structure.....	28
Table 2.3 Sargasso Sea surface pre-concentration.....	31
Table 2.4 Guadiana river water pre-concentration.....	33
Table 3.1a Surface sample composition in the Gulf of Cadiz, April'86.....	75
Table 3.1b Surface sample composition in the Gulf of Cadiz, October'86.....	78
Table 3.2 Sample composition for Gulf of Cadiz profiles.....	79
Table 3.3 Trace metal concentrations for major Iberian rivers.....	80
Table 3.4 Shelf metal enrichments for different coastal regions.....	81
Table 3.5 $^{228}\text{Ra}/^{226}\text{Ra}$ activity ratios and salinity for surface samples.....	82
Table 3.6 Salinity, Cu, Ni, Cd and Zn end-member composition.....	83
Table 4.1 Model matrix.....	91
Table 4.2 Variance normalized model matrix.....	95
Table 4.3 Model parameter covariance matrix.....	97
Table 4.4 Sensitivity of standard error.....	99
Table 4.5 End-member redistribution.....	100

Table 4.6 Simulation of changes in end-member composition.....	103
Table 4.7 Data resolution matrix.....	106
Table 4.Appendix Surface sample composition and inversion results for the Strait of Gibraltar.....	113
Table 5.1 Surface sample composition and inversion results for the Alboran Sea, April '86.....	153
Table 5.2 Surface sample composition and inversion results for the Alboran Sea, June '82.....	154
Table 5.3 Surface sample composition and inversion results for the Alboran Sea, October'86.....	155
Table 5.4 End-member composition for April, June and October.....	156
Table 5.5 Composition of samples from Station 4.....	157
Table 6.1 Metal balance at the Strait of Gibraltar.....	165
Table 6.2 River and aerosol input to the Mediterranean.....	166

CHAPTER ONE

INTRODUCTION

The history of reliable trace metal measurements in the ocean does not reach far back in time. The difficulty in obtaining reproducible results for these elements was due to their presence in sea water at levels on the order of  $10^{-9}$  M. In order to avoid contamination, new sample collection and analysis procedures had to be developed. Boyle et al. (1975) determined dissolved Cu concentrations ranging between 0.9-3.2 nM for surface water south of New Zealand, followed by a number of Pacific profiles showing deep water concentrations increasing to 6 nM (Boyle et al. 1977). Pacific profiles for the element Cd "oceanographically consistent" with the distribution of temperature and salinity in the water column soon followed, and showed concentrations increasing from the surface (.1 $\pm$ .1 nM) to the deep ocean (1.1 pM) (Boyle et al., 1976 and Martin et al., 1976). A linear correlation between Cd and phosphate concentrations in subsurface Pacific water was the first evidence of a link between trace metal and nutrient cycling, i.e. surface uptake by phytoplankton and regeneration by particle dissolution in deeper water. The first profiles of Ni (3 - 12 nM, Sclater et al., 1976) and Zn (0.1 - 10 nM, Bruland et al., 1978) also showed significant enrichments in deep Pacific water relative to surface water. Bruland (1980) subsequently measured Cu, Ni, Cd and Zn concentrations in surface water of the North Pacific gyre as low as 0.5, 2.1, .001 and .07 nM, respectively.

Since these studies on the distributions of dissolved metals concentrations, the composition of phytoplankton in surface water (Bruland et al. 1978, Collier and Edmond, 1985) and that of sinking biogenic particles collected by sediment traps deeper in the ocean was determined. These results showed that internal trace metal cycling in terms of phytoplankton uptake at the surface

and redissolution at depth maintains concentration gradients between the surface/deep ocean and the deep Atlantic/Pacific. On the other hand, the relative importance of external inputs by rivers, aerosols and sediment diagenesis with respect to trace metal distributions has proved more difficult to establish. Early on, the Mediterranean basin was seen to present a unique opportunity to discern these external metal sources for two reasons: (1) the dominant inflow/outflow water transport through the Strait of Gibraltar simplifies the determination of a metal budget for the basin and (2) low nutrient concentrations inhibit metal redistribution by plankton. A first survey of Mediterranean surface waters in 1980 (Spivack et al. 1983) showed that Cu, Ni and Cd are on average enriched relative to eastern Atlantic nutrient-depleted water by factors of 3, 2 and 5, respectively, and raised the possibility of a source for these elements within the basin, natural or anthropogenic. A more detailed look at the Alboran Sea which lies immediately east of the Strait of Gibraltar in 1982 (Boyle et al. 1985), however, showed a metal-enriched plume which appeared to originate from the Atlantic. This was the first indication that Mediterranean metal enrichments are not necessarily caused by a source within the basin.

These considerations of potential trace metal sources for the Mediterranean Sea provided the motivation for this thesis. Three questions were posed at the onset of this work:

- (1) What portion of Cu, Ni, Cd and Zn enrichments observed in the Mediterranean Sea originates in the Atlantic ?
- (2) Are metal enrichment patterns in the surface Alboran Sea systematically

related to contributing Atlantic and Mediterranean water masses ?

(3) Do anthropogenic metal inputs influence trace metal concentrations in the Mediterranean ?

The Gibraltar Experiment (Kinder and Bryden 1987), which involved primarily physical oceanographers concerned with water transport in the Strait of Gibraltar, twice offered the opportunity to sample the Gulf of Cadiz and the Alboran Sea which lie at opposite ends of the Strait. Results from these cruises are interpreted in chapters 3 through 5. Chapter 2 describes an automated trace metal pre-concentration device which was developed in order to facilitate analysis of the many samples required to understand the high variability of trace metal concentrations in the region. The Gulf of Cadiz (the source region for the Atlantic inflow) is examined in detail in Chapter 3 on the basis of 172 samples, including 8 profiles, collected in April and October 1986. Spanish shelf water which is highly enriched in Cu, Cd and Zn is identified on both occasions and shown to dominate the trace metal flux into the Strait of Gibraltar. In Chapter 4, the distribution of trace metals within the Strait (43 surface samples) is subsequently analyzed with respect to conservative mixing of three Atlantic water masses contributing to the inflow (surface Atlantic water, NACW and Spanish shelf water). Alboran Sea surface samples collected in April'86, June'82 and October'86 are compared in Chapter 5 in order to constrain temporal variability of Cu, Ni, Cd and Zn inputs through the Strait. Chapter 6 concludes this thesis by discussing implications of the results with respect to metal inputs within the Mediterranean basin.

## REFERENCES

Boyle E.A. and J.M. Edmond (1975) Copper in surface waters south of New Zealand, Nature 253, 107

Boyle, E.A., F. Sclater and J.M. Edmond (1976) On the marine geochemistry of cadmium, Nature 263, 42

Boyle E.A., F.R. Sclater and J.M. Edmond (1977) The distribution of dissolved copper in the Pacific, Earth Planet. Sci. Lett. 37, 38.

Boyle, E.A., Chapnick, S.D., Bai, X.X. & Spivack, A.J. (1985) Trace metal enrichments in the Mediterranean Sea. Earth Planet. Sci. Lett. 74, 405-419.

Bruland K.W., G.A. Knauer and J.H. Martin (1978) Cadmium in northeast Pacific waters, Limnol. Oceanogr. 23, 618.

Bruland, K.W., G.A. Knauer and J.H. Martin (1978) Zinc in northeast Pacific waters, Nature 271, 741.

Bruland, K.W. (1980) Oceanographic distributions of cadmium, zinc, nickel, and copper in the North Pacific, Earth Planet. Sci. Lett. 41, 461.

Martin, J.H., K.W. Bruland and W.W. Broenkow (1976) Cadmium transport in the California Current, In: Marine Pollutant Transfer, H.L. Windom and R.A. Duce, eds., Heath, Lexington MA.

Kinder, T.H. and H.L. Bryden (1987) The 1985-86 Gibraltar Experiment: Data collection and preliminary results. EOS, Transactions, American Geophysical Union, 68, 786-787, 793-795.

Sclater F.R., E.A. Boyle and J.M. Edmond (1976) On the marine geochemistry of nickel, Earth Planet. Sci. Lett. 31, 119.

Sherrell, R.M. and E.A. Boyle (1988) Zinc, chromium, vanadium and iron in the Mediterranean Sea. Deep-Sea Res. 35 1319-1334.

Spivack, A. J., S. S. Huested & E. A. Boyle (1983) Copper, Nickel and Cd in surface waters of the Mediterranean, In: Trace Metals in Seawater, C. S. Wong, E. Goldberg, K. Bruland and E. Boyle, eds., pp 505-512, Plenum Press, New York, NY.

CHAPTER TWO

AUTOMATED PRE-CONCENTRATION OF TRACE METALS  
FROM SEA WATER AND FRESH WATER

## INTRODUCTION

King and Fritz<sub>1</sub> recently pointed out that separation and concentration of trace metals from sample matrices by solvent extraction<sub>2</sub> is a labour intensive procedure that is not easily automated. In response, these workers developed an alternative method based on the adsorption of complexed metals onto a resin column. Sodium bis (2-hydroxyethyl) dithiocarbamate was shown to form hydrophobic complexes with several metals, including Cu, Ni, Cd, Zn, Co and Pb. These complexes adsorbed quantitatively on XAD-4 resin when seawater or distilled water, both spiked at concentrations on the order of  $10^{-6}M$ , was passed through a column.

A reliable method capable of processing samples at a high rate and requiring a minimum of attention had to be devised for our work on the distribution of trace metals in coastal waters<sub>3</sub>. We present here a low-cost automation of the method of King and Fritz with some significant modifications which proved necessary to determine dissolved metal concentrations of  $10^{-9}M$  or less typically found in seawater. With this procedure, ten 30 ml samples can be pre-concentrated in less than 4 hours without requiring any attention. The device is constructed from commercially available components and could simply be adapted to other column separation techniques requiring trace-metal-clean conditions.

## EXPERIMENTAL SECTION

### Apparatus

Figure 2.1 depicts the configuration of the pre-concentration device. A system of 10 columns and sample reservoirs in parallel, including both air and reagent manifolds with their respective control valves, fits in a laminar flow-bench 2'\*2'\*2 in size (Environmental Air Control, Inc.). As long as laboratory dust levels are not excessive, a complete clean room transformation is not necessary in order to obtain contamination-free sample pre-concentrations using this technique.

Each of the ten extraction units is built around a custom-designed 3 way valve block made of polypropylene and the Teflon cylinder from a Nalgene stopcock (# 6470). The maximum operating pressure is 20 PSI. The valve blocks include four reagent outlets compatible with standard chromatography fittings (1/4-28) used for 1/8' OD teflon tubing.

Connected to each valve are:

(1) a sample reservoir made from a polypropylene syringe (Becton Dickinson & Co., choice of volume: 10 to 60 ml) via a tefzel Luer-lock + 1/4-28 adapter. Each syringe barrel-reservoir is capped by a section of another syringe mounted upside-down. The analyte should not reach the level of this connection to avoid contamination. Each reservoir cap is attached to a common air manifold via a small 3-way stopcock and a Luer connection.

(2) a small resin column (0.3 ml) made of a section of 1/8" OD (.06" ID) teflon tubing. A double layer of 8  $\mu$ M Nuclepore polycarbonate

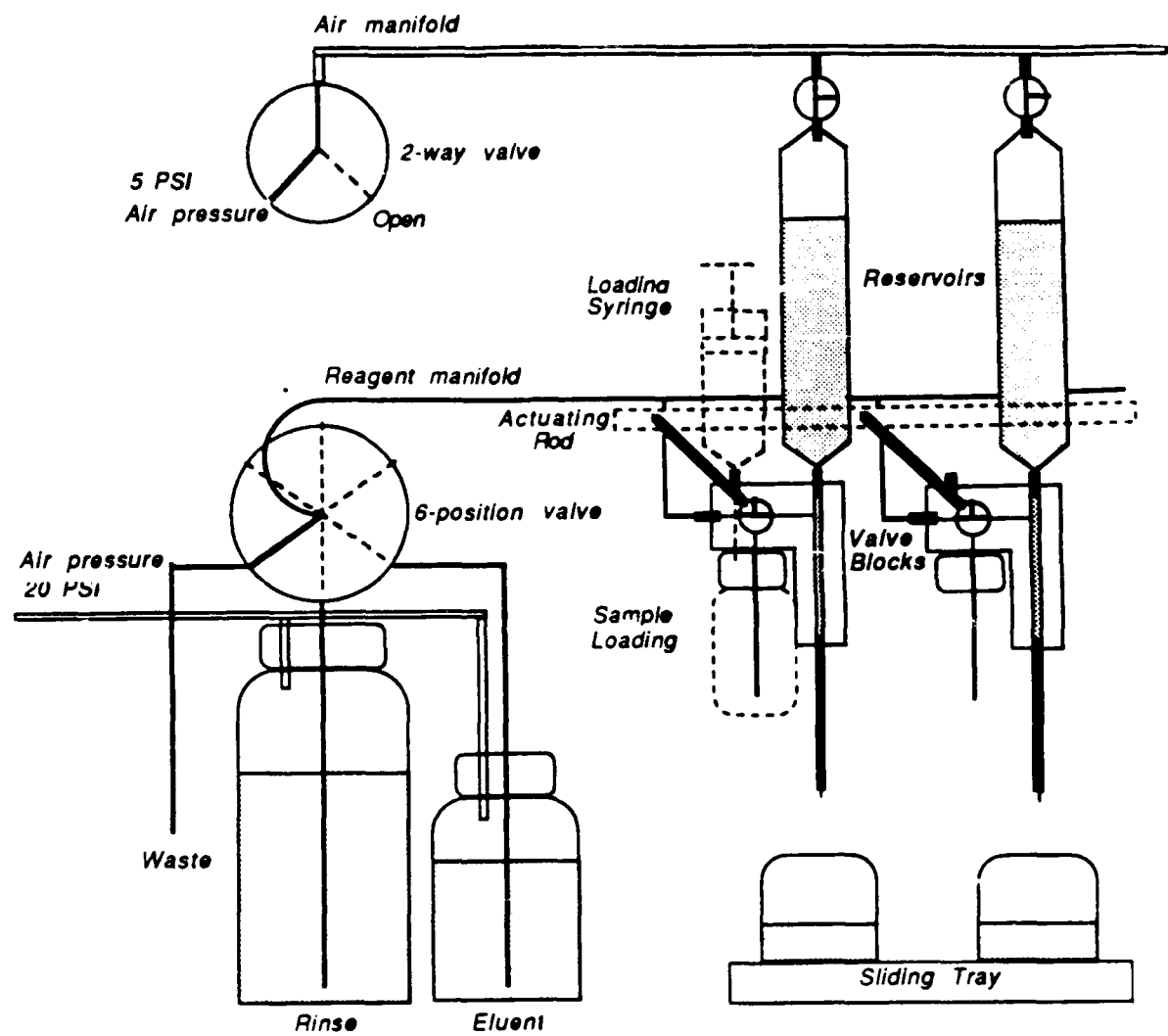


Fig. 2.1 Components of automated pre-concentration device

membrane filter inserted between a standard tubing-to-tubing 1/4-28 connection constitutes the frit.

(3) a sample loading tube (Teflon 1/4-28) with bottle cap matching the sample bottle attached air-tight to the valve block. An additional diagonal conduit in the valve block with 1/4-28 connections directs air flow only.

(4) a branch of the manifold linking each valve unit to the reagent input valve.

The design of the valve-block is such that air-pressure applied over the reservoirs blows out reagent in excess of a fixed volume ( $1 \text{ ml} \pm 0.1$ ) when the reagent manifold is opened to the waste position.

The ten valve units are mounted to a plexiglass frame which also supports a valve actuating rod and a three-position sliding tray. Both actuating rod and sliding tray are controlled by pairs of air-actuated pistons (polypropylene syringes). Pressure at the air manifold is controlled by a 3-way pneumatically controlled Rheodyne (Model 5302) slider valve. A 6-position, chemically inert, Rheodyne valve (Model 5012) switching between rinse solution, eluent and waste is connected to the reagent manifold. Functions of all 8 solenoid air valves controlling these operations as well as the 6-way valve positions are listed Table 2.1.

The custom valve-blocks are disengaged from the actuating rod for individual operation in order to allow each reservoir to be filled manually with the sample solution. The sample bottle is temporarily screwed air-tight onto the matching cap attached to the block.

Table 2.1 Functions for solenoid control channels.

Channel #

- 1 P on columns
- 2 P on bottles
- 3 Actuating rod on Run
- 4 Actuating rod on Load
- 5 Tray to 2nd position
- 6 Tray to 3rd position
- 7 6-way valve\* switch
- 8 6-way valve reset

\* 1:Rinse reagent, 2: Waste, 3: not used 4: Eluent, 5: Rinse, 6: Waste

Air-pressure applied over the loading bottle with a syringe via the diagonal conduit then forces the sample solution into the reservoir. This type of sample inlet to the reservoir avoids handling a removable reservoir cap and reduces the risk of contamination during sample loading. In addition, when the loading bottle is disconnected i.e. in the automated mode, this flowpath permits rinsing of the reagent manifold prior to input to the columns.

#### Reagents

Benson Co. (Reno, NE) kindly supplied the hydrophobic resin in 20 to 30  $\mu\text{M}$  size range (Neutral Porous, BPR-80). Columns were slurry packed with 0.3 ml of resin in ethanol. Two to three complete extraction-elution cycles are usually sufficient to clean the columns. Blanks obtained with Amberlite XAD-2 resin (used by King and Fritz), on the other hand, could not be decreased to acceptable levels even after extensive cleaning. This may be due to impurities in the resin or to contamination during grinding which is necessary for the resin beads manufactured by Amberlite.

Oxidation of the resin by nitric acid can be minimized by rinsing the columns with water after the final elution step if the system is not going to be used within a day. This prevents formation of cation-exchange sites on the resin which retain major seawater cations until the final elution step. When this precaution is taken, Na, Mg, K and Ca levels in the concentrate are typically 0.2% of seawater concentrations if samples are taken up in a final volume of 0.5 ml.

Since concentrates from seawater samples run without ligand contain similar salt concentrations, mechanical trapping of sea water in the first prototype of this system may have contributed to the residual salt.

NaHEDC was synthesized following the procedure of King and Fritz. Ligand crystals have been preserved for two years in a freezer without noticeable degradation. However, for reproducible extractions, the 6% by weight solution of the ligand at pH=8.3 should be less than 6 days old if kept in a refrigerator. The ligand solution is purified by two passages through a resin column similar to that used for samples.

Water is purified with a Corning Mega-Pure glass still after passage through a mixed-ion exchange bed and activated charcoal. Buffer solution of 0.1N NaBO<sub>3</sub> is cleaned by passage through a resin column after addition of 1 ml NaHEDC/1000 ml. Ammonia is added to the buffer (to 0.5 N) in order to neutralize acidified samples. Ammonia is sub-boiling distilled by gently swirling reagent grade ammonia next to an open bottle of distilled water overnight in a closed container. One liter of water rinse solution is buffered to pH=9.0 by addition of 1 ml of purified 0.1N NaBO<sub>3</sub>. The elution solution is composed of glass-distilled ethanol 1N in HNO<sub>3</sub>. Nitric acid is distilled three times in Vycor glass. Elution is not complete when using 1N nitric acid. Phosphoric acid is cleaned by passing a 0.25N solution through a small Dowex AG 50W-X8 cation-exchange column.

Seawater is acidified upon collection with 1 ml of 6N HCl (3 times Vycor-distilled) for a 250 ml sample. In order to obtain good Cu, Ni, Cd and Zn recoveries simultaneously, 30 ml samples are first neutralized to pH=8.4 with 1 ml of NaBO<sub>3</sub>/ NH<sub>4</sub>OH buffer. Then, 0.1 ml of ligand solution, sufficient to complex a solution 250  $\mu$ M in divalent cations, is added to each neutralized 30 ml sample. Samples are also routinely spiked with Co before NaHEDC is added to reach an effective concentration of 10<sup>-9</sup> M which is more than an order of magnitude higher than natural seawater concentrations. Monitoring of Co recovery by GFAAS provides a simple check on ligand degradation, column performance or errors in reagent additions. After weighing and reagent addition, samples can be loaded immediately for extraction. Loading of ten samples takes approximately one-half hour.

#### Procedure

Each action of the device is controlled by a programmable HP 41CX calculator-timer connected to an Oceanics 1000A interface and a simple relay circuit. Eight solenoid air valves are controlled by this circuit and activate each component of the device.

The general sequence of steps, outlined in Figure 2.2, is as follows:

Once each reservoir has been filled with a buffered sample (typically 30 ml) including the ligand, the device is switched to the automated mode. During the first step of the cycle, columns are loaded with metal-ligand complex contained in each sample. In order to sustain a flow rate of 15

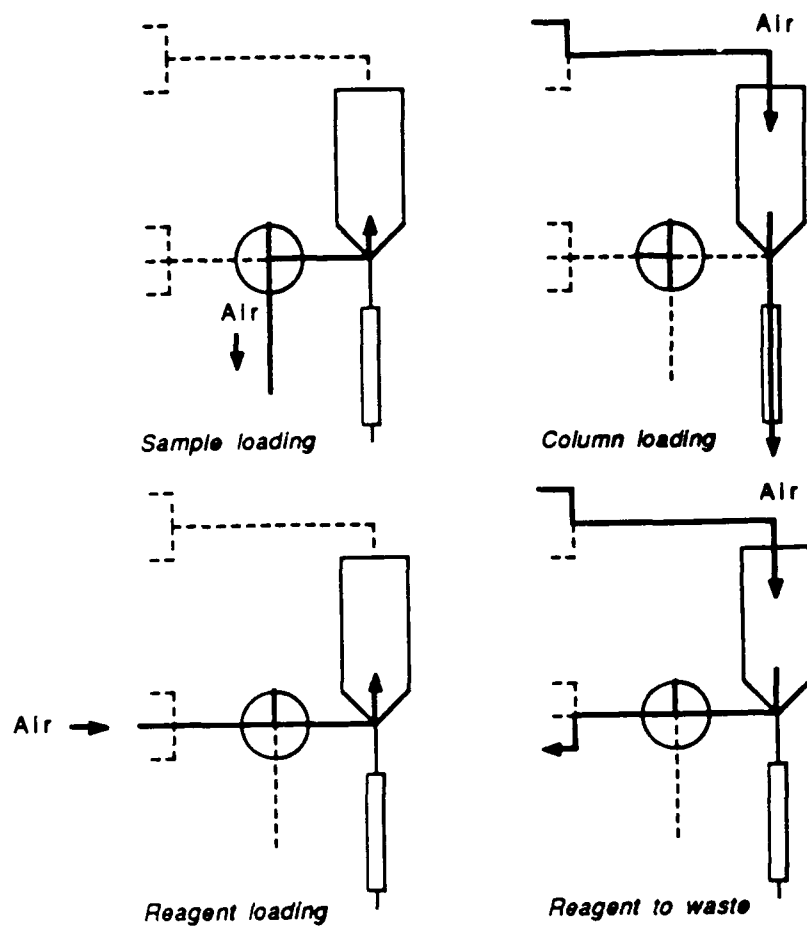


Fig. 2.2 Flow paths for four configurations of the device

Table 2.2 Outline of timer program.

## Main timer program

- 1 Initialize clock
- 2 P on reservoirs
- 3 Delay for 2 hours
- 4 P off
- 5 Tray to 2nd position
- 6 Rinse subroutine
- 7 6-way valve switched to position 5
- 8 Rinse subroutine
- 9 6-way valve switched to position 1
- 10 Rinse subroutine
- 11 6-way valve switched to position 4
- 12 Elute subroutine
- 13 End

## Rinse subroutine

- 1 P on reagent bottles
- 2 Actuating rod to Load position
- 3 Delay for 2 minutes
- 4 P off
- 5 6-way valve to next position (6 or 2)
- 6 P on reservoirs
- 7 Delay for 1 minute
- 8 Actuating rod to Run position
- 9 Delay for 15 minutes
- 10 Return

## Elute subroutine

- 1 P on reagent bottles
- 2 Actuating rod to Load position
- 3 Delay for 30 seconds
- 4 P off
- 5 6-way valve to position 6
- 6 Tray to 3rd position
- 7 P on reservoirs
- 8 Delay for 1 minute
- 9 Actuating rod to Run position
- 10 Delay for 45 minutes
- 11 Return

ml/hour, 5 PSI air pressure is applied over each column reservoir via the air manifold. Samples passing through each column are collected in cups at the first position of the sliding tray for subsequent weighing. Passage of air through the columns towards the end of this step does not adversely affect reproducibilty.

Following the loading phase, all 10 valve blocks are simultaneously isolated or connected to the common reagent manifold by vertical motion of the actuating rod. The collection tray moves to the second (waste) position for three rinse cycles. Table 2.2 contains a detailed description of the steps involved in loading the rinse solution from the 6-position pneumatic reagent flow valve. After the columns have been rinsed of salts which interfere with the analysis of the concentrate by GFAAS, samples are eluted with 1 ml of 1N HNO<sub>3</sub> ethanol solution into teflon beakers placed under the columns in the final position of the sliding tray. This final step ends less than 4 hours after the beginning of the automated procedure. After evaporation to dryness by placing the teflon elution beakers in a hot water bath, concentrates are taken up in typically 0.5 ml of 0.3 N HNO<sub>3</sub> and 0.025 N H<sub>3</sub>PO<sub>4</sub> solution for analysis.

Concentrates were analyzed with a Perkin-Elmer Zeeman 5000 graphite-furnace atomic absorption photometer equipped with an HGA-500 furnace controller/AS-40 autosampler. Standard lamp and furnace conditions were used. For Zn and Cd analyses, a L'vov platfrom was used. Pyrocoated graphite tubes were used for Cu, Ni and Co determinations. Standard curves were established by spiking

concentrates from distilled water processed as a sample. A change in sensitivity in this matrix relative to a pure HNO<sub>3</sub>/H<sub>3</sub>PO<sub>4</sub> solution is significant (10-20%) only for Cd and Zn. Addition of phosphoric acid considerably improves reproducibility of analyses for Cd and Zn.

#### RESULTS AND DISCUSSION

Acidified North Atlantic surface water from the Sargasso Sea was spiked with Cu, Ni, Cd and Zn at levels comparable with typical oceanic waters. Replicate analyses of both spiked and unspiked samples (concentrated from 30 ml to 0.5 ml) are listed in Table 2.3. Reproducibility between days ranged from 5 to 8%. Within a day, reproducibility of replicate analyses on different columns was 3-4%. Recoveries range between 93 to 98% and can be corrected for when determining actual metal concentrations. Trace metal concentrations found in Sargasso Sea surface water are comparable to earlier determinations by different methods in this laboratory as well as by other workers<sup>4,5</sup>: Cu: 0.83 nM, Ni: 1.95 nM, Cd < 1 pM, Zn: 0.1 nM.

Spiked seawater samples buffered to pH=5.0 with 250  $\mu$ l of 0.3 M ammonium acetate and 5N ammonia, instead of NaBO<sub>3</sub>, show 100 % recoveries for Cu and Ni, but Cd and Zn are not retained on the column under these conditions. Depending on the elements of interest, a compromise may have to be made between recovery efficiencies for different elements. Alternatively, extractions could be repeated under optimum conditions for each element. Modification of the pre-concentration method to three

Table 2.3 Sargasso Sea surface water pre-concentrations:  
30 ml to 0.5 ml at pH=8.4

Element	SW (n=13)	SW+spike (n=13)	% Recovery	Blank
Cu nM	0.83 ± .1	3.08 ± .2	93	0.1
Ni nM	1.95 ± .2	5.08 ± .3	94	0.05
Cd pM	1 ± 1	76 ± 5	98	< 1
Zn nM	0.1 ± .1	3.38 ± .3	98	0.3

order of magnitude lower metal concentrations has lowered the working range in pH relative to results reported by King and Fritz.

Blanks were determined by passing seawater a second time through the procedure after adding all reagents except the ammonia whose negligible contribution was checked separately. Results listed in Table 2.3 indicate blanks are small relative to open ocean surface concentrations for all elements except Zn. This limitation is not significant for our purpose since Zn concentrations are typically an order of magnitude higher in coastal or subsurface water than in Sargasso Sea surface water. Blank contributions from the NaHEDC ligand accounts for more than 80% of the total blanks for Cu, Ni and Zn. Further purification of the ligand could, therefore, reduce the blank if necessary. Pb concentrations determined for Sargasso Sea surface water ( $74 \pm 5$  pM, collected June '88) by pre-concentrating 30 ml to 0.1 ml at pH=5.0 are comparable to reported values<sup>6</sup>. Work is ongoing to reduce the current blank of 10 pM to the level obtained for cobalt-APDC coprecipitation (<4 pM).

In order to determine the applicability of this method to fresh water systems with metal concentrations often below the detection limit for analysis by GFAAS via direct injection,<sup>7</sup>, Guadiana river water (Spain) has been analyzed by the pre-concentration method. After filtration through a 0.4  $\mu$ M Nuclepore polycarbonate membrane, fresh water samples are treated in the same way as seawater. As indicated in Table 2.4, recoveries cannot be distinguished from 100% for Cu, Ni and Cd. Even though recovery for Zn is lower (85%), reproducibility remains high for

Table 2.4 Guadiana river water pre-concentrations:  
30 ml to 3 ml at pH=8.4

Element	RW (n=3)	RW+spike (n=2)	% Recovery
Cu nM	11.6 ± .6	19.5 ± .6	101
Ni nM	12.2 ± .1	22.8 ± .8	103
Cd pM	19 ± .6	259 ± 1	101
Zn nM	2.4 ± .2	10.5 ± .1	85

this element. We cannot explain 10-15% lower recoveries from spiked Corning distilled water which were observed for the same metals.

#### CONCLUSION

This device has automated the pre-concentration of trace metals from natural fresh- and seawater by HEDC-metal complex retention on a hydrophobic column. Previous work on dithiocarbamates<sub>g</sub> indicates that other elements should be amenable to this procedure as well. In particular, high recoveries of Ag, Fe, U, V, Bi were obtained by King and Fritz.

Due its flexibility in programming, eluent choice and sample size, this device should allow the automation of other column separation techniques requiring trace metal clean conditions. Chelex and Fractogel immobilized hydroxyquinoline resins, for instance, have successfully been used to preconcentrate from seawater a number of trace elements such as Cd and Zn<sub>9</sub>, Mn<sub>10</sub>, Al<sub>11</sub> and Ga<sub>12</sub>. These methods could easily be automated with this system. Minimal sample handling, and consequently lower risks of contamination, involved in the automated column extraction approach should allow a greater number of laboratories to determine reliably trace metal concentrations in natural waters.

## REFERENCES

- 1 King, J. N.; Fritz, J.S. Anal. Chem. 1985, 57, 1016.
- 2 Bruland, K. W.; Franks, R. P.; Knauer, G. A.; Martin, J. M. Anal. Chim. Acta. 1979, 105, 233.
- 3 van Geen, A.; Rosener, P.; Boyle, E. Nature 1988, 331, 423.
- 4 Boyle, E.A.; Huested, S. S.; Jones, S. P. J. Geophys. Res. 1981, 86, 8048.
- 5 Bruland, K. W.; Franks, R. P. "Trace Metals in Seawater", Plenum Press, New York, 1983.
- 6 Boyle, E. A.; S.D. Chapnick; G.T. Shen J. Geophys. Res. 1986, 91, 8573.
- 7 Shiller, A.M.; Boyle, E.A. Variability of dissolved trace metals in the Mississippi River, Geochim. Cosmochim. Acta 1987, 51, 3273.
- 8 Hulanicki, A. Talanta, 1967, 14, 1371.
- 9 Bruland, K. W.; Coale, K. H.; Mart, L. M. Marine Chem. 1985, 17, 285.
- 10 Landing, W. M.; Haraldsson, C; Paxeus, N. Anal. Chem. 1986, 58, 3031.
- 11 Orians, K. J.; Bruland , K. W. Earth Planet. Sci. Lett. 78, 397.
- 12 Orians, K. J.; Bruland , K. W. Geochim. Cosmochim. Acta, in press.

CHAPTER THREE

Cu, Ni, Cd AND Zn ENRICHMENTS IN THE GULF OF CADIZ

## INTRODUCTION

High Cu, Cd and Zn concentrations have been observed in shelf waters of the Gulf of Cadiz (van Geen et al, 1988). These enrichments are sufficient to influence the composition of the Mediterranean because Spanish coastal water is entrained in the inflow to the Alboran Sea. In fact, the flow averaged composition of the inflow in June'82, determined on the basis of data from the western Alboran Sea (Boyle et al, 1985 and Sherrell and Boyle, 1988), indicates no net source of Cu, Cd and Zn is required within the basin in order to explain metal enrichments in the Mediterranean relative to surface Atlantic water, first reported by Spivack et al, (1983). Here, we support this conclusion by presenting trace metal and ancillary data for 172 samples from the Gulf of Cadiz, collected in April and October'86, which confirm that Spanish shelf water dominates Cu, Cd and Zn fluxes through the Strait of Gibraltar. Following a discussion of the set of 145 surface samples, 8 trace metal profiles , as well as 20 determinations of  $^{228}\text{Ra}/^{226}\text{Ra}$  activity ratios, possible mechanisms causing exceptional metal enrichments over the Spanish shelf are evaluated.

Surface transects extending from the open ocean to nearshore areas generally show increasing trace metal concentrations as coastal waters are entered. However, the cause of these enrichments can differ from one situation to the other. Bruland et al. (1978) related high Cd concentrations in Pacific surface waters to upwelling of metal (and nutrient) enriched subsurface water off central California. On the other hand, Boyle et al., (1981) attributed elevated Cu concentrations

in shelf waters north of the Gulf Stream and in the Gulf of Panama to remobilization from coastal sediments. Heggie (1982) and Heggie et al. (1987) also presented evidence that continental shelf sediments are the major source for Cu (and Mn) enrichments in shelf waters of the eastern Bering Sea. In the North Atlantic, Bruland and Franks (1983) showed Cu, Ni, Cd and Zn concentrations increasing as fresher coastal water over the north-american shelf is approached from the Sargasso Sea. Shelf and riverine metal sources could not be distinguished in this case. In the eastern Atlantic, Kremling (1983) demonstrated that Cd, Cu and Mn concentrations are higher inshore of a hydrographic front off the British Isles. None of these studies, however, have encountered water as enriched in Cu, Cd and Zn as Spanish coastal water off Cadiz.

In this paper, mechanisms which have been proposed to explain metal enrichments in continental shelf waters are examined in the context of the Gulf of Cadiz. It turns out, first, that metal contributions from suspended particles are negligible even in the most turbid waters sampled. Dissolved and particulate inputs by the Guadalquivir river also prove to be too small to account for metal concentrations off Cape Trafalgar, unless these enrichments reflect an exceptional period of erosion. We argue that acid sludge discharges in the Gulf of Cadiz are insufficient as well to explain observed enrichments. For lack of an obvious source of Cu, Cd and Zn from the shelf, we propose a mechanism to explain observed coastal metal enrichments analogous to the nutrient trap found in estuaries. Following a discussion of evidence for this mechanism, the composition of surface Atlantic water, NACW, as well as

seasonal variability in Spanish shelf water, is estimated for salinity and Cu, Ni, Cd and Zn concentrations. The three end-members contributing to the Atlantic inflow are defined for the purpose of tracing their advection through the Strait of Gibraltar and into the Alboran Sea (Chapters 4 and 5).

#### SAMPLING AND ANALYSIS

Two cruises (March 26-April 19 and October 12-17 1986) of USNS Lynch during the Gibraltar Experiment (Kinder and Bryden, 1987) offered the opportunity to collect surface samples with a contamination-free underway pumping apparatus. Profiles and additional surface samples were also collected during RV Oceanus cruise 176 on 14-16 April 1986. Five liter Niskin bottles modified and cleaned as described in Boyle et al. (1985) were used for the profiles. Salinity and nutrients were determined using standard techniques (Guildline Autosal salinometer and colorimetry, respectively) described in Strickland and Parsons (1968).

Trace metal analyses on 30 ml samples followed a resin pre-concentration procedure which has been automated (Chapter 2). Comparison of this procedure for selected samples with modified Co-APDC (cobalt-ammonium pyrrolinedithiocarbamate) co-precipitation (Boyle et al. 1981) showed no significant differences for Cu, Ni, Cd and Zn. All sample concentrates were analyzed by graphite-furnace atomic absorption (Perkin-Elmer Zeeman 5000, HGA 500). One-sigma precision for this data set is 5% or 0.1 nM for Cu and Ni whichever is larger, 5% or 5 pM for Cd and 6% or 0.2 nM for Zn. Blank corrections averaged 0.1 nM, 0.01 nM, <1 pM and 0.3 nM.

for Cu, Ni, Cd and Zn respectively. A number of samples spanning the range of metal concentrations in the Gulf were also filtered through 0.4  $\mu\text{m}$  Nuclepore filters before acidification.

Trace metal concentrations were determined for several Iberian rivers by direct injection GFAAS with calibration by standard addition. Results for the Guadalquivir river by this method agree with trace metal concentrations determined by the automated pre-concentration procedure, indicating river water may also be analyzed by resin extraction.

Finally, dissolved  $^{228}\text{Ra}/^{226}\text{Ra}$  activity ratios for 20 surface samples were determined with towed Mn impregnated fibers following the method of Moore (1976) during RV Oceanus cruise 176.

## RESULTS

In April 1986, surface salinity in the Gulf of Cadiz outside the region influenced by continental shelf waters ranged from 36.25 to 36.4  $\text{\textperthousand}$ . (Fig. 3.1a). Over the Spanish continental shelf, salinities ranged from 35.6 to 36.0  $\text{\textperthousand}$ . In contrast, salinity in Moroccan shelf water remains above 36.14  $\text{\textperthousand}$ . Extensive CTD coverage obtained during this cruise indicates an average surface mixed layer depth of 60 m (Bray, 1986). This, and profile data to be presented, implies that surface samples taken with the underway pumping apparatus (intake depth between 1 and 3 m) are representative of a significant portion of the water column rather than a thin surface layer. Phosphate and silicate concentrations ranged from 0.98  $\mu\text{M}$  to 0.05  $\mu\text{M}$  and from 3.2 to 0.3  $\mu\text{M}$ ,

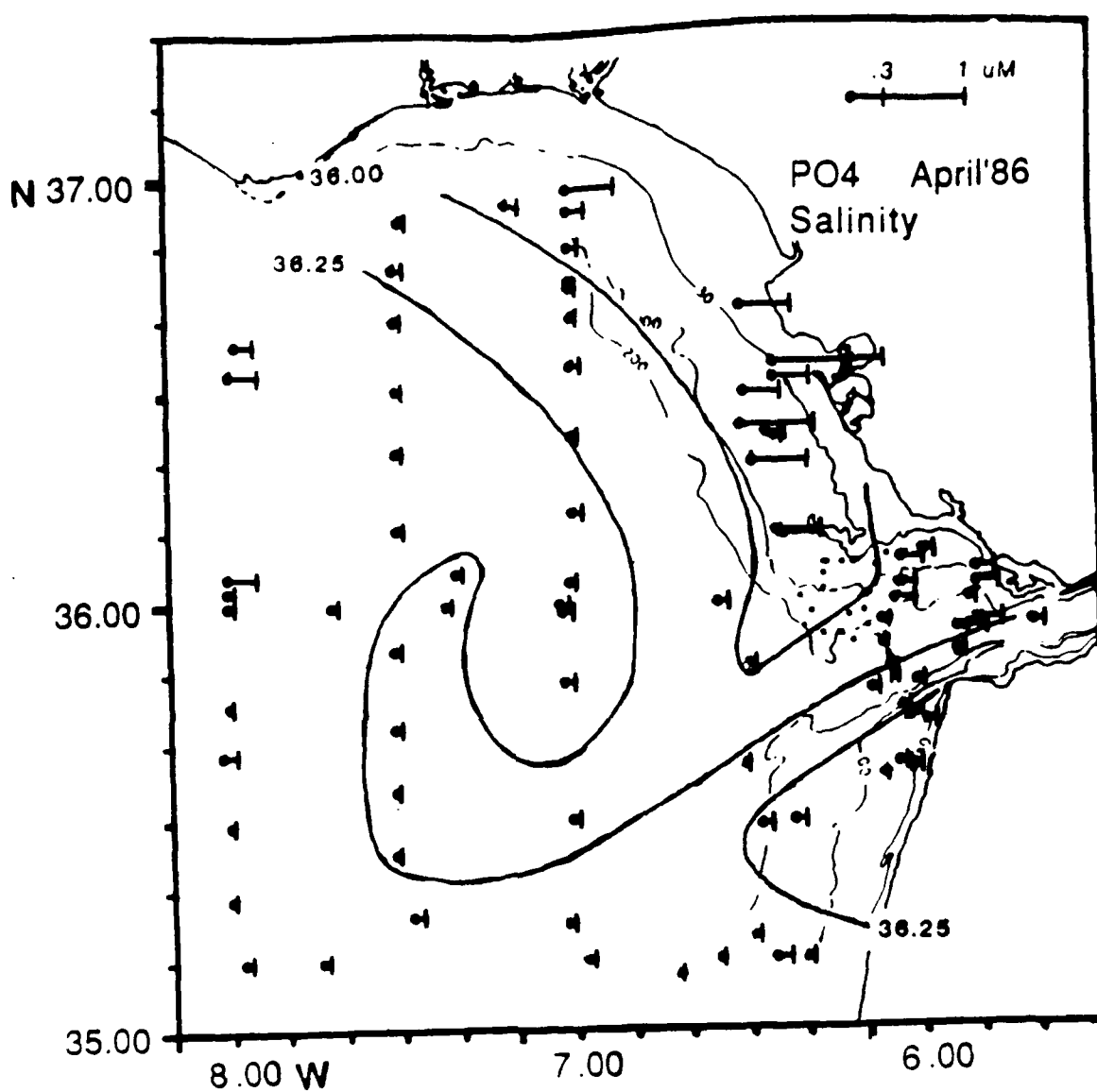
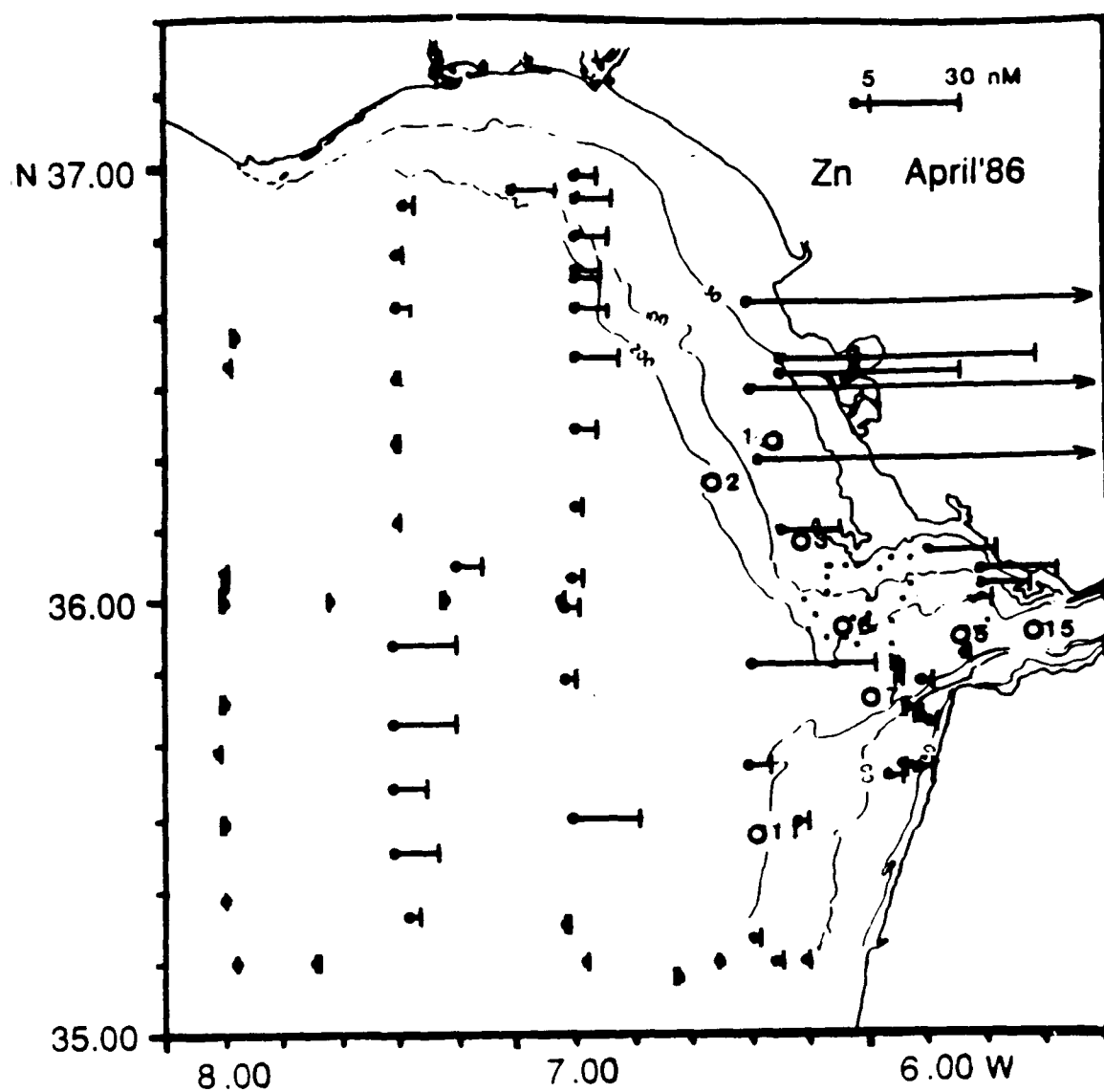


Fig. 3.1a Salinity in ‰(contours) and phosphate (bars) in Gulf of Cadiz surface water.



respectively (Fig. 3.1a and Table 3.1a). Elevated nutrient concentrations were restricted to less saline water overlying the continental shelf and the highest values were found near the mouth of the Guadalquivir river.

Zn concentrations generally follow the distribution of salinity and nutrients, even though patterns differ in detail (Fig. 3.1b). Zn concentrations range between 0.3 - 1 nM for samples with salinity higher than 36.25 ‰. Zn levels over the Spanish shelf, on the other hand, are elevated by at least an order of magnitude: Zn > 50 nM over a distance of 40 km from the estuary of the Guadalquivir river (sample # 1) to shelf water off Cadiz south of the estuary (sample # 73, 2, 3 and 0.1!). Mimicking Zn enrichments, Cu and Cd concentrations in shelf water (Fig. 3.2) are also extremely high, eg. for sample # 0.1: Zn= 51nM, Cu=20 nM and Cd=340 pM. Cu, Cd and Zn concentration for shelf samples between the estuary of the Guadalquivir and the shelf off Cadiz increase linearly with decreasing salinity (Fig. 3.3). Ni enrichments over the Spanish shelf are much weaker. Only a single sample (# 1), the freshest sample from the estuary of the Gaudalquivir (35.42 ‰), reaches a concentration greater than 5 nM (twice typical open ocean concentrations).

The offshore Zn distribution agrees with surface samples collected in September 1980 (Spivack et al, 1983) and a profile, collected in June 1982 at 35°46'N, 06°30'W, which shows Zn concentrations increasing from 0.8 nM at the surface to 1.5 nM at 400 m depth (Sta. 3 of Sherrell and

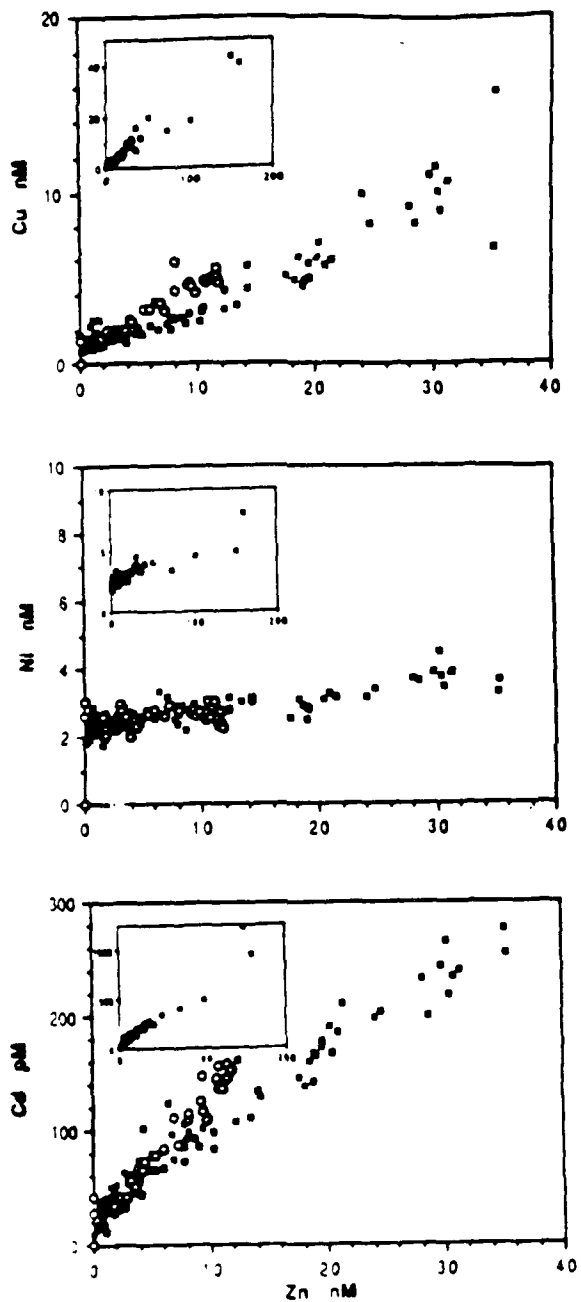


Fig. 3.2a Zn vs. Cu for surface samples, April (filled squares)  
October (open circles)

b Zn vs. Cd               "  
c Zn vs. Ni               "

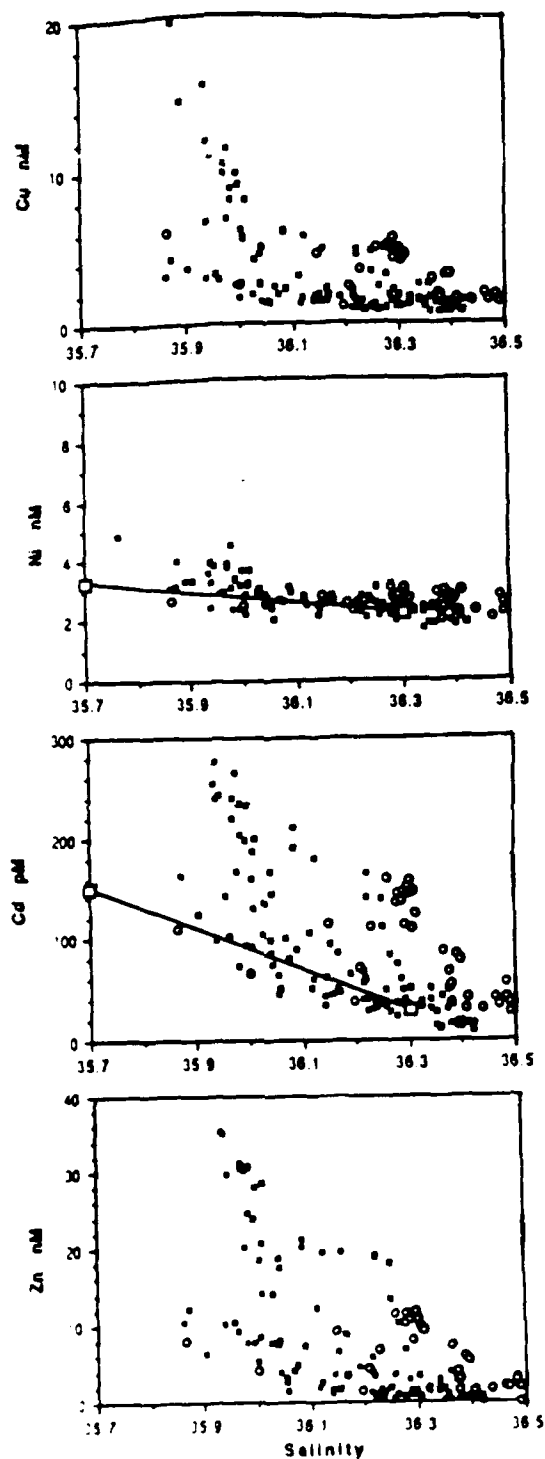


Fig. 3.3a Salinity vs. Zn for surface samples, April (filled squares)  
October (open circles)

b Salinity vs. Cu  
c Salinity vs. Ni  
d Salinity vs. Cd

Boyle, 1988). Since changes in Zn concentrations with depth down to 400 m are negligible relative to enrichments in Spanish shelf water, surface enrichments in the deeper portion of the Gulf of Cadiz can not be due to upwelling. For this reason, an anticyclonic tongue of high Zn concentrations extending beyond the shelf south-west of Cadiz over a distance of 100 km. (barely detectable on the basis of salinity) is most likely due to advection of shelf water (Fig. 3.1b). Cu and Cd ratios relative to Zn for enriched offshore samples are consistent with conservative mixing of open ocean and shelf water. However, nutrients phosphate and silicate are depleted within the tongue to levels close to the detection limit and salinity is higher by 0.2 ‰ than expected for shelf water of equal metal concentrations. Such discrepancies suggest that nutrients and salinity are not conservative relative to Cu, Cd and Zn on the advection time scale of this feature. This example illustrates the potential uses of dissolved metals as tracers of cross-shelf circulation.

Profile data are consistent with tracer distributions in surface water. There are two distinct water masses in the Gulf of Cadiz in addition to surface Atlantic water and shelf water: the saline Mediterranean outflow (38.4 ‰) and fresher NACW (35.7 ‰ at 400 m depth). All four end-members are represented in the set of profiles whose locations are indicated in Fig. 3.1b. In order of decreasing latitude, the composition of these profiles for salinity, Si, P, Cu, Ni, Cd and Zn is depicted in Fig. 3.4. Briefly, stations 1 and 3, and a 15 m thick surface layer at station 6 show the characteristic shelf water

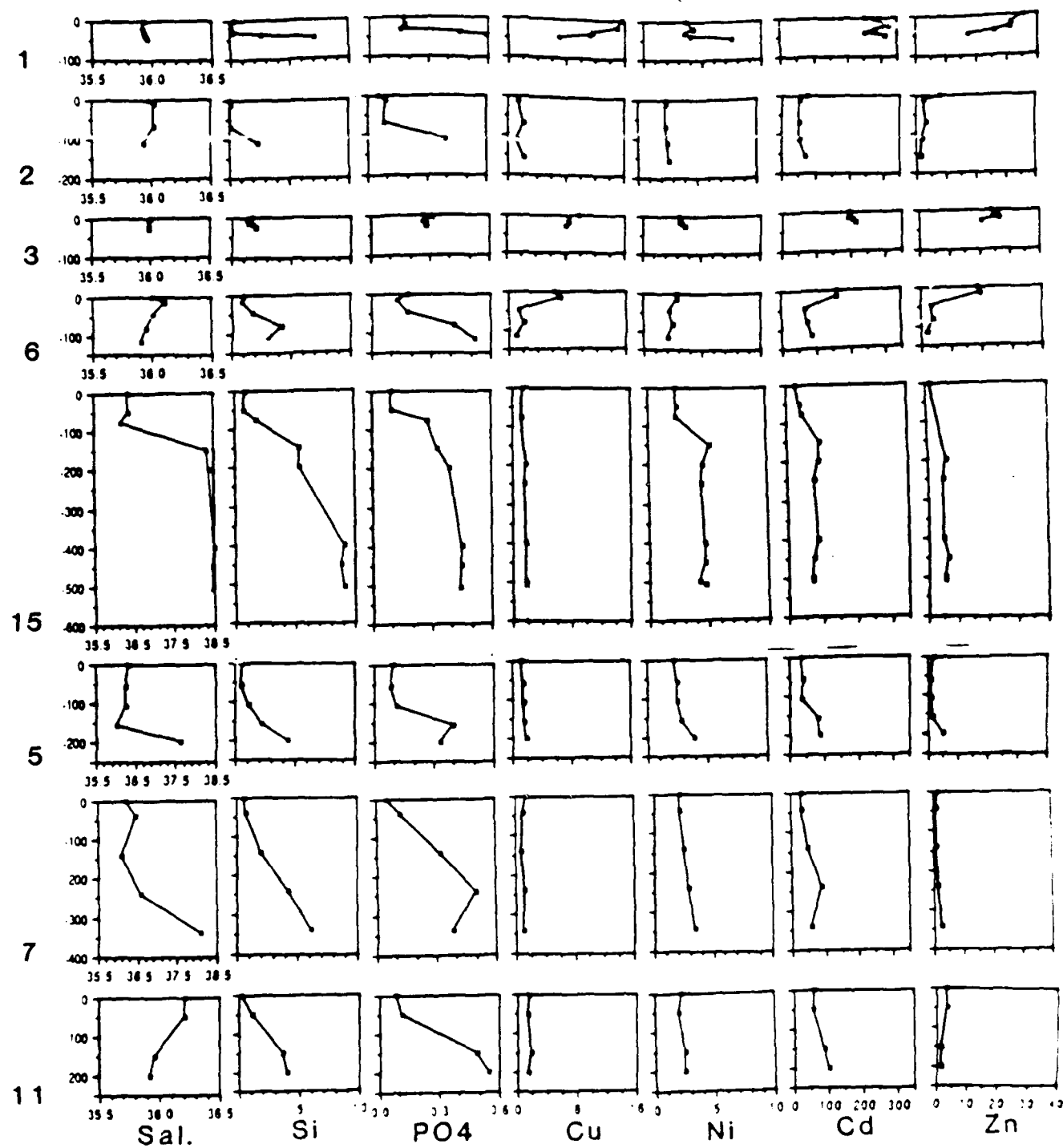


Fig. 3.4 Stations 1, 2, 3, 6, 15, 5, 7, 11(order of decreasing latitude)  
 Sal. %, Si  $\mu\text{M}$ , PO<sub>4</sub>  $\mu\text{M}$ ,  
 Trace metals Cu, Ni, Zn in nM, Cd in pM.  
 Station locations in Fig. 3.1b, data from Table 3.2

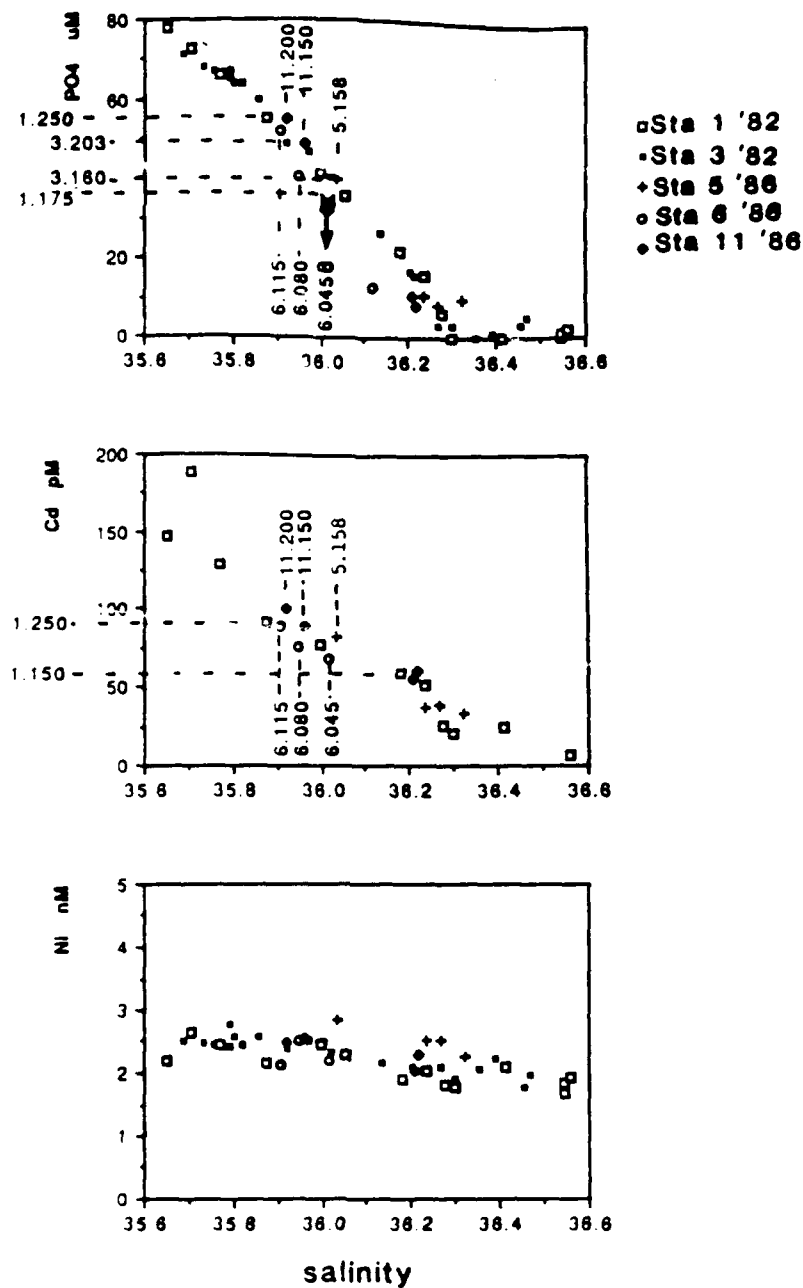


Fig. 3.5a Salinity vs.  $\text{PO}_4$  for subsurface samples outside shelf region  
 Dashed lines identify sample by Sta# depth(m)  
 Arrow indicates  $\text{PO}_4$  depletion (see text)  
 b Salinity vs. Cd for subsurface samples outside shelf region.  
 c Salinity vs. Ni " "

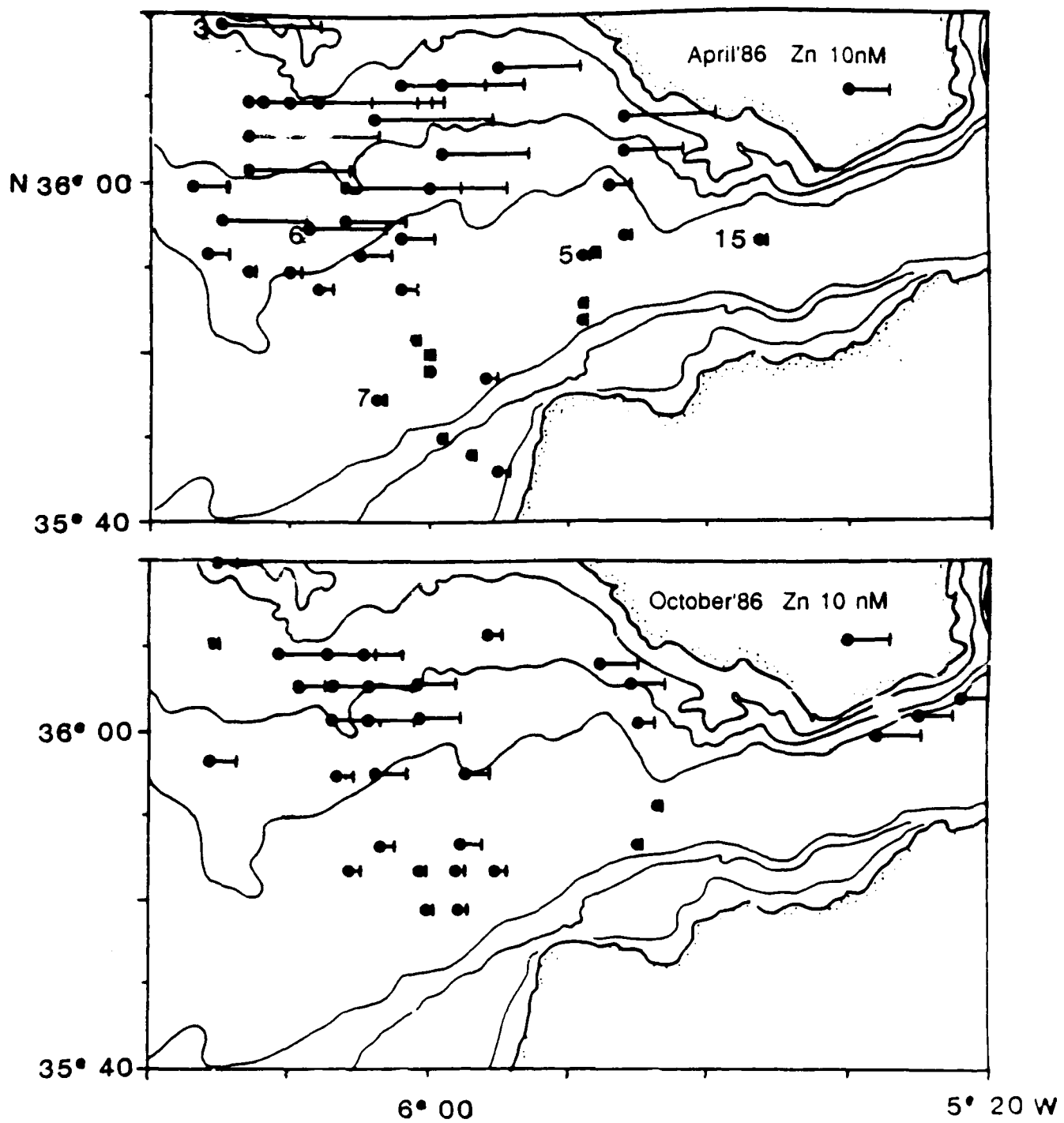


Fig. 3.6 Zn in surface waters, western approaches to the Strait.  
 a April  
 b October

signature. Profiles at stations 2 and 11 can simply be accounted for by mixing of surface Atlantic water and NACW. Only Cd and, to a lesser extent Ni, are significantly enriched in NACW. For Cu, Ni, Cd, Zn, and salinity, the upper 400 m of an Atlantic profile can be described mathematically as mixtures of surface Atlantic water and NACW. Vertical concentration gradients are significant only for Cd and Ni and the linear relationship with salinity is indicated in Fig. 3.5. Surface Atlantic water and NACW are also indicated in Fig. 3.3 b,c to show that shelf enrichments can not be attributed to upwelling of subsurface water only. The deeper portions of profiles 15, 5 and 7 contain the Mediterranean outflow. Salinities greater than 37.3 ‰ (approximately 50% Mediterranean outflow contribution) are found at 150 m, 200m and 340 m depth at Stations 15, 5 and 7 respectively, which is also the order of increasing distance from the source of this water mass. Trace metal concentrations of 1.7 nM, 4.5 nM, 75 pM and 5.1 nM for Cu, Ni, Cd and Zn in the ouflow (Sta. 15) match the composition of Mediterranean deep water determined in June 1982 from an Alboran Sea profile (Boyle et al., 1985 and Sherrell and Boyle, 1988).

Due to greater sampling density in the western approaches to the Strait of Gibraltar, the Zn distribution in this region has been enlarged in Fig. 3.6a. Shelf enrichments are clearly restricted to waters shallower than 200 m. A smaller set of surface samples collected in October'86 (Fig. 3.6b) shows significant changes occurred over 6 months. First, the range in metal concentrations is much smaller in October than in April (Fig. 3.2). To some extent, this reflects that the October cruise

collected fewer samples from the area where highest enrichments were observed in April. However, even samples from the same location have trace metal concentrations which are roughly a factor of two lower than in April. In addition, within the October data set, several samples (1, 2, 3, 103, 104 and 105) show very low metal enrichments relative to salinity (Fig. 3.3). The composition of these samples is comparable to that found in waters over the north western shelf of the Gulf of Cadiz in April'86. Another difference between the two trace metal data sets is that at a given Zn concentrations, Cu and Cd concentrations in shelf water are significantly higher in October than in April (Fig. 3.2). These differences must somehow be related to changes in circulation and/or variations in the strength of the metal source to the shelf.

Over the Moroccan shelf, Cu, Ni and Cd concentrations in surface samples do not show evidence of enrichment other than by mixing with Atlantic subsurface water. Zn levels of 3 nM, on the other hand, are higher than concentrations found in the Gulf of Cadiz outside the region influenced by Spanish shelf water. One reason for this may be that a small degree of shelf enrichment does occur off the Moroccan coast, but to an extent detectable only for Zn which is more sensitive to this process than other metals. In any case, Zn concentrations around 1 nM in surface waters in the southern half of the Strait of Gibraltar (Fig. 3.6a) indicate that little Moroccan shelf water is entrained with the inflow to the Alboran Sea. Due to its negligible contribution to metal fluxes through the Strait, this water mass can be neglected.

## DISCUSSION

Offshore surface water concentrations of Cu (1.2 nM), Cd (15-30 pM) and Zn (1 nM) in metal-depleted water at the center of the Gulf of Cadiz are higher than in the Sargasso Sea: 0.8 nM, 2 pM, and .06 nM, respectively, determined by Bruland and Franks (1983). Given the presence of a strong subsurface source in the the case of Cd (NACW), surface enrichments could be due to upwelling. A more likely explanation for surface enrichments is simply that mixing with enriched shelf water raises offshore surface Cd concentrations, as it does in the case of Cu and Zn. Ni, which is not enriched in shelf water to the same extent as Cu, Cd and Zn, is found at comparable concentrations in both the Atlantic central gyre and offshore waters of the Gulf of Cadiz. Evidently, Spanish shelf can not be traced far beyond the Gulf of Cadiz since metal concentrations for samples 38-46 and 49,50 at the south-west border of the large scale survey (Fig. 3.1b) already approach typical surface Sargasso Sea values.

Despite unusually high Cu, Cd and Zn concentrations found in Spanish coastal water, several arguments allow us to rule out the possibility of contamination during sampling or analysis. First, surface sampling procedures which were followed in the Gulf of Cadiz have repeatedly yielded consistent results for contamination prone elements such as Cu, Zn and Pb in Sargasso Sea surface water where metal concentrations are lower. Second, remarkably constant inter-element ratios between Zn and Cu, Ni, Cd (Fig. 3.2 a,b,c) for the suite of enriched shelf samples argue against contamination. Metal-salinity relationships (Fig. 3.3

a,b,c,d) for enriched shelf samples off Cadiz are roughly linear over a range in metal concentrations of more than one order of magnitude. It is unlikely such a relation would have been preserved if samples were randomly contaminated. The Cu/Zn ratio in shelf waters off Cadiz is equal to that found in metal-enriched surface samples from the Alboran Sea which lies downstream of the flow path of Spanish coastal water (Sherrell and Boyle, 1988). This a final argument against contamination since these samples were collected on different cruises and analyzed by two different methods.

The particulate metal contribution to total Cu, Cd and Zn concentrations is known to be small in the open ocean (Boyle et al., 1981). Filtered and unfiltered samples were compared over a wide range of metal concentrations. As it turns out, even in samples with very high metal levels, the difference between filtered and unfiltered samples is less than 10% of the total concentration. Total Cu, Ni, Cd and Zn concentrations mainly reflect the dissolved component. Observed coastal enrichments are, therefore, not simply due to higher concentrations of particles in shelf water.

#### Riverine metal source

Despite linear metal-salinity relationships in the region between the Guadalquivir river and the shelf off Cadiz, conservative mixing of river water over the continental shelf is unlikely. Extrapolation of metal-salinity relationships to zero salinity requires unrealistically high riverine dissolved metal concentrations (eg. Zn= 10  $\mu\text{M}$ ). In order

to confirm that fluvial metal input to this region is not exceptional, major rivers reaching the Atlantic flank of the Iberian peninsula were sampled. Cu, Cd and Zn concentrations for the Guadalquivir river (Table 3.3) are not significantly different from levels found in the Mississippi or even in an unperturbed system such as the Amazon (Shiller and Boyle, 1987) and, therefore, insufficient by several orders of magnitude to explain observed shelf enrichments. For desorption from riverine suspended particulate matter in the Guadalquivir estuary to account for shelf enrichments, dissolution of Zn from a suspended load greater than 11 g/l would be required. This estimate is based on a Mississippi suspended matter Zn concentration of 60 ppm determined by Shiller and Boyle (1985). Such an unrealistically high particulate load disqualifies the normal Guadalquivir river as a likely source of Cu, Cd and Zn enrichments in waters overlying the Spanish shelf. Since exceptional erosion events may contribute more sediment than normal particulate transport, it is not possible to entirely rule out input of sufficient leachable Zn to the shelf.

Factors controlling the distribution of Ni in the Gulf of Cadiz are ambiguous due to the lack of strong enrichments anywhere for this element. Vertical profiles from June '82 and April '86 are consistent with the Ni-salinity relationship determined in June 1982 for samples unaffected by the shelf (Fig. 3.5 c). As it turns out, all Gulf of Cadiz surface water samples, with the exception of # 1, 2, 3 which are closest to the estuary of the Guadalquivir, conform to the mixing relationship for vertical profiles (Fig. 3.3 c). From these

observations, it appears that a distinct shelf end-member does not need to be invoked (with the exception of samples with Ni > 3.5 nM) for this element. Ni also distinguishes itself from Cu, Cd or Zn by being enriched in the Guadalquivir river (Table 3.3). In fact, extrapolating the dominant surface trend to zero salinity yields a river concentration very similar to the measured concentration xx miles upstream from the estuary. Since both riverine and NACW sources of Ni are of similar magnitude relative to salinity, shelf enrichments cannot be attributed with certainty to input from either or both of these sources.

#### Anthropogenic discharges

C. Lambert (pers.comm.) argues that metal enrichments over the Spanish shelf may be due to "chemical mud discharges" presumably identified on a CZCS image of the Gulf of Cadiz dated August 24th 1981. The image was processed by Andre and Morel (unpubl. manuscript) and shows high concentrations of suspended matter (measured by radiance at 550 nm) in a pattern closely following the distribution of Zn in April 1986 outside the shelf area. Even though an anthropogenic source may be suggested by the similarity between the clockwise rotating gyre (Fig. 3.1b) and the feature in the CZCS image, several observations argue against this assertion.

One source of metals to the Gulf of Cadiz are acidic effluents from a nearby titanium dioxide production plant (Tioxide Espana, S.A.) which are discharged daily at 36°30'N, 07°00'W from two 750 m<sup>3</sup> capacity tankers and have been the subject of publicized environmental concern

(Oslo Commission, 1986). If this source were the cause of trace metal enrichments in Spanish shelf waters, the implications would be very significant since by extension Cu, Cd and Zn enrichments in the Alboran Sea and throughout the Western Mediterranean basin would also be due to these discharges. The total metal transport to the Mediterranean through the Strait of Gibraltar was estimated recently (van Geen et al., 1988) and turns out to be two orders of magnitude greater than acidic effluent inputs for Zn (Oslo Commission, 1986). Since probably only a fraction of the metal flux causing Spanish shelf enrichments contributes to the Atlantic inflow, the sludge discharge can a fortiori not be sufficient to sustain Spanish shelf water enrichments. In addition, highest metal concentrations are observed near the mouth of the Guadalquivir river rather than at the dumping site which lies 50 km offshore. The particulate plume identified on the CZCS image may simply have been due to a phytoplankton bloom in advected shelf water initially enriched in nutrients. If this interpretation is correct, the CZCS image can be taken as evidence for recurrence of the tongue-like circulation feature that we observe in this work.

#### Shelf sediments

Since none of the mechanisms discussed above can explain observed shelf enrichments, sediments must be considered as a potential source of Cu, Cd and Zn. For comparison, Table 3.4 lists representative coastal enrichments and corresponding salinities determined for various coastal regions of the Atlantic and the Pacific. Since samples were not chosen within estuaries, tabulated salinities are representative of shelf water

rather than a particular mixing proportion with river water. Clearly, Zn, Cu and to a lesser extent Cd enrichments off Cadiz are considerably higher than in other regions. More accurately, only the portion of the Gulf of Cadiz south of the estuary of the Guadalquivir river stands out relative to other coastal waters since enrichments are significantly lower over the shelf north-west of the estuary.

The region off Cadiz does not show any striking features which might explain the unusual degree of metal enrichments. The shelf, approximately 20 n.mi wide to the 100 m isobath, is much narrower than, for instance, the continental shelf of the Eastern Bering Sea where Cu concentrations do not rise above 5 nM (Heggie et al., 1987). Total dissolvable Mn concentrations determined by G. Klinkhammer (unpubl. data) for a selected number of unfiltered shelf surface samples are very high off Cadiz: 157, 163, 25 nM for # 0.1, 14.7 and 287, respectively, vs. a maximum of 20 nM in Bering Sea surface water. Concentrations in offshore samples of the Gulf of Cadiz were 1.7 and 2.0 nM for # 262 and 256, respectively. This may indicate that anoxia in shelf sediments sustains unusually important diagenetic metal flux in this portion of the Gulf.

Even though processes releasing metals and  $^{228}\text{Ra}$  from shelf sediments are different, this tracer can be used as a measure of shelf water-sediment interactions. Moore (1987) has shown that the dissolved  $^{228}\text{Ra}/^{226}\text{Ra}$  activity ratio is supported by sedimentary fluxes in estuaries as well as near-shore fine grained sediments. The range of  $^{228}\text{Ra}/^{226}\text{Ra}$  activity ratios found in shelf waters both North and South

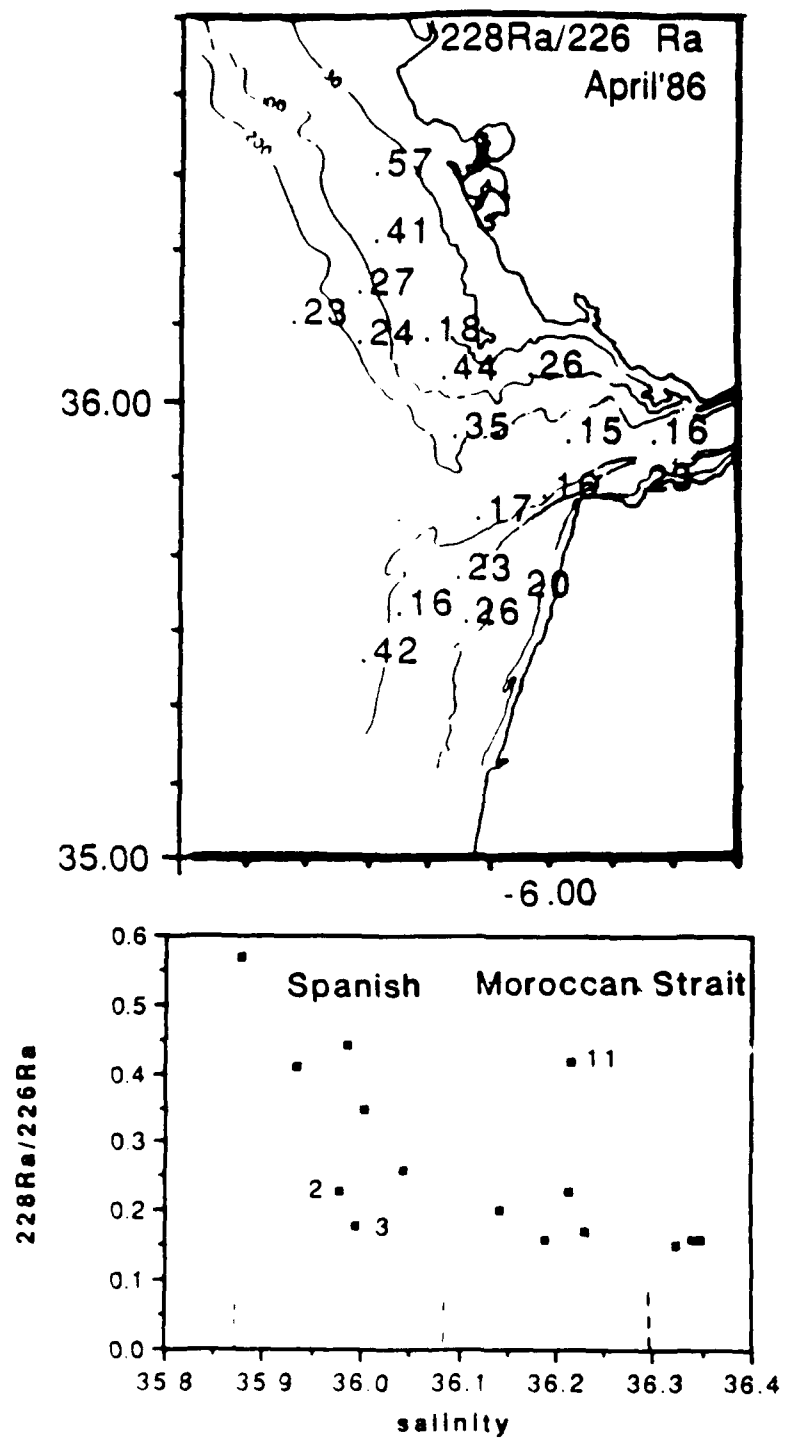


Fig. 3.7a 228Ra/226Ra activity ratio (dpm/dpm) in surface waters  
 b 228Ra/226Ra vs. salinity in ‰.

of the entrance to the Strait of Gibraltar (Table 3.5 and Fig. 3.7a) is comparable to that found previously in the South Atlantic Bight (Moore, 1987) and over the shelf of the Amazon outflow (Moore et al., 1986). With the exception of sample #11 whose high activity ratio cannot be explained, the data contain three groups of samples indicated in Fig. 3.7b: Spanish shelf water with activity ratios up to .57, more saline Moroccan shelf water with ratios not exceeding .26, and surface Atlantic water within the Strait (.16). Higher ratios in Spanish shelf water could be due to either to input from the Guadalquivir or the broader portion of the shelf shallower than 30m relative to Morocco. Even though these possibilities cannot be distinguished, the Ra data are compatible with trace metal distributions.

Current meter moorings of Grundlingh (1981) show that surface currents over the shelf follow the coastline of the Gulf of Cadiz in a general southern direction. The implication is that a metal source specific to the shallow area off Cadiz may be superimposed on enrichments originating upstream along the Iberic coast. Profiles collected in shallow waters west of the Strait, however, do not show metal gradients indicative of a strong pore water source. At station 3 (25 m deep) uniform profiles for all tracers indicate a well mixed water column. Evidence of either a shallow (less saline) or a bottom (pore waters) metal source is obscured at this site. At station 1 which is slightly deeper (45 m) and closer to the Guadalquivir estuary, Cu and Zn concentrations are significantly higher in the upper water column rather than towards the sediment. As indicated earlier, station 6 (115 m deep)

shows highest metal concentrations only within a 15 m thick surface layer. Such concentration gradients indicate that sediments underlying the deepest sample at stations 1 and 6 (45 and 115 m) cannot be the dominant source of Cu, Cd and Zn to shelf waters off Cadiz. Perhaps high shelf water Cu, Cd, and Zn concentrations are sustained by pore water fluxes from sediments shallower than 45 m depth. If this interpretation is correct, then enrichments extending beyond the shallowest portion of the shelf are due to lateral advection. It is worth noting that nutrient concentrations increase with depth at station 1. The divergent distributions of trace metals and nutrients may again be due to greater reactivity of nutrients in surface water.

Box model for shelf metal enrichments

High water column metal concentrations in Spanish coastal water provide circumstantial evidence for a strong "source" over the shelf. The previous discussion has shown that neither a riverine nor an anthropogenic origin for these enrichments is likely. A diagenetic sediment source, on the other hand, can not be excluded but would have to be considerably stronger than elsewhere in the ocean based on reported water column concentrations. To reconcile these observations, we propose a different mechanism, analogous to the "nutrient trap" observed in estuaries (Redfield et al. 1963), which could account for observed shelf enrichments without requiring an external metal source other than open-ocean subsurface water laterally advected towards the shore.

There are two prerequisites for this mechanism to hold, one physical and the other geochemical: (1) an estuarine circulation pattern across the shelf and, (2) metal removal by phytoplankton in coastal water followed by regeneration. The role of these processes is indicated in Fig. 3.8 for a section perpendicular to the coastline. Briefly, subsurface Atlantic water containing Cu, Cd and Zn is advected onto the shelf (water transport  $Q_d$ ). Due to plankton production in shelf water stimulated by upwelling, trace metals are stripped from the dissolved phase onto biogenic particles. These metal "trapping" particles remain in the shelf box (eg. by sinking to shelf sediments) while shelf water (now metal depleted) is advected offshore at the surface ( $Q_s$ ). Finally, trapped trace metals are released by

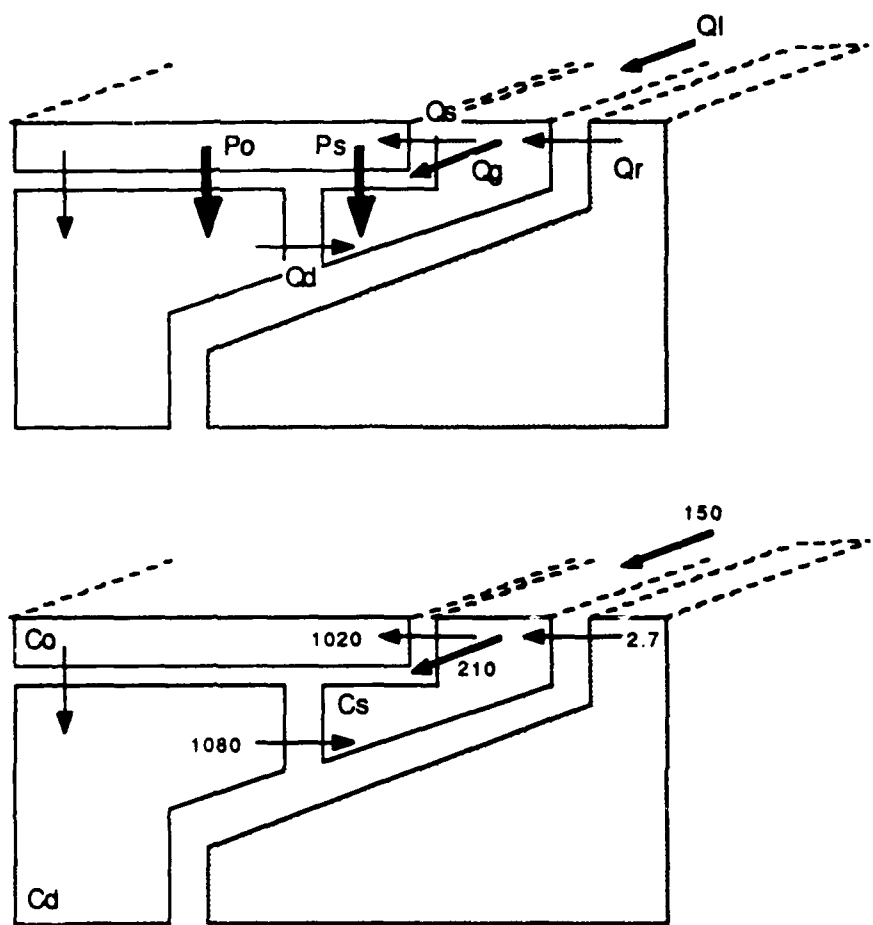


Fig. 3.8 Metal-trap Box model

Advective water fluxes indicated as thin arrows

Thick arrows represent particulate metal from box of origin  
and redissolution in destination box.

Water transport in  $10^3 \text{ m}^3/\text{s}$  for 1000 km long shelf box.

plankton decomposition which maintains elevated shelf water concentrations.

The following section discusses details of the box model. Salinity of 36.0 ‰ ( $S_s$ ) is chosen for the shelf box based on the CTD survey of the Gulf of Cadiz in April'86 by Bray (1986). The shelf box is freshened relative to the offshore mixed layer (36.2 ‰) by river input and upwelling of NACW. The mean salinity of 36.1 ‰ ( $S_d$ ) for the top 300 m of the water column is chosen for the offshore subsurface box. Also indicated in Fig. 3.8 are river discharge to the shelf box ( $Q_r$ ), a longshore current flowing south along the Iberian peninsula ( $Q_l$ ) and entrainment of shelf water with the Atlantic inflow through the Strait of Gibraltar ( $Q_g$ ). For mass balance in the shelf box, these water fluxes must satisfy:

$$(1) \quad Q_l + Q_d + Q_r = Q_s + Q_g$$

Three terms of equation (1) can be estimated from the hydrography of the region. Peak discharge (March) by the four main rivers on the Atlantic coast of the Iberian peninsula (Guadalquivir, Guadiana, Tejo and Douro) sums up to  $2.7 \cdot 10^3$  m<sup>3</sup>/s (UNESCO, 1969). The distance separating the Guadalquivir from the Douro is approximately 900 km of coastline. A longshore current of 15 cm/s was determined off the south coast of Portugal by Grundlingh (1981) and corresponds to a transport rate of  $150 \cdot 10^3$  m<sup>3</sup>/s for a shelf box 20 km wide and 50 m deep. Finally, the Atlantic inflow through the Strait of Gibraltar ( $700 \cdot 10^3$  m<sup>3</sup>/s, from Sarmiento and Toggweiler (1988) based on data of Bryden and Pillsbury

(1988)) is composed of 30% shelf water of salinity 36.0 ‰. Therefore  $Q_g$  equals  $210 \cdot 10^3 \text{ m}^3/\text{s}$ . The salt balance for the shelf box is the second constraint that allows us to determine  $Q_d$  and  $Q_s$ :

$$(2) S_s \cdot Q_l + S_d \cdot Q_d + 0. Q_r = (Q_s + Q_g) \cdot S_s$$

Replacing the sink term  $Q_s + Q_g$  by its equivalent given in equation (1) yields:

$$(3) Q_d = (Q_r \cdot S_s) / (S_d - S_s)$$

The resulting upwelling flux  $Q_d$  is  $1080 \cdot 10^3 \text{ m}^3/\text{s}$  for a shelf box length of 1000 km. River discharge is assumed to be proportional to coast length. Most of the upwelling flux returns offshore at the surface since equation (1) dictates:

$$Q_s = 150 + 1080 + 3 - 210 = 1020 \text{ units of } 10^3 \text{ m}^3/\text{s}.$$

This flux could be wind-driven since Ekman transport and coastal boundary result in an upwelling rate of 360 to  $1100 \cdot 10^3 \text{ m}^3/\text{s}$  from:

$$U = \tau \cdot L / \rho \cdot f$$

where  $\rho$  is the density of sea water ( $\sim 1 \text{ g/cm}^3$ ),  $L$  the length of coastline ( $10^8 \text{ cm}$ ),  $f$  the Coriolis parameter ( $9.3 \cdot 10^{-5} \text{ /s}$  at  $40^\circ$  latitude) and  $\tau$  the wind stress which varies between 0.3 (winter) and 1 dyne/cm<sup>2</sup> (summer) from the North along the Portuguese coast (May, 1986).

In order to quantify the metal-trap mechanism, mass-balances can be expressed for any trace element following the example of equation (2) for advective fluxes and by adding metal particulate fluxes:

$$(3) \quad C_s \cdot Q_1 + C_d \cdot Q_d + C_r \cdot Q_r + F_s = (Q_s + Q_g) \cdot C_s$$

Following the description in Fig. 3.8, the particulate flux which strips offshore surface water of dissolved metals can be divided in two components: (1)  $F_o$  which is regenerated into the deep offshore box and (2)  $F_s$  which is decomposed into the shelf box. Following the approach of Broecker and Peng (1982), mass balance for the offshore surface box is expressed as:

$$(4) \quad Q_s \cdot (C_s - C_o) - F_o = 0$$

If the trapping efficiency  $f$  is defined as the proportion of the total particulate flux which is recycled into the shelf box,  $f = F_s / (F_s + F_o)$ , then substitution in equation (4) expresses  $F_s$  in terms of advective metal fluxes:

$$(5) \quad F_s = f \cdot Q_s \cdot (C_s - C_o)$$

Replacing  $F_s$  with this expression in the mass balance equation for the shelf box (equation 3) yields an expression for the shelf box metal concentration as a function of the trapping efficiency and water transport fluxes:

$$(6) \quad C_s = (Q_s(1-f) + Q_g)^{-1} \cdot (C_o \cdot (Q_1 - f \cdot Q_s) + C_d \cdot Q_d + C_r \cdot Q_r)$$

Rearranging equation (6) yields the expression for the trapping efficiency which can be applied to Cu, Cd, and Zn:

$$(7) f = ( Q_1 \cdot (C_s - C_o) + Q_d \cdot (C_s - C_d) + Q_r \cdot (C_s - C_r) ) / ( Q_s \cdot (C_s - C_o) )$$

Taking first the example of Cd, box concentrations are determined based on surveys of the Gulf of Cadiz in June '82 and April'86. Details on end-member definitions follow in the final section of this chapter. As in the case of salinity, the deep offshore box concentration is an average of the top 300 m of the water column. River concentrations are from Table 6.2 which is discussed later. Resulting box model concentrations are:  $C_s = 190$  pM,  $C_o = 30$  pM,  $C_d = 75$  pM and  $C_r = 1200$  pM taking into account desorption to obtain the effective river concentration. The relative importance of the different terms is shown by the following expression which follows the order of equation (6):

$$C_s = ( 1020 \cdot (1-f) + 210 )^{-1} \cdot ( 30 \cdot (150 - f \cdot 1020) + 75 \cdot 1080 + 1200 \cdot 3 )$$

Transport rates Q are in units of  $10^3$  m<sup>3</sup>/s. For trapping efficiencies of 100 and 50 %, for instance, the shelf box Cd concentration could range between 280 and 100 pM, respectively. In this case, the trapping efficiency of Cd is:

$$f = (2.4 + 12.4 - 0.3) / (16.3) = 89 \%$$

Each term in this expression is in units of  $10^4$  pM.m<sup>3</sup>/s. The implication is that a considerable metal sink through the Strait of Gibraltar and elevated concentrations in shelf water can be sustained for a 1000 km long shelf box if the trapping efficiency is 89 %. Since

$Q_d$  and  $Q_e$  are not very different and the effects of river input or longshore transport are relatively small (with respect to the metal balance, clearly not the salt balance), the dominant term in equation (7) for the trapping efficiency is the ratio  $(C_s - C_d)/(C_s - C_o)$ . In other words, the greater the difference between deep water and shelf water metal concentrations, or the smaller the difference between surface water and shelf water, the greater the trapping efficiency has to be. A minimum shelf box length of 630 km required to sustain the flow pattern in Fig. 3.8 can also be recalculated from equations (3) and (6). This case corresponds to a 100 % Cd trapping efficiency, a smaller river input and, consequently, a lower upwelling rate.

In the case of Zn ( $C_s = 21$  nM,  $C_o = 0.5$ ,  $C_d = 1.5$ ,  $C_r = 33$ ) and Cu ( $C_s = 6$  nM,  $C_o = 1.3$ ,  $C_d = 1.3$ ,  $C_r = 24$ ), the calculated trapping efficiencies are greater than one (115 and 119 %) respectively, indicating this configuration of the box model cannot sustain the metal sink through the Strait of Gibraltar. Equation (6) can be rearranged to determine the fraction of the flux through the Strait which could be supported given a 100 % trapping efficiency and a 1000 km shelf box length. In effect, this modification of  $Q_g$  involves redirecting a portion of this flux to the offshore surface box where metals can be taken up and recycled to the shelf box. As it turns out, only 27 and 8 % of the actual Zn and Cu fluxes through the Strait, respectively, can be supported by this configuration. Alternatively, the difference could be accounted for if the length of the shelf box were increased to 3,700 and 14,500 km for Zn and Cu, respectively, assuming 100 % trapping efficiency. Keeping in

mind the extreme simplification of this model, it appears that while coastal Cu enrichments could not be sustained against metal output through the Strait of Gibraltar, a metal-trap along the Iberian coast may play a significant role in the case of Cd and Zn.

In the following section, three tracers (salinity, Cd and phosphorous) are shown to support the existence of the circulation pattern required for the "metal-trap" in the Gulf of Cadiz using their conservative properties. Throughout the upper 400 m of the water column, salinity, Cd and phosphorous are linearly related to each other (Fig 3.5a, b). As indicated in this figure, the relationship based on two profiles collected in June'82 (Boyle et al., 1985) also holds for stations 5, 6, and 11 in April'86 as long as samples are unaffected by shelf processes. While these tracers follow a common relation, the depth of occurrence of a given salinity, Cd and P composition rises significantly from the center of the Gulf of Cadiz in the direction of the shelf. At offshore stations 1 and 3 (June'82), for instance, water of composition salinity equal to 35.95 ‰, PO<sub>4</sub>-0.5 μM and Cd=80 pM is found at approximately 200 m depth. At the western entrance to the Strait of Gibraltar (Sta. 5), water of similar composition is found at 160 m depth in April'86. Near the shelf edge, however, the same signature occurs at depths as shallow as 80 m at Sta. 6 (off Cape Trafalgar) and 100 m at station 11 (Moroccan coast). Since agreement between such different tracers would have been very fortuitous were they not behaving conservatively, this is strongly suggestive of subsurface advection and upwelling from the center of Gulf towards the shelf. Finally, there is also evidence in

surface water of the circulation pattern described in Fig. 3.8: offshore flow of coastal water is indicated by the metal-enriched plume which leaves the shelf off Cadiz towards the center of the Gulf. Summarizing, in addition to satisfying mass balance constraints in the case of Cd and (marginally) Zn, tracer distributions support two features of the metal-trap: upwelling and offshore advection at the surface.

An additional test of metal-trap is given by the plankton flux required to strip upwelling water from its metal content. Given the average composition of plankton determined by Collier and Edmond (1985),  $0.4 \cdot 10^{-6}$  mole Cd/ gC,  $0.4 \cdot 10^{-6}$  mole Cu/ gC and  $10^{-6}$  mole Zn/ gC, and considering the respective  $C_d$  concentrations for these elements, carbon fluxes ranging from 0.2 (Cd) to  $3.5 \cdot 10^6$  gC/s (Cu) would be required for 1000 km long shelf box. These values are equivalent to gross production rates ranging between 0.3 and  $5.5 \cdot 10^3$  gC/m<sup>2</sup>.year. For comparison, production rates in the Peru upwelling region are on the order of  $2 \cdot 10^3$  gC/m<sup>2</sup>.year. In the case of all three metals, therefore, primary production required to strip upwelling subsurface water of dissolved metals is reasonable for a high productivity region. If a trapping efficiency is close to 100%, then the required plankton flux must be multiplied by the ratio  $C_s/C_d$  which is 2.5 for Cd. The resulting primary productivity flux of  $0.8 \cdot 10^3$  gC/m<sup>2</sup>.year is still reasonable for this element, in contrast to Cu and Zn where the high  $C_s/C_d$  requires too high primary productivity rates for 100 % trapping efficiency.

Three observations concerning features of the metal-trap must still be explained: (1) the absence of comparable enrichments off the Moroccan

coast, (2) the relation between variability in trace metal enrichments and seasonality in the physical forcing for the trap circulation and (3) the lack of particularly high nutrient concentrations in coastal water. Given the mechanism invoked for metal enrichments along the Iberian coast, two features specific to the Moroccan coast can account for low metal concentrations in coastal water. First, river input per unit length of the Moroccan coastline is an order of magnitude lower (UNESCO, 1969) than in Spain and Portugal. In addition, the southern direction of the coastal current supplies metal-depleted open ocean water to the Moroccan shelf and enrichments due to metal-trapping in the water column are therefore limited. Seasonal variability in Spanish metal enrichments is more difficult to explain. Indeed, the two physical forcing mechanisms of the trap circulation are opposite in phase: river discharge decreases by an order of magnitude along the Iberian coast between March and August, but wind stress along the Portuguese coast is much stronger during the summer months. The decrease in water column enrichments observed between April and October'86 can, therefore, not be explained at present.

Finally, a tentative explanation for the lack of nutrient enrichments comparable to metals concentrations is presented on the basis of the salinity-Cd-PO<sub>4</sub> relationship at Sta. 6 (April'86). As indicated in Fig. 3.5a, b, while the Cd and salinity composition at 45 m depth for station 5 conforms to the relationship for the upper 400 m of the water column, phosphate is depleted by approximately 0.2  $\mu\text{M}$  relative to the predicted nutrient concentration. Greater reactivity of phosphate relative to Cd

within the photic zone (indicated previously for offshore advection of shelf water) is also confirmed by the breakdown of the salinity-phosphate relation within 50 m of the surface (Fig. 3.5a). One could therefore speculate that the absence of unusual nutrient enrichments off Cadiz is due to uptake by phytoplankton before subsurface water reaches the shallow portion of the shelf where recycling takes place. Within the framework of the model, the implication is that nutrient uptake reduces the effective deep water box concentration before the shelf region is reached and limits the effect of particulate recycling.

#### Composition of water masses entering the Strait of Gibraltar

Surface samples from the Alboran Sea have been analyzed for Cu, Cd and Zn for June'82, April'86 and October'86 (Boyle et al., 1985, Sherrell and Boyle, 1988, and van Geen and Chapter 5). In order to determine variability in the Atlantic inflow composition to this region, contributors are reduced to three end-members (1) surface Atlantic water, (2) NACW and (3) Spanish shelf water, following the approach of van Geen et al.(1988). End-members are redefined here based on the more extensive data set presented in this paper. Sample coverage in April'86 is more complete than in October'86 when a smaller number of surface samples is restricted to the western approaches to Strait of Gibraltar. For June'82, only two profiles are available west of the Strait of Gibraltar.

The composition of surface Atlantic water in the Gulf of Cadiz is estimated first. Salinity in Atlantic surface water entering the Strait is approximately 0.2 ‰ higher in October (eg. samples 106, 107: 36.5 ‰) than in April (samples 253, 254: 36.3 ‰). For June 1982, an end-member value of 36.5 ‰ is chosen based on surface salinities at stations 1 and 3. Surface concentrations of Cu, Ni, Cd and Zn in metal-depleted offshore water do not differ significantly from one season to the other: 1.0 nM, 2.3 nM, 30 pM and 0.8 nM, respectively. For the definition of NACW, salinity, Cu, Ni, Cd and Zn concentrations are based on June'82 profiles 1 and 3. The resulting composition for both surface Atlantic water and NACW is given in Table 3.6. Estimates for the combination of natural variability and analytical uncertainty are also tabulated.

Defining seasonal variability for the final end-member, Spanish shelf water, is critical since it dominates metal transport through the Strait of Gibraltar. As discussed above, the distribution and magnitude of Spanish shelf water enrichments for each season differ. Even though Cu and Cd concentrations in shelf water increase linearly as a function of Zn concentrations on both occasions, the slope of this relation is approximately 30% higher in the Fall than in the Spring. As noted earlier, absolute Zn concentrations decrease by approximately a factor of two when comparing similar locations (Fig. 3.6). Despite such variations in the magnitude of metal enrichments west of the Strait of Gibraltar, Cu and Cd concentrations for this metal enriched end-member are defined relative to a constant Zn concentration of 21 nM. This

choice is based on the highest value observed within the Strait in April'86 (Chapter 4) and avoids obtaining shelf water contributions greater than 100%. Corresponding salinity and Cu, Ni, Cd concentrations are 36.0 ‰, 6.1 nM, 190 pM, respectively in April'86 (eg. sample # 259).

It should be noted that according to the definition above, no pure Spanish shelf water was sampled in October'86 and metal concentrations must be extrapolated in order to define the end-member relative to the same Zn concentration (Table 3.6). Choosing a particular composition is in any case somewhat arbitrary given the continuum of observed enrichments. A shelf end-member of, for instance, 10.5 nM Zn could have been defined instead with corresponding salinity, Cu, Cd and Ni concentrations based on linear relationships between tracers. For a given sample in the Alboran Sea, the nominal shelf end-member contribution would then simply be doubled. For lack of data, the composition of the June'82 Spanish shelf end-member is simply linearly interpolated with respect to time, assuming changes in inter-element ratios are seasonal. The estimated uncertainty in the composition of Spanish shelf water for most tracers is doubled relative to that for surface Atlantic water and NACW.

## CONCLUSION

Cu, Cd and Zn concentrations over a 40 km long portion of the Spanish continental shelf are an order of magnitude higher than enrichments generally found in coastal water. A consequence of these exceptional enrichments is that geochemical processes involving trace metals over the Spanish shelf influence the composition of a basin as large as the Mediterranean for these elements. Seasonal variability in Spanish shelf water enrichments was demonstrated based on samples collected in April and October '86. For lack of direct evidence for the source of metal enrichments off Cadiz, a metal-trap mechanism based on estuarine circulation and metal uptake and regeneration over the Spanish shelf is proposed. While this explanation remains tentative, the model indicates that trapping should be active over the whole length of the Iberian coast in order to sustain the significant metal sink through the Strait of Gibraltar.

## ACKNOWLEDGEMENTS

Space and time were generously provided during the Gibraltar Experiment by Dr Tom Kinder and Dr Nan Bray on board USNS Lynch. We thank A. Spivack, S. Chapnick, D. Lea, W. Moore, E. Callahan, C. Measures and H. Yee who helped collecting samples and P. Rosener for assistance in analyses. A. Cantos-Figuerola brought the Oslo Commission report to our attention. Dr. Robert Beardsley offered helpfull suggestions for the box model.

Station	Latitude	Longitude	Salinity	Si	PO4	Cu	Ni	Cd	Zn
1.0	36.700	-6.500	35.418	3.22	0.45	40.7	8.0	947	159.5
2.0	36.500	-6.483	35.763	0.45	0.30	43.4	4.9	1231	150.2
3.0	36.333	-6.500	35.630	0.18	0.12	18.2	4.5	496	101.0
4.0	35.850	-6.483	35.939	0.25	0.08	6.7	3.3	277	35.2
5.0	35.617	-6.500	36.278	0.80	0.05	3.1	3.2	75	6.9
6.0	35.217	-6.483	36.341	0.93	0.05	2.5	1.7	51	1.6
7.0	35.167	-6.333	36.291	1.05	0.05	2.2	2.2	40	0.9
8.0	35.167	-6.417	36.287	1.07	0.11	1.5	1.9	50	1.5
9.0	35.167	-6.583	36.350	1.25	0.05	1.1	1.9	15	0.3
10.0	35.133	-6.700	36.392	0.84	0.04	1.4	2.4	18	0.5
11.0	35.167	-6.967	36.357	0.85	0.05	2.5	2.5	11	1.0
12.0	35.250	-7.017	36.382	0.75	0.05	1.4	2.5	34	0.5
13.0	35.500	-7.000	36.220	0.65	0.07	4.8	2.8	165	19.0
14.0	35.817	-7.017	36.284	0.84	0.07	1.8	2.6	61	2.8
15.0	36.050	-7.000	36.302	0.89	0.08	1.8	2.8	51	3.4
16.0	36.217	-6.983	36.321	0.89	0.08	1.7	2.3	38	1.6
17.0	36.400	-6.983	36.214	0.85	0.04	2.1	2.6	68	6.0
18.0	36.567	-6.983	36.113	0.49	0.07	3.1	2.8	107	12.2
19.0	36.683	-6.983	36.164	0.87	0.04	2.4	2.8	86	8.9
20.0	36.750	-6.983	36.152	1.04	0.04	1.9	2.7	96	6.6
21.0	36.767	-6.983	36.087	0.95	0.05	2.3	2.9	89	7.4
22.0	36.850	-6.983	35.962	0.80	0.08	3.0	3.0	102	9.3
23.0	36.933	-6.983	35.862	1.25	0.15	3.2	3.1		10.4
24.0	36.983	-6.983	35.903	3.07	0.40	3.6	3.3	124	6.3
25.0	36.950	-7.167	35.870	1.07	0.12	4.3	3.2	162	12.2
26.0	36.083	-7.333	36.039	0.93	0.08	2.6	2.5	86	7.7
27.0	36.917	-7.483	36.168	1.11	0.06	1.8	2.6	47	3.7
28.0	36.800	-7.500	36.248	0.85	0.09	1.1	2.6	36	1.9
29.0	36.683	-7.500	36.254	0.91	0.06	1.2	2.1	49	3.8
30.0	36.517	-7.500	36.305	0.93	0.05	1.1	2.9	31	0.7
31.0	36.367	-7.500	36.254	0.93	0.07	1.0	2.5	33	0.5
32.0	36.183	-7.500	36.297	1.02	0.07	1.4	2.4	31	1.2
33.0	35.900	-7.517	36.222	0.58	0.06	4.5	2.5	141	18.9
34.0	35.717	-7.517	36.248	0.71	0.07	4.8	3.1	139	18.1
35.0	35.567	-7.517	36.261	0.67	0.05	2.5	2.5	84	10.2
36.0	35.417	-7.517	36.248	0.58	0.05	3.4	3.0	111	13.3

Table 3.1a. part 1. Surface samples, April'86  
 Surface sample #, latitude and longitude in decimal units,  
 salinity in ‰, Si and P in µM, Cu, Ni and Zn in nM,  
 Cd in pM

Station	Latitude	Longitude	Salinity	Si	Po4	Cu	Ni	Cd	Zn
37.0	35.267	-7.467	36.371	0.80	0.07	1.4	2.2	32	2.6
38.0	35.167	-7.733	36.398	0.85	0.05	1.0	2.3	19	0.8
39.0	35.167	-7.967	36.378	0.96	0.07	0.8	2.3	17	0.1
40.0	35.317	-8.000	36.420	0.87	0.04	0.8	1.9	9	0.1
41.0	35.483	-8.000	36.418	0.82	0.05	1.4		16	0.6
42.0	35.650	-8.017	36.408	0.87	0.13	0.9	2.0	17	0.8
43.0	35.767	-8.000	36.387	0.96	0.05	1.0	2.4	14	0.3
44.0	36.000	-8.000	36.391	0.84	0.07	0.7	1.9	13	0.2
46.0	36.033	-8.000	36.361	0.87	0.08	0.8	1.9	13	0.2
47.0	36.550	-7.983	36.276	1.09	0.25	1.0	2.1	24	0.7
48.0	36.617	-7.967	36.222	1.15	0.17	1.4	2.2	30	0.6
49.0	36.067	-8.000	36.057	1.62	0.26	1.3	2.0	51	1.5
50.0	36.000	-7.700	36.399	0.76	0.09	0.7	1.8	13	0.1
52.0	36.000	-7.367	36.399	1.20	0.09	0.9	2.2	13	0.2
53.0	35.983	-7.017	36.359	1.13	0.10	1.8	2.4	43	4.0
54.0	36.000	-7.033	36.317	1.15	0.09	1.2	2.4	33	1.7
56.0	36.000	-6.567	36.054	0.51	0.06	1.5	2.4	46	3.3
57.0	36.000	-6.350	35.992	0.51	0.09	2.5	2.4	93	7.9
58.0	36.000	-6.350	36.005	0.67	0.10	2.6	2.2	92	8.6
70.0	36.167	-6.400	36.043	0.40	0.40	5.1	2.5	145	17.6
71.0	36.333	-6.467	35.954	0.49	0.49	3.3	2.9	143	10.4
72.0	36.417	-6.500	35.937	0.64	0.64	3.0	2.4	98	10.2
73.0	36.567	-6.400	35.887	0.98	0.98	14.5	3.4	407	72.4
253.0	35.867	-5.883	36.298	0.00	0.00	1.1	2.6	34	1.6
254.0	35.883	-5.883	36.214	0.00	0.06	1.0	2.6	41	1.1
255.0	35.933	-5.867	36.234	0.00	0.20	0.9	2.8	38	0.7
256.0	35.950	-5.833	36.153	0.83	0.24	1.4	2.7	45	1.7
257.0	36.000	-5.850	36.074	0.83	0.07	2.0	2.6	80	4.9
258.0	36.033	-5.833	36.029	1.32	0.20	4.3	3.0	135	14.1
259.0	36.067	-5.833	36.086	1.46	0.15	6.1	3.1	211	21.3
260.0	35.717	-5.983	36.119	0.60	0.11	1.7	2.5	60	2.8
261.0	35.733	-6.017	36.141	0.63	0.07	1.6	2.1	35	1.2
262.0	35.750	-6.050	36.278	0.99	0.06	1.0	2.4	36	0.8
263.0	35.817	-6.067	36.262	0.89	0.04	0.8		28	0.9
264.0	35.833	-6.067	36.238	0.70	0.03	0.8	2.6	33	1.1
265.0	35.850	-6.083	36.219	0.73	0.03	1.0	2.7	40	1.1

Table 3.1a, part 2. Surface samples, April'86  
 Surface sample #, latitude and longitude in decimal units,  
 salinity in ‰., Si and P in µM, Cu, Ni and Zn in nM,  
 Cd in pM

Station	Latitude	Longitude	Salinity	Si	PO4	Cu	Ni	Cd	Zn
266.0	35.900	-6.100	36.067	0.60	0.04	2.4	2.7	101	4.1
267.0	35.950	-6.100	36.038	0.79	0.07	2.6	2.9	99	8.1
268.0	36.000	-6.067	36.038	1.39	0.19	4.6	2.8	167	18.8
269.0	36.033	-6.050	36.007	1.46	0.15	5.7	3.2	186	20.8
271.0	36.117	-5.983	36.123	1.06	0.11	5.8		179	19.4
272.0	36.100	-6.050	36.156	1.06	0.11	5.0		173	19.4
273.0	36.100	-6.100	36.085	1.69	0.34	6.2		191	20.2
274.0	36.083	-6.200	35.976	2.42	0.31	11.4	4.5	266	30.2
275.0	36.083	-6.233	35.969	2.28	0.26	9.9	3.8	219	30.4
276.0	36.083	-6.267	35.938	1.59	0.27	11.9	4.0	240	40.5
277.0	36.083	-6.283	35.946	1.82	0.23	10.9	3.9	243	29.7
278.0	36.050	-6.283	35.970	1.72	0.21	10.5	3.9	240	31.3
279.0	36.017	-6.283	35.983	1.23	0.17	8.2	3.4	203	24.6
280.0	35.967	-6.317	35.977	0.46	0.08	7.0	3.1	167	20.3
281.0	35.933	-6.333	35.999	0.63	0.08	1.7	2.8	66	5.3
282.0	35.917	-6.283	36.114	0.73	0.09	1.3	2.6	52	1.9
283.0	35.917	-6.233	36.052	0.66	0.10	1.5	2.6	64	2.7
284.0	35.900	-6.200	36.042	0.70	0.07	1.5	2.7	75	3.8
285.0	35.933	-6.150	36.025	0.66	0.09	1.9	2.9	105	7.8
286.0	35.967	-6.167	36.009	0.89	0.13	5.6	3.2	129	14.2
287.0	36.000	-6.167	35.996	1.29	0.17	9.1	3.7	232	28.0
288.0	36.067	-6.133	36.010	1.75	0.24	8.2	3.6	200	28.5
0.1	36.530	-6.400	35.876	1.13	0.31	19.7	4.0	340	51.0
1.0	36.400	-6.420	35.935	0.33	0.17	15.6	3.6	255	35.3
2.0	36.390	-6.400	35.979	0.04	0.05		2.4	73	7.8
3.0	36.157	-6.316	35.995	1.63	0.26	9.9	3.2	198	24.0
5.0	35.930	-5.882	36.323	0.66	0.10	1.3	2.3	33	1.9
6.0	35.960	-6.210	36.003	1.05	0.18	6.2	2.9	160	18.5
7.0	35.790	-6.130	36.231	0.62	0.05	1.5	2.1	32	1.6
7.1	35.900	-6.200	36.141	0.25	0.06	1.4	2.5	44	1.6
8.0	35.610	-6.010	36.142	0.46	0.06	1.9	2.4	62	3.7
8.1	35.790	-6.130	36.340	0.81	0.05	1.6	2.4	31	2.1
9.0	35.620	-6.060	36.215	0.33	0.08	1.9	2.4	57	3.9
10.0	35.590	-6.100	36.188	0.41	0.04	1.7	2.4	65	4.7
11.0	35.480	-6.450	36.217	0.28	0.08	1.6	2.3	61	3.3
11.1	35.490	-6.360	36.165	0.74	0.10	1.4	2.5	52	3.5
13.0	35.810	-6.000	36.339	0.50	0.04	1.4	2.2	41	2.9
14.2	36.160	-6.380	35.982	1.37	0.24	8.9	3.4	235	30.6
15.0	35.942	-5.673	36.349	0.82	0.10	1.4	2.4	28	1.7

Table 3.1a, part 3. Surface samples, April '86  
 Surface sample #, latitude and longitude in decimal units,  
 salinity in ‰, Si and P in µM, Cu, Ni and Zn in nM,  
 Cd in pM

Station	Latitude	Longitude	Salinity	Si	Po4	Cu	Ni	Cd	Zn
1	36.165	-6.318	36.207	0.40	0.05	2.5	2.3	72	4.4
2	36.085	-6.323	36.197	0.33	0.03	1.1	2.6	39	1.5
3	35.970	-6.328	36.228	0.33	0.10	3.6	2.6	111	6.8
5	35.820	-6.150	36.490	0.33	0.06	1.4	2.6	27	0.0
6	35.822	-6.112	36.409	0.33	0.03	1.6	3.0	42	
7	35.823	-6.068	36.436	0.46	0.05	1.5	2.3	31	1.3
8	35.823	-6.028	36.490	0.46	0.04	1.4	2.3	37	1.8
10	35.860	-5.985	36.481	0.40	0.08	1.8		42	2.8
11	35.860	-6.032	36.461	0.43	0.06	1.9		42	2.3
12	35.860	-6.077	36.470	0.43	0.05	1.4	2.1	35	1.8
13	35.860	-6.160	36.378	0.36	0.05	1.9	3.0	55	3.0
15	35.885	-6.123	36.374	0.33	0.10	1.9	2.6	51	3.5
17	35.888	6.027	36.396	0.36	0.12	3.1	2.7	79	5.3
19	35.957	-6.022	36.387	0.46	0.09	3.1	2.8	84	5.9
21	35.957	-6.128	36.365	0.43	0.09	3.0	2.9	87	7.2
22	35.955	-6.175	36.376	0.46	0.06	2.0	2.0	67	3.8
23	36.010	-6.180	36.280	0.53	0.14	5.1	2.7	145	11.5
24	36.010	-6.138	36.260	0.40	0.19	5.0	2.3	159	11.4
25	36.012	-6.075	36.304	0.30	0.12	4.2	2.8	110	9.7
26	36.047	-6.080	36.308	0.17	0.15	4.4	2.6	147	9.4
27	36.045	-6.138	36.300	0.20	0.14	4.8	3.0	145	10.5
28	36.045	-6.180	36.301	0.07	0.14	4.7	2.5	157	10.7
30	36.075	-6.245	36.291	0.13	0.15	5.6	2.3	146	11.4
31	36.075	-6.188	36.298		0.14	4.8	2.3	152	11.7
32	36.075	-6.143	36.311		0.15	4.6	2.7	125	9.2
81	36.093	-5.993	36.481		0.02	1.8	2.8	56	3.2
88	36.032	-5.433	36.288		0.22	4.8	2.8	137	10.8
89	36.015	-5.482	36.290		0.13	4.3	2.8	114	8.0
90	35.997	-5.530	36.276		0.14	5.0	3.0	136	10.2
103	36.067	-5.862	36.148		0.12	4.7	2.8	116	9.3
104	36.047	-5.822	35.865		0.11	5.9	2.7	109	8.0
105	36.007	-5.813	36.002		0.07	2.6	2.5	65	4.2
106	35.925	-5.792	36.378		0.02	1.7	2.4	36	1.4
107	35.887	-5.815	36.406		0.02	1.4	2.2	31	1.4

Table 3.1b Surface samples, October'86

Surface sample #, latitude and longitude in decimal units,  
 salinity in '/.., Si and P in  $\mu\text{M}$ , Cu, Ni and Zn in  $\text{nM}$ ,  
 Cd in  $\text{pM}$

	Depth m	Salinity	Si	PO4	Cu	Ni	Cd	Zn
Station 1 36.400 N 6.420 W	0	35.935	0.33	0.17	15.6	3.6	255	35.3
	20	35.931	0.18	0.18	15.0	4.3	328	31.5
	30	35.932	0.21	0.16	11.7	3.4	284	31.0
	40	35.945	2.63	0.46	11.1	4.0	253	26.2
	45	35.963	7.12	0.59	7.0	7.5	317	17.7
Station 2 36.390 N 6.400 W	0	35.979	0.04	0.05		2.4	73	7.8
	10	36.020	0.07	0.09	1.4	2.4	54	2.5
	70	36.024	0.18	0.08	2.1	2.4	54	3.5
	110	35.941	2.34	0.39	1.2	2.5	54	2.0
	155				2.2	2.6	70	1.5
Station 3 36.160 N 6.320 W	0	35.995	1.63	0.26	9.9	3.2	198	24.0
	5	35.983	1.29	0.31	8.5	3.3	198	25.9
	15	35.984	1.32	0.26	8.4	3.1	191	24.6
	20	35.984	1.78	0.28	8.3	3.3	205	26.7
	25	35.984	1.94	0.28	8.0	3.7	213	20.3
Station 5 35.930 N 5.880 W	0	36.323	0.66	0.10	1.3	2.3	33	1.9
	58	36.267	0.49	0.08	1.4	2.5	39	1.2
	108	36.236	1.13	0.11	1.4	2.5	37	1.2
	158	36.035	2.20	0.40	1.7	2.8	83	1.6
	200	37.613	4.33	0.33	1.8	3.9	87	5.0
Station 6 35.960 N 6.210 W	0	36.003	1.05	0.18	6.2	2.9	160	18.5
	15	36.117	0.82	0.13	7.0	2.9	162	19.3
	45	36.017	1.79	0.18	1.5	2.2	69	3.7
	80	35.949	4.14	0.41	2.0	2.5	78	4.0
	115	35.907	3.03	0.52	1.0	2.1	89	2.1
Station 7 35.790 N 6.130 W	0	36.231	0.62	0.05	1.5	2.1	32	1.6
	40	36.471	0.80	0.12	1.0	2.1	30	1.1
	140	36.101	1.95	0.32	0.8	2.5	47	1.2
	240	36.600	4.29	0.50	1.2	2.9	88	1.7
	340	38.072	6.09	0.38	1.1	3.4	59	2.7
Station 11 35.480 N 6.450 W	0	36.217	0.28	0.08	1.8	2.3	61	3.3
	50	36.207	1.11	0.11	1.4	2.0	58	3.4
	150	35.963	3.62	0.49	1.8	2.5	89	1.7
	200	35.920	3.94	0.55	1.3	2.5	101	1.4
Station 15 35.942 N 5.673 W	0	36.349	0.82	0.10	1.4	2.4	28	1.7
	50	36.365	0.72	0.10		2.5	40	
	75	36.174	1.75	0.28	1.2	2.4	43	
	150	38.303	5.42	0.33		5.2	97	
	200	38.372	5.37	0.39	1.8	4.8	94	6.0
	250				1.6	4.5	78	5.2
	400	38.517	9.18	0.45	1.7	4.8	87	5.0
	450	38.450	8.93	0.45		4.8	73	6.4
	500				1.8	4.3	69	5.7
	510	38.450	9.15	0.44	1.7	4.8	72	5.3

Table 3.2 Profile data, April'86  
 Sample #, station position indicated for surface sample, depth m.

Table 3.3 Trace metal concentrations for major Iberian rivers determined by GFAAS direct injection and standard additions. Cd concentrations below detection limit of  $\leq 100$  pM. Seawater contribution (%) estimated from Mg concentration determined by flame AA.

River	Location	% SW (Mg)	Cu nM	Ni nM	Zn nM
Guadalquivir	Sevilla	2	9.5	21.3	13.0
Guadalquivir #1	2/3 upstr	2	15.7	64.1	33.2
Guadalquivir #2	2/3 upstr	2	14.3	78.6	40.2
Guadiana	Merida	<1	10.1	7.0	3.1
Tejo	Trujillo	<1	.6	58.8	7.0
Tejo #1	Lisboa	<1	9.6	20.8	418
Tejo #2	Lisboa	<1	7.5	14.0	392

Table 3.4 Shelf enrichments for areas indicated

Location	Salinity	Cu nM	Ni nM	Cd pM	Zn nM	Mn nM	Reference
Cadiz	35.95	11.0	3.9	250	30.0	160	this work
Huelva	35.95	3.0	3.0	100	9		this work
Morocco	36.20	1.9	2.4	60	4.2		this work
NW Atlantic	30.00	4.0	6.0	200	2.5	20	Bruland, 1983
NE Atlantic	35.00	2.5		250		12	Kremling, 1983
Calif. Bight	33.50			150			Martin, 1976
Bering Sea	31.50	5.0				30	Heggie, 1987

Station	Latitude	Longitude	228Ra/226Ra	+/-	salinity
0.100	36 530	-6.400	0.570	0.050	35.878
1.000	36 400	-6.420	0.410	0.010	35.935
	36 280	-6.480	0.270	0.010	
2.000	36 220	-6.580	0.230	0.020	35.978
	36 180	-6.450	0.240	0.010	
3.000	36 157	-6.318	0.180	0.010	35.995
3.100	36 100	-6.270	0.440	0.030	35.987
4.000	36 080	-6 000	0.280	0.010	36.043
5.000	35 930	-5.882	0.150	0.010	36.323
6.000	35 960	-6.210	0.350	0.010	36.003
7.000	35 790	-6.130	0.170	0.020	36.231
8.000	35 810	-6.010	0.200	0.010	36.142
9.000	35 820	-6.060	0.230	0.020	36.215
	35 580	-6.100	0.260	0.020	
10.000	35 590	-6.100	0.160	0.020	36.188
11.000	35 480	-6.450	0.420	0.050	36.217
13.000	35 810	-6.000	0.160	0.010	36.339
14.000	35 950	-5 590	0.160	0.010	35.982
15.000	35 942	-5 673	0.160	0.010	36.349
	35 850	-5 720	0.230	0.020	

Table 3.5 Nearest trace metal station, location,  $^{228}\text{Ra}/^{226}\text{Ra}$  activity ratio, uncertainty and salinity in ‰, when available.

Table 3.6 End member composition for surface Atlantic water, Spanish shelf water, NACW and Mediterranean deep water. Estimate of combination of natural variability and analytical uncertainty indicated in parentheses.

	Surface Atlantic	NACW	Mediterr.
Sal. ‰	36.3 (.1)	35.7 (.05)	38.45 (.02)
Cu nM	1.0 (.3)	1.3 (.3)	1.9 (.3)
Ni nM	2.2 (.3)	3.3 (.3)	4.6 (.3)
Cd pM	30 (10)	150 (10)	77 (10)
Zn nM	0.8 (1.)	1.5 (.5)	4.8 (.5)
Spanish Shelf	April '86	June '82	October '86
Sal. ‰	36.0 (.2)	36.0 (.2)	36.1 (.2)
Cu nM	6.1 (.6)	6.7 (.6)	8.0 (.6)
Ni nM	3.4 (.3)	3.4 (.3)	3.4 (.3)
Cd pM	190 (20)	210 (20)	260 (20)
Zn nM	21 (1.)	21 (1.)	21 (1.)

## REFERENCES

Boyle, E.A., S.S. Huested and S.P. Jones (1981) On the distribution of Cu, Ni, and Cd in the surface waters of the North Atlantic and North Pacific Ocean. *J. Geophys. Res.* 86, 8048-8066.

Boyle, E.A., Chapnick, S.D., Bai, X.X. & Spivack, A.J. (1985) Trace metal enrichments in the Mediterranean Sea. *Earth Planet. Sci. Lett.* 74, 405-419.

Bray, N. (1986) Gibraltar Experiment CTD data report, SIO Reference series #86-21, Scripps Institution of Oceanography

Broecker, W.S. and T.H. Peng (1982) *Tracers in the Sea*, LDGO Press, Palissades, NY.

Bryden H.L. and R.D. Pillsbury (1988) Measurement of flow through the Strait of Gibraltar, Proceedings of international conference on computer methods and water resources, Computer Mechanics Publication, Southampton.

Bruland, K.W., G. A. Knauer and J.H. Martin (1978) Cadmium in northeast Pacific waters, *Limnol. Oceanogr.* 23, 119-128.

Bruland K.W. and R.P. Franks (1983) Mn, Ni, Cu, Zn, and Cd in the western North Atlantic. In: *Trace Metals in Seawater*, C. S. Wong, E. Goldberg, K. Bruland and E. Boyle, eds., pp 505-512, Plenum Press, New York, NY.

Grundlingh, M. (1981) On the observation of a solitary event in the Mediterranean outflow west of Gibraltar, *Meteor Forschungsergebnisse A/B*, 23, 15-46.

Heggie, D.T. (1983) Copper in surface waters of the Bering Sea. *Geochim. Cosmochim. Acta* 46, 1301-1306.

Heggie, D., G. Klinkhammer and D. Cullen (1987) Manganese and copper fluxes from continental margin sediments. *Geochim. Cosmochim. Acta* 51, 1059-1070.

Kinder, T.H. and H.L. Bryden (1987) The 1985-86 Gibraltar Experiment: Data collection and preliminary results. *EOS, Transactions, American Geophysical Union*, 68, 786-787, 793-795.

Kremling, K. (1983) Trace metal fronts in European shelf waters. *Nature* 303 226-227.

May, P. (1986) Heat and momentum flux calculations for the Mediterranean, NORDA Technical Report.

Martin, J.H., K.W. Bruland and W.W. Broenkow (1976) Cadmium transport in the California Current, In: Marine Pollutant Transfer, H.L. Windom and R.A. Duce, eds., Heath, Lexington MA.

Moore, W.S. (1976) Sampling  $^{228}\text{Ra}$  in the deep ocean, Deep-Sea Res. 23 647-651.

Moore, W.S., J.L. Sarmiento and R.M. Key (1986) Tracing the Amazon component of surface Atlantic water using  $^{228}\text{Ra}$ , salinity and silica. J. Geophys. Res. 91 2574-2580.

Moore, W.S. (1987) Radium 228 in the South Atlantic Bight. J. Geophys. Res. 92 5177-5190.

Ochoa, J.L. and N.A. Bray Exchange of Mediterranean and Atlantic water masses in the Gulf of Cadiz. In press, Deep Sea Res.

Oslo Commission (1986) Environmental impact assessment of dumping titanium dioxide wastes in the Gulf of Cadiz by Tioxide Espana, S.A., 12 th meeting, Madrid, June 1986.

Redfield, A.C., B.H. Ketchum and F.A. Richards (1963) The influence of organisms on the composition of seawater, In: The Sea, M.N. Hill, ed., v 2, 61-63, Wiley, NY.

Sarmiento J.L. and J.R. Toggweiler (1988) Mediterranean nutrient balance and episodes of anoxia, Global Biogeochem. Cycles 2, 427-444.

Sherrell, R.M. and E.A. Boyle (1988) Zinc, chromium, vanadium and iron in the Mediterranean Sea. Deep-Sea Res. 35 1319-1334.

Shiller, A.M., and Boyle E.A. (1985) Dissolved zinc in rivers. Nature 317 49-52.

Shiller, A.M., and E.A. Boyle (1987) Variability of dissolved trace metals in the Mississippi River. Geochim. Cosmochim. Acta 51 3273-3277.

Spivack, A. J., S. S. Huested & E. A. Boyle (1983) Copper, Nickel and Cd in surface waters of the Mediterranean, In: Trace Metals in Seawater, C. S. Wong, E. Goldberg, K. Bruland and E. Boyle, eds., pp 505-512, Plenum Press, New York, NY.

Strickland, J.D.H., and T.R. Parsons (1968) A practical handbook of seawater analysis, Fisheries Research Board of Canada.

UNESCO (1969) Discharge of selected rivers of the world, Studies and Reports in Hydrology # 5, v.1, Paris.

van Geen, A., P. Rosener and E. Boyle, 1988. Entrainment of trace metal-enriched Atlantic shelf-water in the inflow to the Mediterranean Sea. Nature 331, 423-426.

CHAPTER FOUR

VARIABILITY OF TRACE METAL FLUXES THROUGH THE STRAIT OF GIBRALTAR

## INTRODUCTION

Three water masses west of the Strait of Gibraltar show sharp contrasts in trace metal concentrations: (1) Atlantic surface water, (2) North Atlantic Central Water and (3) Spanish coastal water. The first goal of this paper is to exploit these circumstances and follow the advection of these water masses into the Strait of Gibraltar. A regression model decomposes each sample into these end-members; sensitivity of the model is discussed in detail. The second objective is to examine the distribution of Cu, Ni, Cd and Zn within the Strait with respect to the mass balance of these elements in the Mediterranean basin.

Surface samples collected in March-April and October 1986 have recently allowed us to establish that Spanish Atlantic shelf water is highly enriched in Cu, Cd and Zn relative to nutrient depleted Atlantic surface water (van Geen et al., 1988). A distinction is made between shelf waters and upwelling of North Atlantic Central Water (NACW), which is also enriched in certain metals (profiles collected during Donde Va?, Boyle et al., 1985). By comparing profile and shelf water metal-salinity relationships, surface enrichments can be attributed in part to mixing with deeper water in the case of Cd. In the case of Cu and Zn, levels of Cu and Zn in Spanish coastal water are higher by an order of magnitude than in subsurface Atlantic water of the same salinity (van Geen et al., 1988). Profiles collected in April'86 indicate that shallow advection onto the shelf region and "metal-trapping" along the Iberic peninsula is the most likely source of

these enrichments (Chapter 3). Riverine and anthropogenic inputs are not sufficient to explain Spanish shelf-water metal enrichments.

#### SAMPLING AND ANALYSIS

We present here new data for 43 surface samples distributed across the Strait of Gibraltar on April 11th, 12th and 16-18th. Surface samples were collected on USNS Lynch during the Gibraltar Experiment (Kinder and Bryden, 1987) with a contamination-free underway pumping apparatus. Salinity and nutrients were determined using standard techniques (Guildline Autosal salinometer and colorimetry, respectively) described in Strickland and Parsons (1968). Trace metal analyses on 30 ml samples followed a resin pre-concentration procedure which has been automated (Chapter 2). All sample concentrates were analyzed by graphite-furnace atomic absorption spectroscopy (Perkin-Elmer Zeeman 5000 and HGA 500). One-sigma precision for this data set is 5% or 0.2 nM for Cu and Ni whichever is larger, 6% or 6 pM for Cd and 6% or 0.3 nM for Zn. Blank corrections average 0.1 nM, 0.05 nM, <1 pM and 0.3 nM for Cu, Ni, Cd and Zn respectively.

#### THE CONSERVATIVE MIXING MODEL

Distributions of trace metals and salinity in the western approaches to the Strait of Gibraltar can be described as conservative mixing of the three end-members mentioned above, even though non-conservative processes most likely play a role in shallow Spanish coastal waters (Chapter 3). As indicated by end-member compositions in Table 4.1,

Atlantic surface water (1) is depleted in all trace metals. Only Cd enrichment in less saline NACW (2) is comparable to concentrations found in Spanish coastal water (3) which is highly enriched in Cu and Zn. Given the continuum of linear salinity-trace metal relationships over the shelf, the shelf end-member end-member is somewhat arbitrarily defined by a salinity of 36.0 ‰ and corresponding Cu, Cd, Zn concentrations. This description corresponds to water found at the north-west entrance to the Strait. End-member definitions have been revised relative to earlier work (van Geen et al., 1988) based on a more extensive data set (Chapter 3). The main differences are that metal concentrations are roughly halved for the definition of "100 %" Spanish shelf water, and that Cd concentrations are increased to 30 pM for surface Atlantic water.

Trace metal and salinity data for 43 surface stations within the Strait (Fig. 4.1) can be related to the end-members defined above. Station tracer data are listed in the appendix. Mediterranean deep water, defined on the basis of a second profile collected during Donde Va? (Boyle et al., 1985) is added to the list of end-members in order to describe the northernmost stations in the western Alboran Sea where this water mass outcrops at the surface. A fifth tracer (Ni) not as dramatically enriched as other metals in Spanish shelf waters, and only slightly enriched in NACW, is included in the definition of the four sources (Table 4.1).

Assuming conservative mixing of salinity and trace metals, each surface sample can be described as a linear combination of four distinct end

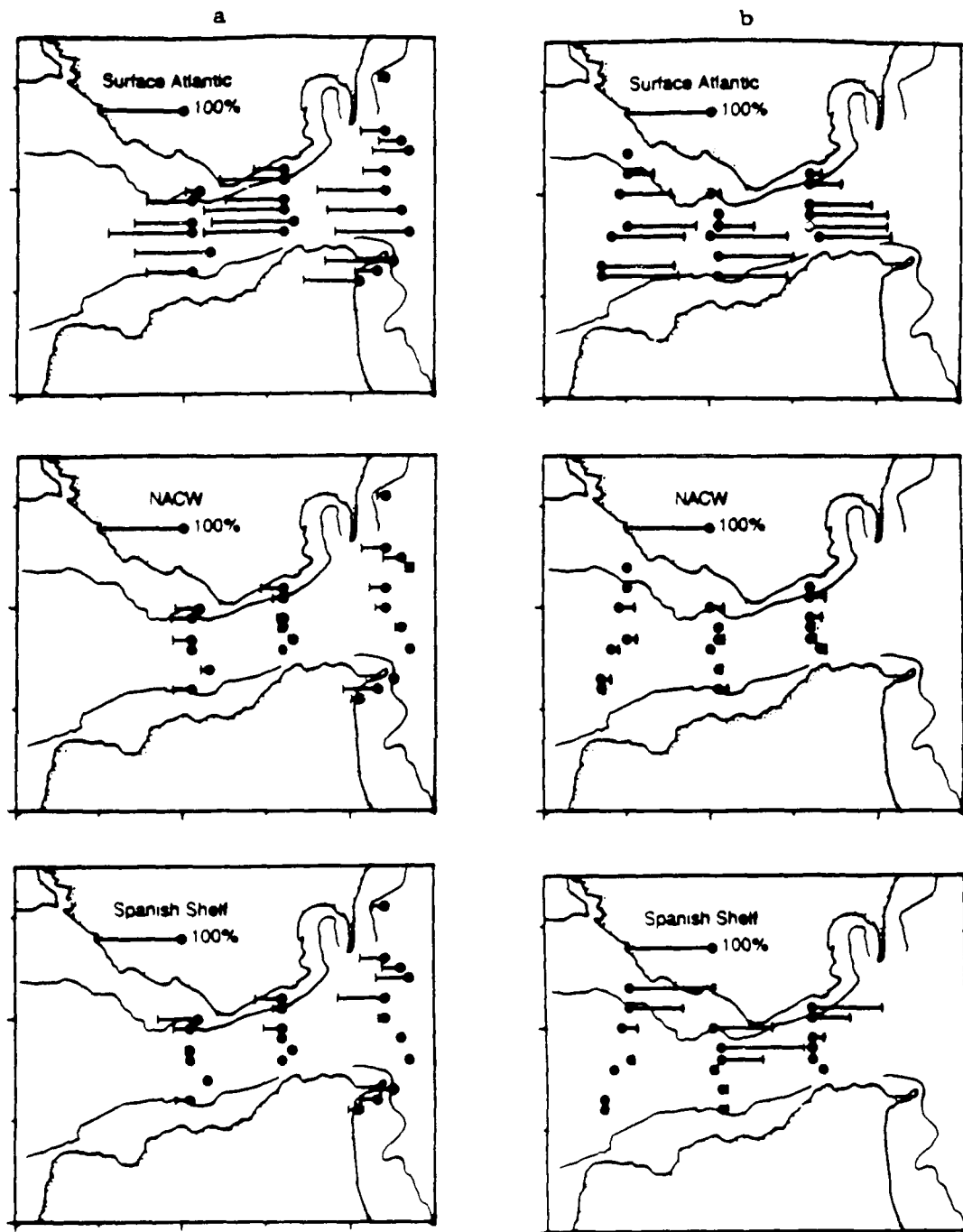


Fig. 4.1 End-member distributions on April 11th, and 16-18th. Length of bar is proportional to contribution. Filled circle indicates station location.

Table 4.1 Model matrix A

	Surface Atlantic	Spanish Shelf	NACW	Mediterranean Deep	Standard Error
Salinity	36.30	36.00	35.70	38.45	0.1 °/..
Cu	1.0	6.1	1.3	1.9	0.33 nM
Ni	2.2	3.4	3.3	4.6	0.33 nM
Cd	30	190	150	77	10 pM
Zn	0.8	21.0	1.5	4.8	1.0 nM
Closure	1	1	1	1	0.001

members. In this expression, the weight of an end-member is the fraction of the total sample contributed by each source. In matrix notation, this relationship can be expressed as:

$$(1) \quad A \cdot f = d$$

where A is the (6\*4) model matrix whose top five rows contain the tracer composition of each end-member (= Table 4.1), (6\*1) vector d contains the composition of a specific sample and f is a (4\*1) vector whose four elements are the fractions of each contributing source which we want to estimate (Mackas et al., 1987). The fractions are constrained to be positive and to sum to unity: a final line of factors equal to unity added to the model matrix and to each column data vector expresses this additional closure condition. The system is over-determined since there are 4 unknowns (the end-member fractions) and 6 linear equations (one for each tracer + the closure condition).

The solution need not match the data perfectly due to analytical errors and "real world" deviations from the model. For each tracer, a residual is defined as the difference between observed and model-predicted data. Assuming the data follow Gaussian statistics, the best fit to each set of equations corresponding to a sample is obtained by minimizing the sum of the squared residuals (i.e. the  $L_2$  norm, Menke (1984)). However, residuals must first be normalized with respect to each other by giving proper weights to each tracer equation. This is achieved by dividing all tracer values by their respective estimated standard errors which are also listed in Table 4.1. Error estimates are greater than

(salinity) or comparable to (trace metals) analytical errors and represent the degree to which the model is required to fit the data for a given tracer. If  $W$  is a diagonal matrix composed of the inverse of estimated uncertainties for each tracer, the weighted model matrix becomes  $A_w = W \cdot A$  (Table 4.2). Similarly, tracer data at each station are converted to  $d_w = W \cdot d$ . By this transformation, the variance of each tracer datum is, by definition, equal to one. The closure condition is given a high weight of 1000, i.e. an error of 0.001, and forces the model parameters to add up to 1 within 0.01% for all samples.

The dynamic range separating end-members for each tracer, expressed in  $A_w$ , is compared on the same scale in Fig. 4.2. The greater the range for a given tracer, the more useful it will be in resolving end-member contributions. Salinity dominates the estimate for the fraction of deep Mediterranean water, Zn and Cu dominate the estimate for the shelf end-member fraction, and Cd best resolves the deep Atlantic contribution after correction for Cd of shelf origin. The least-squares solution to equation (1) for each surface sample is:

$$(2) \quad f = (A_w^T \cdot A_w)^{-1} \cdot A_w^T \cdot d_w.$$

Taking the additional inequality constraints into account, an iterative solution is found using the Kuhn-Tucker theorem (Menke, 1984). By this procedure, if the unconstrained best fit requires one of the end-member fractions to become negative, the solution becomes the next best fit with that fraction set to zero. This simple program was applied to each sample on a Tektronix 4052 computer. Matrix inverses are calculated by

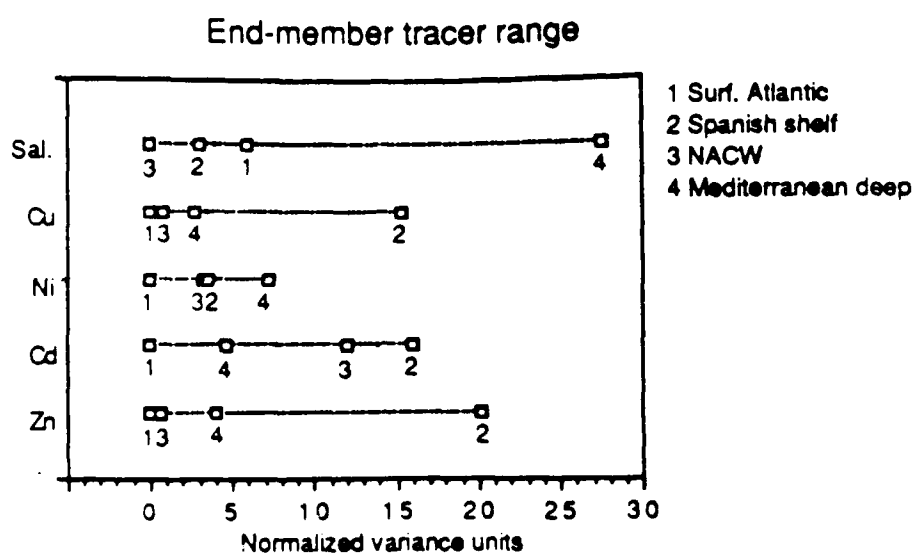


Fig. 4.2 Range of tracer composition of end-members for normalized model-matrix. Lowest concentration was subtracted for each tracer.

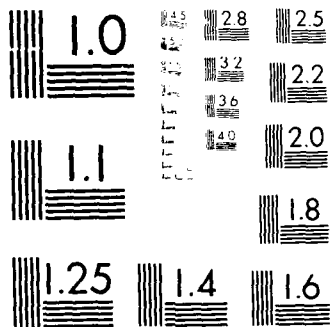
UNCLASSIFIED

MEDITERRANEAN SEA(U) MASSACHUSETTS INST OF TECH  
CAMBRIDGE A F VAN GEEN JUN 89 N00014-86-K-0323

F/G 8/3

ML

END  
FILMED  
X-7  
DTIC



MICROCOPY RESOLUTION TEST CHART  
NATIONAL BUREAU OF STANDARDS Spec. A

Table 4.2 Variance normalized model matrix  $A_w$ 

	Surface Atlantic	Spanish Shelf	NACW	Mediterranean Deep	Standard Error
Salinity	363	360	357	384.5	1
Cu	3.0	18.3	3.3	5.7	1
Ni	6.6	10.2	9.9	14.7	1
Cd	3	19	15	7.7	1
Zn	0.8	21	1.5	4.8	1
Closure	1000	1000	1000	1000	1

a supplied subroutine based on Gauss-Jordan triangularization. Before discussing in detail the distribution of the four end-members in the Strait of Gibraltar and the Alboran Sea (Fig. 4.1), the uncertainty in these solutions must be estimated.

#### HOW ROBUST ARE THE SOLUTIONS ?

Since both the model matrix A and the data d were premultiplied by the weight matrix W in the expression of the generalized inverse, the data covariance matrix becomes the identity matrix. Assuming errors in the data are uncorrelated (not necessarily true for "real world" errors ), off-diagonal elements of the data covariance matrix can be set to zero. How errors in the data are amplified as uncertainty in the model parameters can be estimated from the unit covariance matrix of the model parameters:

$$(3) \quad \text{cov } f = (A_w^T \cdot A_w)^{-1}$$

Diagonal elements of cov f (see Table 4.3) are the variances of the model parameters. The uncertainty in each model parameter is estimated from the square root of the variance: 10% for surface Atlantic water, 4% for Spanish shelf water, 9% for NACW and 5% for Mediterranean deep water. These estimates depend on the structure of the model matrix and not on the composition of a specific sample. Non-zero off-diagonal terms of the covariance matrix indicate that the model parameters are not mutually independent.

Table 4.3 Model parameter covariance matrix cov f

	Surface Atlantic	Spanish Shelf	NACW	Mediterranean Deep
Surface Atlantic	.0092	.0015	-.0077	-.0029
Spanish Shelf		.0020	-.0027	-.0008
NACW			.0091	.0014
Mediterranean Deep				.0023

The contribution of each tracer to the solution can be illustrated by removing the constraint imposed by each tracer in turn. Standard errors for each model parameter are calculated from the modified covariance matrix (Table 4.4). This procedure quantifies the role of each tracer in determining the solution which was discussed qualitatively earlier. Without the salinity constraint, uncertainty in the Mediterranean contribution increases by a factor of three to 17%. Estimates of surface Atlantic and NACW contributions are strongly dependent on the Cd constraint: uncertainties increase to 24 and 22%, respectively, when neglecting this tracer. The contribution of the final end-member, Spanish shelf water, is better constrained than other members. Removal of either Cu or Zn does not significantly affect the variance of the solution. This indicates that, of these two tracers, one is redundant because of strong Cu and Zn enrichments in the same end-member. Simultaneously neglecting these two tracers, however, increases the uncertainty in shelf end-member proportion to 38%.

The model parameter covariance matrix can be decomposed in greater detail. The redistribution of end-member fractions due to a one standard error unit change in each tracer datum is derived from equation (2):

$$\frac{\partial f}{\partial d} = A \cdot (A_t \cdot A)^{-1} \quad (\text{subscript } w \text{ becomes implicit})$$

Table 4.5 contains this (6\*4) matrix (neglecting the closure condition) and lists individual changes in end-member fractions. The squares of

Table 4.4 Sensitivity of standard error (%) to disregarding each tracer in inversion.

	Surface Atlantic	Spanish Shelf	NACW	Mediterranean Deep
All 6 tracers	10	4	9	5
no Salinity	12	5	11	17
no Cu	10	5	10	5
no Ni	11	4	10	5
no Cd	24	5	22	6
no Zn	10	7	12	5

Table 4.5 End-member redistribution (%)  $\partial f/\partial d$ 

	Surface Atlantic	Spanish Shelf	NACW	Mediterranean Deep
Salinity	-1.4	-0.6	1.9	3.8
Cu	1.4	2.6	-3.3	-0.7
Ni	-3.6	-0.9	2.4	2.0
Cd	-7.2	-0.4	5.9	1.7
Zn	2.0	3.5	-4.6	-0.9

entries in each column of Table 4.5 sum up to the diagonal terms of the model parameter covariance matrix discussed above.

Standard errors in model parameters (due to errors in the data) range from 4% for Spanish shelf water to 10% for surface Atlantic water. It is more difficult to establish the regression sensitivity to the assumptions of the model. These are (1) the structure of the model matrix, i.e. the choice and composition of end-members, and (2) conservative mixing. Assumption (2) of the mixing model implies the absence of significant external input or output mechanisms that could affect dissolved trace metal concentrations in surface water. This is reasonable given the time scale of mixing in the Strait (on the order of days) and the oceanic geochemistry of trace metals (Bruland, 1983). To get an intuitive understanding of assumption (1), a simple mixing model  $A \cdot f = d$  is solved algebraically for two end-members of arbitrary composition  $(S_1, Z_1)$  and  $(S_2, Z_2)$ , respectively.

$$\text{For } A = \begin{matrix} S_1 & Z_1 \\ S_2 & Z_2 \end{matrix}, \quad f = \begin{matrix} f_1 \\ f_2 \end{matrix} \quad \text{and } d = \begin{matrix} S_d \\ Z_d \end{matrix} \quad \text{as defined for equation (1)}$$

the best fit solution minimizes:

$$\Sigma (\text{residual})^2 = (S_d - (f_1 \cdot S_1 + f_2 \cdot S_2))^2 + (Z_d - (f_1 \cdot Z_1 + f_2 \cdot Z_2))^2$$

recalling that  $f_1 + f_2 = 1$  and

setting  $\partial \Sigma (\text{residuals})^2 / \partial f_1 = 0$  yields:

$$f_1 = (S_d - S_2) / (S_1 - S_2)$$

The sensitivity of the solution to variations in the data ( $S_d$ ) or the composition of either of the end-members ( $S_1$ ,  $S_2$ ), becomes:

$$(4) \partial f_1 / \partial S_d = 1/(S_1 - S_2)$$

If for a given sample:  $S_d = x \cdot S_1 + (1-x) \cdot S_2 \quad (0 < x < 1)$ , then:

$$(5) \partial f_1 / \partial S_1 = -x/(S_1 - S_2)$$

$$(6) \partial f_1 / \partial S_2 = (x-1)/(S_1 - S_2)$$

As discussed above and shown again by equation (4), the uncertainty in the solution due to errors in the data does not depend on the composition of a specific sample. Changes in end-member fractions caused by a variation in the model matrix (equations (5) and (6)), however, do depend on the composition of a specific sample. As indicated for the simple two end-member case, the closer a sample is to the composition of one of the end-members (eg.  $x$  close to 1), the more sensitive the solution will be to variations in the composition of that same end-member. Since a general derivation of this problem is cumbersome, changes in end-member composition for a sample composed of equal (25%) proportions of each of the end-members were simulated instead. Van Geen et al. (Chapter 3) recently estimated uncertainties for the composition of Atlantic end-members: 1 standard error unit (listed in Table 4.1) for each tracer in surface Atlantic water, NACW, and Mediterranean deep water and 2 units for Spanish shelf water. Results from this computer simulation are summarized in Table 4.6. End-member fraction deviations from 25% were squared and

Table 4.6 Simulation results for changes in end-member composition (%).

	Surface Atlantic 1S	Spanish Shelf 2S	NACW 3S	Mediterranean Deep 4S
Salinity	1.2	0.5	0.9	2.6
Cu	0.7	1.6	2.0	0.4
Ni	2.7	0.4	1.9	1.2
Cd	5.4	0.3	4.8	1.0
Zn	0.9	2.3	2.8	0.4
E e <sup>2</sup>	6.3	2.9	6.3	3.1
Total %	11.5	5.3	11.4	5.7

added to each other. Adding the squared uncertainties due to errors in salinity composition (from the covariance matrix) yields the total error estimate for the model parameters: surface Atlantic water and NACW, 11%; Spanish shelf water, 5%, and Mediterranean deep water, 6%.

Finally, the model chosen to describe trace metal concentrations in the Strait of Gibraltar can be evaluated by graphically by comparing measured and model-derived tracer data for the set of surface stations (Fig. 4.3). How much weight a tracer datum carries in its own prediction in the least-square solution is first calculated from the (6\*6) data resolution matrix  $N$  (Menke, 1984) which relates observed and model-predicted data:  $d_{pre} = N \cdot d$ . Predicted data,  $d_{pre}$ , are calculated by applying the forward problem to estimated model parameters:  $d_{pre} = A \cdot f$ . Substitution from (2) yields:

$$N = A \cdot (A^T \cdot A)^{-1} \cdot A^T$$

Table 4.7 lists the data resolution matrix calculated for this problem. Since predicted data are the product of observed data by the data resolution matrix, deviations from the identity matrix indicate that a predicted tracer value is a linear combination of its own and other observed tracer values. Diagonal entries of the data resolution matrix are defined as the importance of the data in their own prediction. In decreasing order, the importance of the closure condition is .99, salinity: .94, Cd: .86, Zn: .64, Cu: .35, and Ni: .21. Off-diagonal entries are small for tracers with a high weight in their own prediction, such as salinity and Cd. Perhaps surprisingly, Zn and Cu

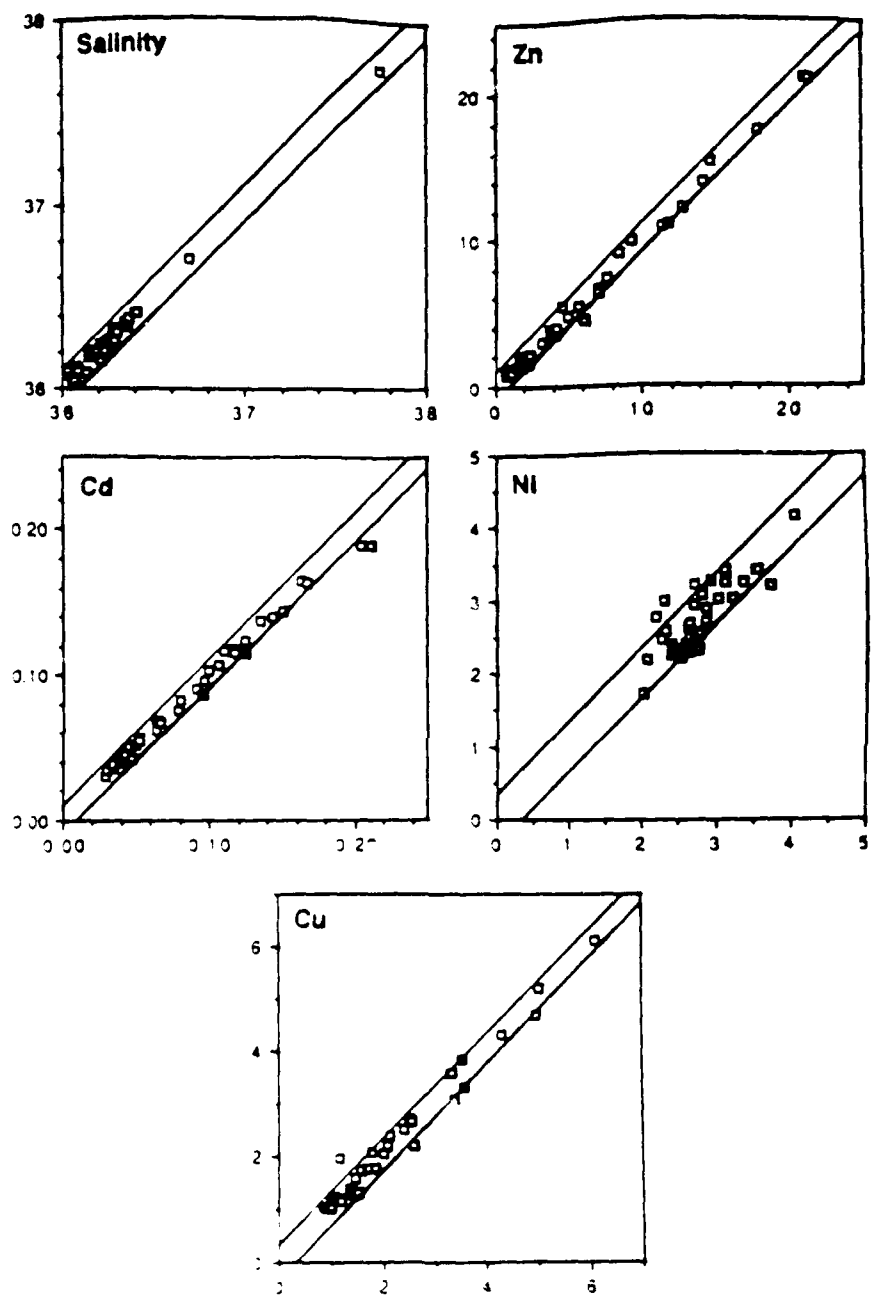


Fig. 4.3 Observed vs. model-predicted data from best fit. Diagonals indicate one standard error deviation from one to one correspondence.

Table 4.7 Data resolution matrix

	Salinity	Cu	Ni	Cd	Zn	I
Salinity	.94	.00	.21	-.09	.02	.02
Cu		.35	-.04	.03	.47	-.00
Ni			.21	.33	-.06	-.07
Cd				.86	.01	.03
Zn					.64	-.01
I						.99

have a low importance relative to their wide dynamic range. This is due to high co-linearity in the distributions of these two tracers which are dominated by the same end-member (Spanish shelf water). Examination of the off-diagonal term relating these two tracers (0.47) indicates that the individual importances of Cu and Zn is replaced by a role in predicting each other.

It should be expected that tracers with a high importance, such as salinity and Cd, follow a one to one line in Fig. 4.3 within the a priori error bands. This is because these tracers almost independently determine Mediterranean and NACW contributions, and therefore also control their own prediction. In contrast, tracers that are redundant (e.g. Ni vs. all other tracers, or Cu vs. Zn) and therefore do not control their own prediction, provide a verification of the conservative mixing hypothesis as well as the composition chosen for the end-members. As it turns out, residuals are small also for the "weaker" tracers. The fact that no systematic errors can be detected supports the choice of end-members; the model is consistent with the data. It is worth noting that end-members were chosen on the basis of observed profiles and surface samples from the Gulf of Cadiz (Chapter 3), i.e. independently from data for the Strait of Gibraltar.

#### DISTRIBUTION OF END-MEMBERS IN THE STRAIT OF GIBRALTAR

On the basis of the distribution of Atlantic end-members (Fig. 4.1), surface waters in the Strait can be divided in two regions by a boundary roughly equidistant from each shore throughout the Strait during both

sampling periods (Fig. 4.1) The southern half is rather uniformly composed of 90-95% Atlantic surface water and 10-5% North Atlantic Central Water. The reduction of an Atlantic profile to mixing of two end-members, mentioned in the introduction, limits the depth resolution of the model. Indeed, two mixing equivalent scenarios for surface Cd enrichments, such as (1) discrete mixing of the surface and 400 m deep extrema or, (2) continuous mixing to a shallower depth can not be distinguished in principle.

CTD data from USNS Lynch (Bray, 1986) obtained at the time of chemical surface sampling (Sta. GB1131, GB 1198) along 50°40'W indicate that at the center of this section, below a 50m mixed layer, the inflow is not homogeneous down to the interface with the saline outflow (150 m). The intrusion of NACW causes a salinity minimum at approximately 90 m depth. This recurrent feature was discussed in detail by Gascard and Richez (1985). Surface transects at 50°40' W were taken after LW on both April 11th and April 17th. At that time, the preceding 6 hours have seen the strongest inflowing currents as the interface separating in- and outflow deepens. This explains the strong subsurface presence of NACW in the CTD profile and implies that surface samples at this section of the Strait may underestimate the proportion of NACW in the inflow. Further east, the interface is shallower: 40 to 70 m deep at 05°30' W. The inflow at this section is vertically homogeneous on April 12th (1 day after spring tide), but not on April 17th (Sta. GB 1193) when a small subsurface salinity minimum due to NACW is again detectable. Gascard

and Richez (1985) also discuss the greater penetration through the Strait of NACW at neap tide.

The northern half of the Strait is more heterogeneous in composition. Spanish coastal water dominates samples close to the shore and is gradually diluted towards the center of the Strait. Spanish shelf water is a combination of Atlantic surface water, NACW and some river water that has passed over a shallow portion of shelf in the Gulf of Cadiz (Chapter 3). Surface water at the northwest entrance to the Strait is composed almost exclusively of Spanish shelf water defined in Table 4.1 (sample # 259). This end-member contributes as much as 50% to the surface Alboran Sea at 5°15' W (# 178). Since CTD profiles of the northern portion of the Strait show a vertically homogeneous inflow layer, one can assume that surface data along this section are representative and that metal enrichments from the Spanish shelf entering the Alboran Sea are not restricted to very shallow depths. It should be noted that this end-member could not have been quantified by standard tracers because shelf-water and NACW are both less saline sources relative to surface Atlantic water. Nutrients and temperature would be uncertain tracers since both are strongly non-conservative in surface water.

Transects across the Strait on April 11, 12th and 16-18th show that the shelf water fraction at 5°40' W in the northern portion of the Strait is much greater during the later period. This change is not simply due to patchiness in the area since it is confirmed over five stations: # 144, 148, 151, 168-170 and 239-247. Cross-strait sections at 5°40' W started

from the North roughly at LW on both April 11th and 17th and samples are spaced evenly over the two hours required to reach the Moroccan coast. Therefore, the greater proportion of shelf water on April 17th can not be due to a difference in sampling time relative to the tide. Perhaps spring tides are accompanied by less entrainment of Spanish shelf water. This possibility may be worth further study.

Contribution of Mediterranean deep water to surface water is significant only in the Alboran Sea: 71, 14, 28 and 12% at stations # 184, 181, 180 and 179 respectively. Only three (Atlantic) end-members are represented at half the locations in the Strait and the mixing model changes configuration for these samples. There are still 6 equations to be satisfied in the least square sense but only three unknown model parameters. The new covariance matrix for this reduced system decreases the uncertainty due to errors in the data for surface Atlantic, NACW and Spanish shelf water to 7%, 9%, and 4%, respectively.

Four samples at the southern end of the Alboran Sea section (# 171, 172, 173, 174) indicate caution must be used when interpreting trace metal data in this area. Model results indicate up to 19% contribution from the Spanish shelf end-member. However, in view of the dominant current direction in the Strait, it seems unlikely that this water mass could cross over to the Moroccan shore south of Ceuta. This feature should probably be interpreted as a different water mass influenced by the Mediterranean shelf, which is not included in our analysis.

## CONCLUSION

Distributions of dissolved constituents Cu, Ni, Cd, Zn and salinity in the Strait of Gibraltar were shown to be consistent with conservative mixing of water masses contributing to the Atlantic inflow. These three water masses, (1) surface Atlantic water, (2) NACW and (3) Spanish shelf water, can be followed into the Alboran Sea. The data confirm that Atlantic metal-enriched water masses entering through the Strait of Gibraltar can account for Cu, Zn and Cd enrichments of the Mediterranean relative to nutrient-depleted Atlantic surface waters. However, high current shear across the Strait makes it difficult to flow-average the relative contributions of Atlantic water masses to the inflow at this location. In addition, the proportion of NACW may be underestimated by considering surface samples only. Even though Ni is enriched in the Mediterranean outflow, Spanish shelf water cannot be the source of this element. Interestingly, surface samples from the Mediterranean (Spivack et al., 1983) show larger relative enrichments towards the eastern basin for Ni than for Cu, Cd and Zn. This observation is consistent with a source, eolian or riverine, internal to the Mediterranean for this element.

Results from surface samples collected in the Alboran Sea at three times of the year, April '86, June '82 and October '86, also indicate significant variations in the relative proportion of the three Atlantic end-members over longer time scales (Chapter 5). This may be related to seasonal changes in the circulation through the Strait predicted by Bormans et al. (1987) on the basis of tide gauge and meteorological data

and confirmed by direct measurements made during the Gibraltar Experiment (Ochoa and Bray, manuscript and J. Candela, pers. comm.).

Over even longer time scales, climate change may have affected source waters for the inflow and therefore the composition of the Mediterranean. Lowering of sea-level during glacial time would have exposed the Atlantic Spanish shelf and limited processes which give rise today to very high dissolved metal concentrations in that region. Given the short residence time of water in the Mediterranean relative to the inflow (100 years), such a signal could be looked for in both planktonic and benthic foraminifera of the Mediterranean if skeletons of these organisms reflect ambient Cu or Zn concentrations (Boyle, 1981).

#### ACKNOWLEDGEMENTS

Space and time was generously provided during the Gibraltar Experiment by Drs. Tom Kinder and Nan Bray on board USNS Lynch. We thank Liz Callahan for assistance in collecting a large number of samples and M. Benno Blumenthal for very formative discussions on the regression model.

## APPENDIX

Station	Latitude	Longitude	Salinity	Si	Po4	Qu	Ni	Cd	Zn	Surf All	Sp Shell	NACW	Med	Residual Sq
144	36 000	-5 633	36.131	1.49	0.20	3.3	2.7	0.150	11.4	0.11	0.48	0.35	0.07	3.92
145	35 983	-5 650	36.091	0.94	0.08	1.8	2.7	0.091	5.5	0.56	0.19	0.25	0.00	1.07
151	35 950	-5 650	36.161	1.04	0.10	1.4	2.8	0.064	2.0	0.70	0.05	0.23	0.02	0.64
154	35 933	-5 650	36.285	0.92	0.19	0.9	2.1	0.029	0.8	1.00	0.00	0.00	0.00	0.18
157	35 900	-5 617	36.285	2.68	0.10	1.2	2.0	0.047	1.0	0.89	0.02	0.08	0.01	1.15
160	35 867	-5 650	36.282	1.44	0.16	1.2	2.2	0.095	6.1	0.55	0.17	0.23		12.52
165	35 933	-5 467	36.253	0.99	0.13	0.9	2.5	0.031	0.9	0.96	0.00	0.04	0.00	0.95
166	35 950	-5 450	36.251	1.39	0.13	0.9	2.5	0.030	1.0	0.97	0.00	0.03	0.00	1.23
167	35 967	-5 467	36.267	1.56	0.18	0.9	2.4	0.035	0.8	0.95	0.00	0.05	0.00	0.30
168	35 983	-5 467	36.231	1.66	0.14	2.1	2.3	0.079	5.6	0.69	0.23	0.07	0.01	0.84
169	36 017	-5 467	36.181	1.64	0.17	1.5	2.3	0.063	3.2	0.77	0.10	0.13	0.00	0.52
170	36 033	-5 467	36.215	1.46	0.19	2.5	2.3	0.124	7.6	0.36	0.31	0.27	0.05	6.15
171	35 850	-5 317	36.409	1.17	0.09	1.7	2.9	0.066	4.0	0.66	0.13	0.11	0.10	0.34
172	35 867	-5 283	36.354	1.09	0.08	2.6	3.1	0.117	4.6	0.25	0.19	0.40	0.16	2.14
173	35 877	-5 245	36.356	1.19	0.10	1.7	2.6	0.052	4.2	0.80	0.14	0.00	0.05	0.45
174	35 888	-5 250	36.363	1.22	0.09	1.8	2.7	0.053	3.8	0.80	0.14	0.01	0.06	0.62
175	35 933	-5 217	36.299	1.22	0.12	1.1	2.5	0.040	1.8	0.90	0.03	0.04	0.02	1.27
176	35 967	-5 233	36.218	1.09	0.12	1.2	2.5	0.042	1.6	0.89	0.03	0.08	0.00	0.34
177	36 000	-5 267	36.193	1.27	0.12	1.4	2.6	0.053	2.4	0.81	0.07	0.12	0.00	0.37
178	36 033	-5 267	36.063	1.41	0.20	3.5	2.8	0.144	12.7	0.26	0.55	0.19	0.01	2.18
179	36 067	-5 217	36.400	2.11	0.19	3.4	3.2	0.100	8.5	0.44	0.38	0.05	0.12	1.75
180	36 083	-5 233	36.693	2.41	0.22	2.4	3.5	0.106	7.0	0.26	0.23	0.23	0.28	0.33
181	36 100	-5 267	36.284	3.18	0.22	2.6	3.7	0.110	7.6	0.29	0.28	0.14	0.14	3.40
184	36 183	-5 267	37.742	3.20	0.17	2.1	4.0	0.097	7.1	0.07	0.14	0.08	0.71	1.07
239	35 933	-5 450	36.282	0.83	0.14	1.0	2.6	0.042	2.2	0.87	0.03	0.07	0.02	1.23
240	35 950	-5 467	36.283	0.90	0.13	1.0	2.4	0.039	1.6	0.91	0.02	0.05	0.01	0.25
241	35 967	-5 467	36.280	0.08	1.0	2.7	0.035	1.7	0.92	0.02	0.04	0.02	0.02	1.61
242	35 983	-5 467	36.143	0.09	1.6	2.7	0.065	4.0	0.73	0.13	0.14	0.00	0.97	
243	36 017	-5 467	36.051	0.17	3.5	2.7	0.124	9.2	0.37	0.44	0.19	0.00	0.00	1.30
244	36 033	-5 467	36.060	0.23	5.0	3.4	0.163	17.8	0.14	0.82	0.02	0.01	0.56	
245	36 000	-5 667	36.061	0.38	5.0	2.9	0.167	14.6	0.12	0.71	0.16	0.02	0.02	2.39
246	35 967	-5 650	36.054	0.22	6.1	3.6	0.204	20.9	0.00	1.00	0.00	0.00	0.00	2.44
247	35 950	-5 650	36.038	0.10	3.3	2.9	0.118	11.8	0.43	0.50	0.07	0.00	0.02	1.13
248	35 933	-5 667	36.347	0.05	1.1	2.5	0.035	2.2	0.92	0.04	0.00	0.04	0.00	0.95
249	35 900	-5 650	36.245	0.12	1.5	2.5	0.043	1.7	0.89	0.06	0.05	0.00	0.00	0.79
251	35 867	-5 650	36.167	0.16	1.5	2.4	0.050	1.7	0.83	0.06	0.11	0.00	0.00	0.72
253	35 867	-5 883	36.298	1.1	2.6	0.034	1.6	0.93	0.02	0.03	0.02	0.00	0.00	
254	35 883	-5 883	36.214	0.06	1.0	2.6	0.041	1.1	0.87	0.00	0.12	0.01	0.00	1.09
255	35 933	-5 867	36.234	0.20	0.9	2.8	0.036	0.7	0.89	0.00	0.10	0.01	0.00	2.12
256	35 950	-5 833	36.153	0.83	0.24	1.4	2.7	0.045	1.7	0.84	0.05	0.11	0.00	1.80
257	36 000	-5 850	36.074	0.83	0.07	2.0	2.6	0.080	4.9	0.62	0.19	0.19	0.00	0.39
258	36 033	-5 833	36.029	1.32	0.20	4.3	3.0	0.135	14.1	0.32	0.65	0.03	0.00	0.39
259	36 067	-5 833	36.086	1.46	0.15	6.1	3.1	0.211	21.3	0.00	1.00	0.00	0.00	5.79

## REFERENCES

Bormans, M., Garrett, C., Thompson, K., 1986. Seasonal variability of the surface inflow through the Strait of Gibraltar. *Oceanol. Acta* 9,4, 403-414.

Boyle, E.A., 1981. Cadmium, zinc, copper, and barium in Foramimifera tests. *Earth Planet. Sci. Lett.* 53,11-35.

Boyle, E.A., Chapnick, S.D., Bai, X.X. & Spivack, A.J., 1985. Trace metal enrichments in the Mediterranean Sea. *Earth Planet. Sci. Lett.* 74, 405-419.

Bruland, K.W. 1983, Trace elements in Sea-water, In: *Chemical Oceanography*, v. 8, Academic Press, London.

Bray, N., 1986. *Gibraltar Experiment CTD data report*, SIO Reference series #86-21, Scripps Institution of Oceanography

Gascard, J.C. and C. Richez, 1985. Water masses and circulation in the Western Alboran Sea and in the Strait of Gibraltar, *Prog. Oceanog.* 15, 157-216.

Kinder, T.H., Z.R. Hallock, D.A. Burns and M. Stirgus, 1983. *Donde Va?*, Hydrographic measurements in the Western Alboran Sea, June 1982, NORDA Technical Note 202.

Kinder, T.H. and H.L. Bryden (1987) The 1985-86 Gibraltar Experiment: Data collection and preliminary results. *EOS, Transactions, American Geophysical Union*, 68, 786-787, 793-795.

Mackas, D.L., Denman, K.L. & Bennett, A.F., 1987. Least squares multiple tracer analysis of water mass composition. *J. Geophys. Res.* 92, 2907-2918.

Menke, W. *Geophysical data analysis-Discrete inverse theory*, 1985. Academic Press, Orlando Ca.

Spivack, A. J., S. S. Huested & E. A. Boyle, 1983. Copper, Nickel and Cd in surface waters of the Mediterranean, In: *Trace Metals in Seawater*, C. S. Wong, E. Goldberg, K. Bruland and E. Boyle, eds., pp 505-512, Plenum Press, New York, NY.

van Geen, A., P. Rosener and E. Boyle, 1988. Entrainment of trace metal-enriched Atlantic shelf-water in the inflow to the Mediterranean Sea. *Nature* 331, 423-426.

CHAPTER FIVE

VARIABILITY OF Cu, Ni, Cd AND Zn DISTRIBUTIONS  
IN SURFACE WATERS OF THE ALBORAN SEA

## INTRODUCTION

Atlantic shelf water off the Spanish coast is strongly enriched in certain trace metals, and may dominate the flux of Cu, Cd and Zn to the Mediterranean Sea through the Strait of Gibraltar (van Geen et al, 1988). The initial data suggested that the integrated surface input of these elements through the Strait roughly matched the output by the underlying Mediterranean outflow to Atlantic. However, determination of the average composition of the inflow is complicated by recently observed temporal variability of metal enrichments in Spanish shelf water (Chapter 3) and day to day changes in the proportion of shelf water entrainment within the Strait (Chapter 4).

The first goal of this paper is to address this problem by presenting new trace metal data for 99 surface samples collected during the Gibraltar Experiment on two cruises in the Alboran Sea (Kinder and Bryden, 1987). The second objective is to quantitatively relate dissolved metal distributions to the composition of water masses contributing to the Alboran Sea. A major factor controlling these distributions is vigorous surface circulation as indicated by the distributions of two classical tracers: temperature and salinity. Infra-red satellite images generally show a clockwise rotating gyre with a diameter on the order of 50 n.mi (The ?Donde Va? Group, 1984). The IR pattern shows entrainment in the gyre of colder water from the northern Alboran Sea and from the Atlantic inflow through the Strait of Gibraltar. High surface salinities in the northern Alboran Sea indicate outcropping of Mediterranean deep water in that region. Complementing this picture, geostrophic calculations

(Parilla and Kinder, manuscript) and direct current measurements show that a narrow jet with velocities often greater than 100 cm/s enters the Alboran Sea from the Strait of Gibraltar (La Violette, 1985). Such features are examined in this paper by integrating information from five tracers (salinity, Cu, Ni, Cd, Zn) at each surface station. To this end, a conservative mixing model is solved by weighted least-squares in terms of four end-members: Atlantic surface water, North Atlantic Central Water, Spanish shelf water, and Mediterranean deep water. The model provides a common basis from which to compare tracer distributions in April'86, October'86, as well as earlier results from June'82 (Boyle et al., 1985).

#### ANALYSIS

Surface samples were collected on two USNS Lynch cruises, March 26-April 19 and October 12-17 1986, with a contamination-free underway pumping apparatus. Salinity and nutrients were determined using standard techniques (Guildline Autosal salinometer and colorimetry, respectively) described in Strickland and Parsons (1968). Trace metal analyses on 30 ml samples followed a resin pre-concentration procedure which has been automated (Chapter 2). All sample concentrates were analyzed by graphite-furnace atomic absorption spectroscopy (Perkin-Elmer Zeeman 5000 and HGA 500). One-sigma precision for this data set is 5% or 0.1 nM for Cu and Ni whichever is larger, 5% or 5 pM for Cd and 6% or 0.2 nM for Zn. Blank corrections averaged 0.1 nM, 0.01 nM, <1 pM and 0.3 nM for Cu, Ni, Cd and Zn respectively.

## RESULTS

Although five tracers display a remarkable dynamic range in surface waters of the Alboran Sea (salinity: 36-38 ‰, Cu: 1-5 nM, Ni: 2-5nM, Cd: 40-150 pM and Zn: 1-13 nM), changes in the main circulation features of the Alboran Sea can be followed over the three sampling periods by restricting our attention to two tracers: salinity and Zn. The location of samples listed in Table 5.1 (April'86) and Table 5.2 (October'86), as well as June'82 (Table 5.3, data from Boyle et al., 1985) is indicated in Fig. 5.1. In April'86, saline Mediterranean deep water clearly outcrops over a greater portion of the northern Alboran Sea: the 36.5 ‰ isohaline is shifted 20 n.mi. to the south relative to June'82 and October'86 (Fig. 5.1). This may be related to greater wind stress from the northwest in November through March (Bormans et al, 1986). Such variability is not unusual for the Alboran Sea on shorter time scales as well, as indicated by a suite of satellite IR images covering October 11-13th '82 (La Violette, 1986). South of the region of Mediterranean water upwelling, the Atlantic inflow sustains a less saline layer over the upper 200 m of the water column. The extent of this layer is brought into perspective when considering that water transport by the inflow is 30 times greater than all fresh water inputs to the Mediterranean (Tchernia, 1980).

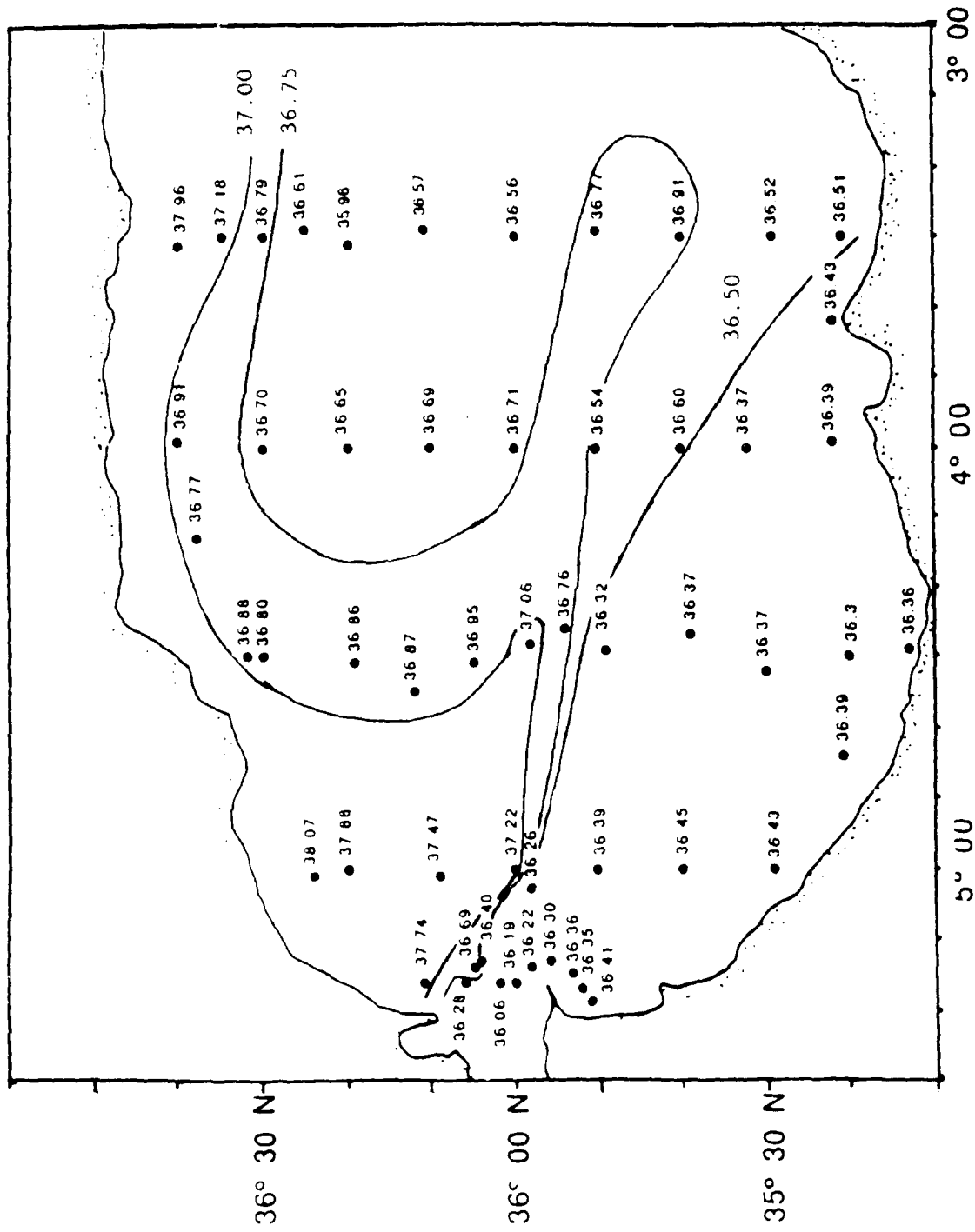


Fig. 5.1a Salinity in surface Alboran Sea, April '86  
Contours at 36.5, 36.75 and 37.00 ‰.

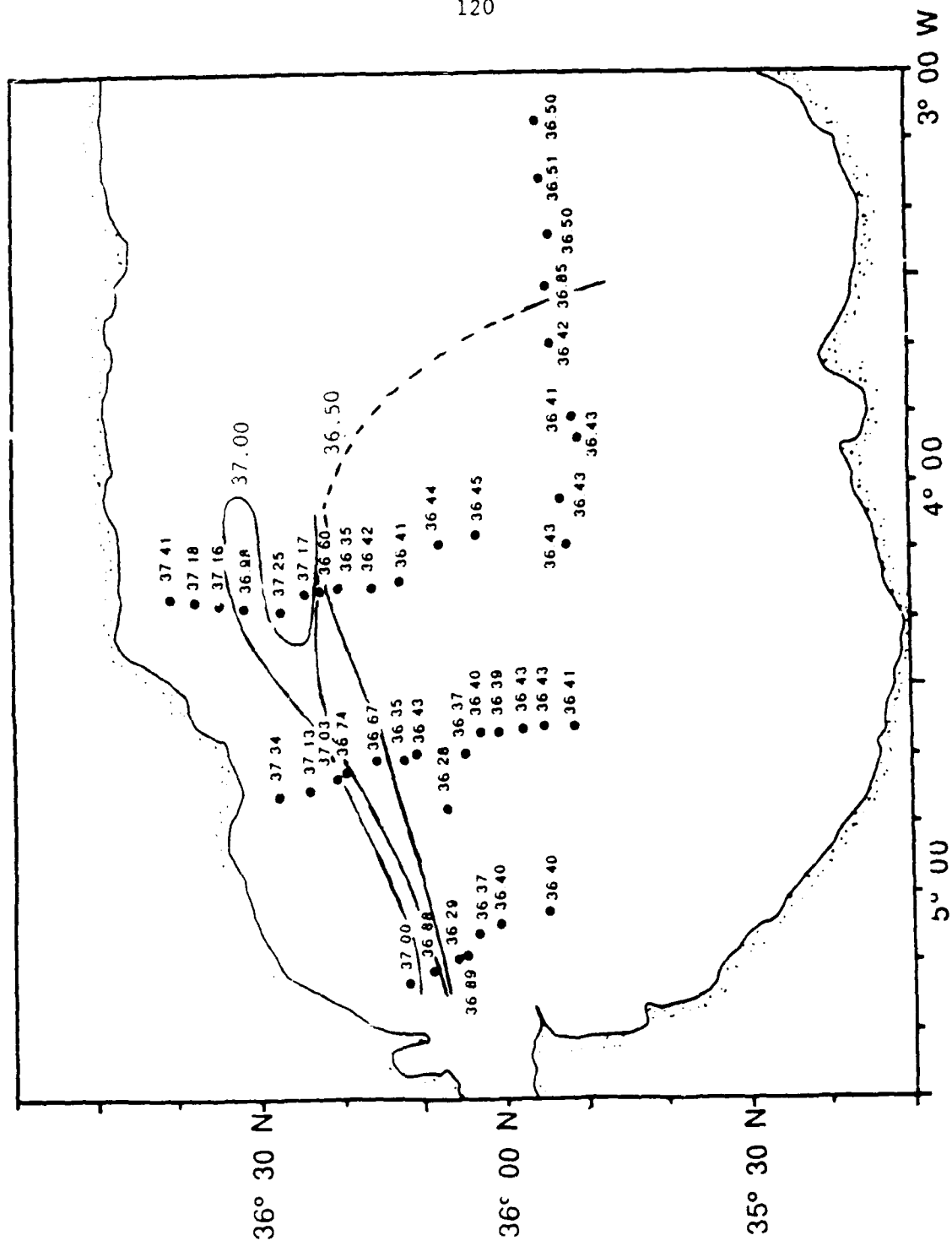


Fig. 5.1b Salinity in surface Alboran Sea, June'82  
Contours at 36.5, 36.75 and 37.00 ‰.

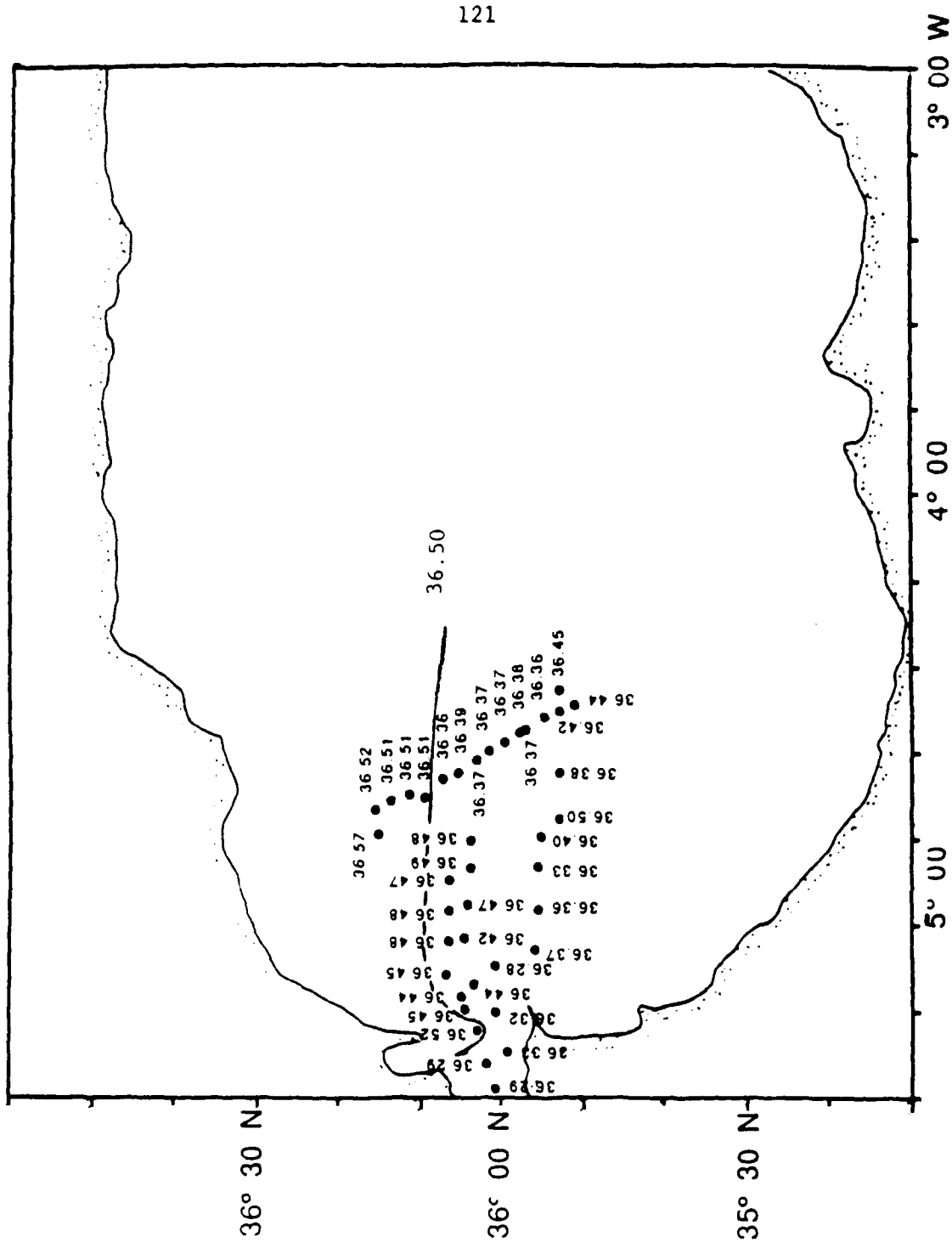


Fig. 5.1c Salinity in surface Alboran Sea, October'86  
Contours at 36.5, 36.75 and 37.00 ‰.

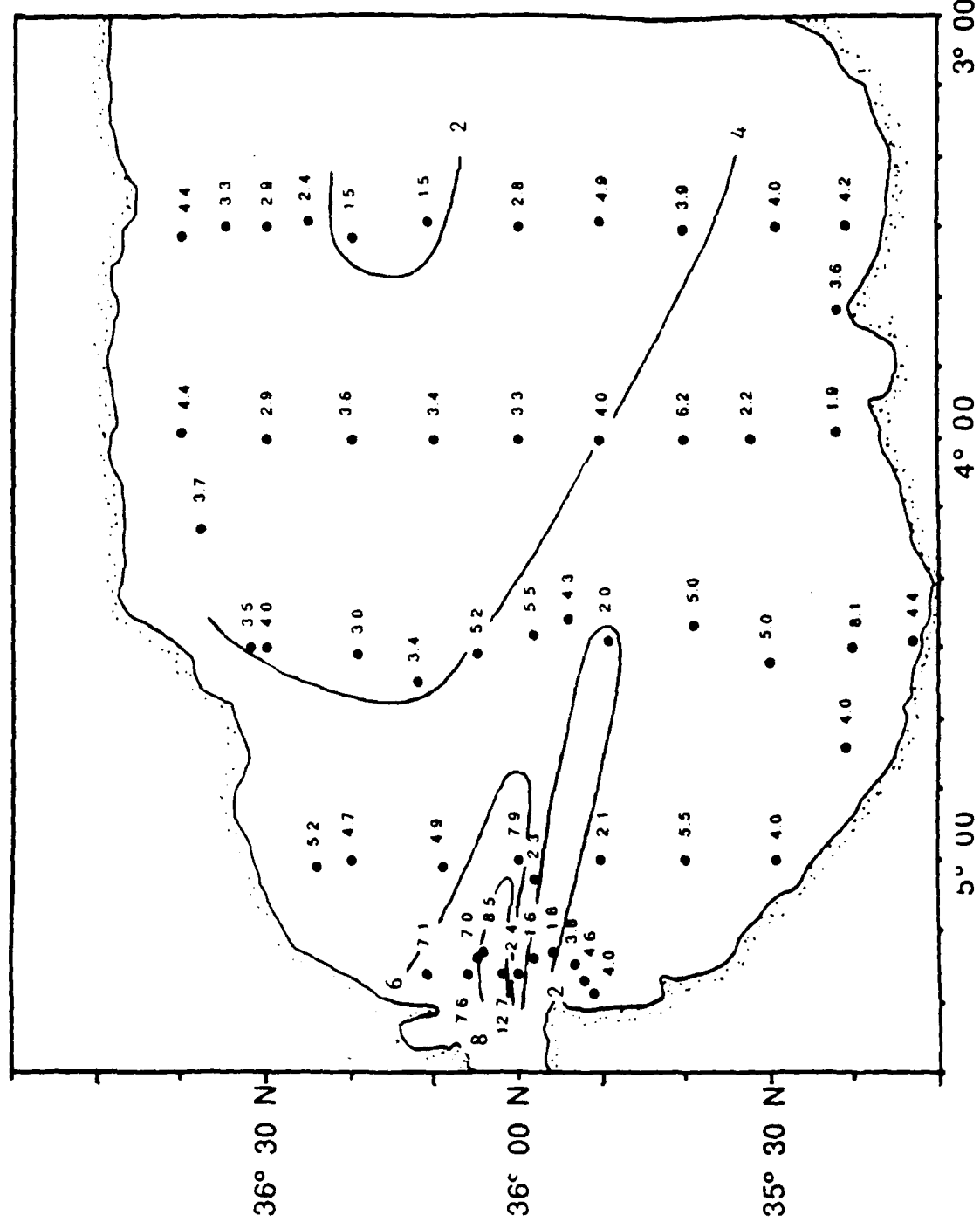


Fig. 5.2a Zn concentrations in surface Alboran Sea, April '86  
 Contours at 2, 4, 6, and 8 nM  
 Area with  $Zn < 2$  nM hatched horizontally  
 Area with  $Zn > 6$  nM hatched vertically

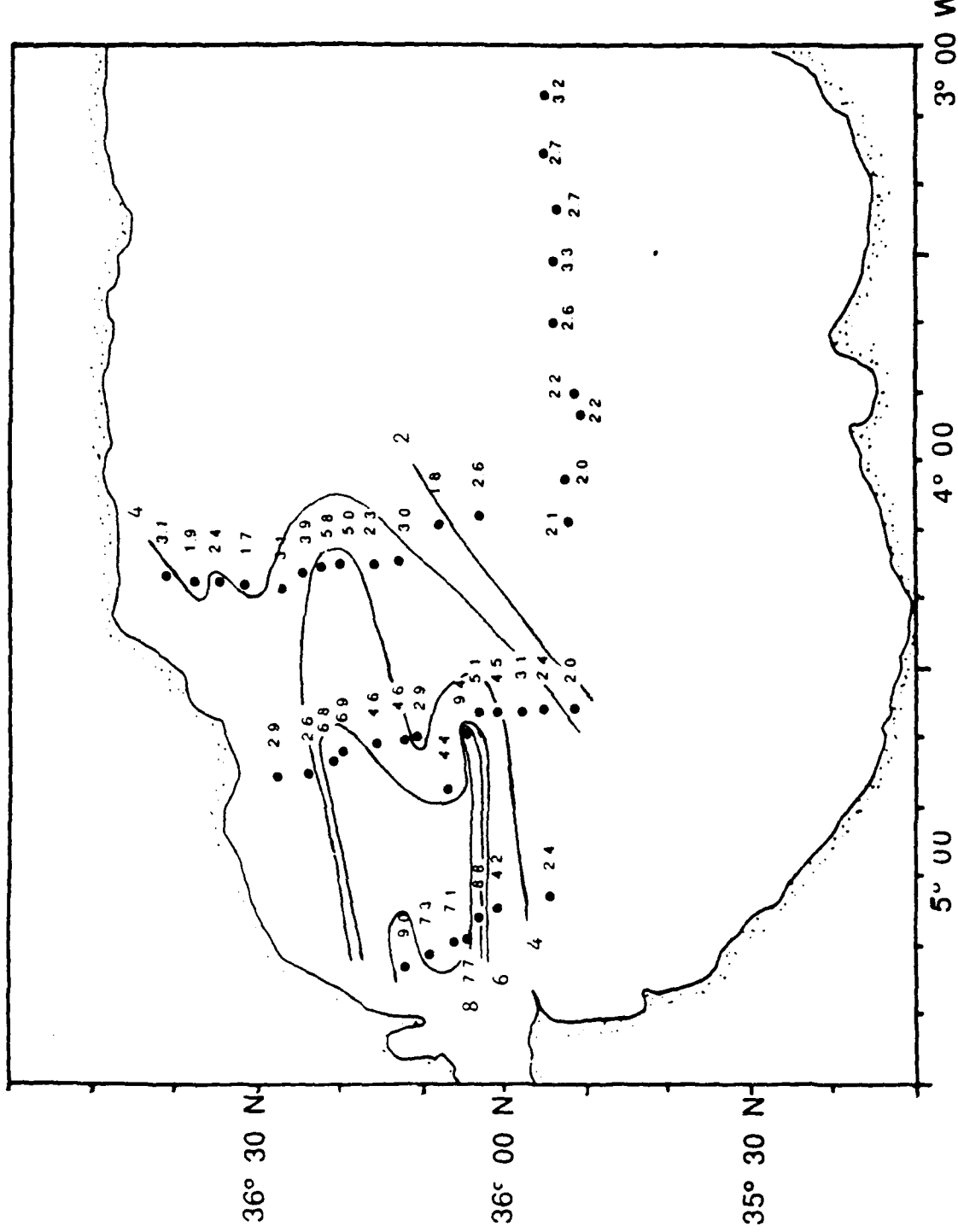


Fig. 5.2b Zn concentrations in surface Alboran Sea, June '82  
 Contours at 2, 4, 6, and 8 nM  
 Area with  $Zn < 2$  nM hatched horizontally  
 Area with  $Zn > 6$  nM hatched vertically

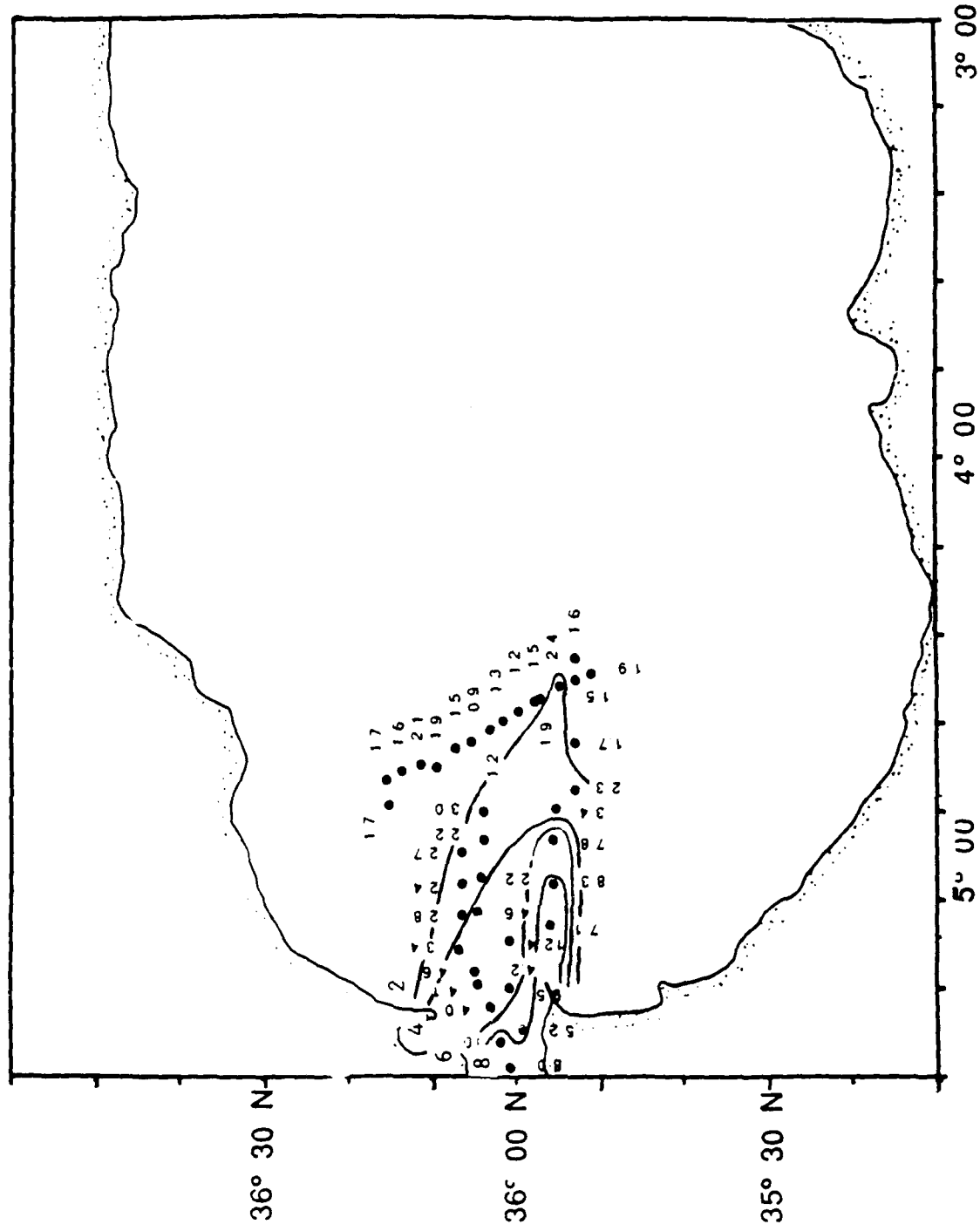


Fig. 5.2c Zn concentrations in surface Alboran Sea, October '86  
 Contours at 2, 4, 6, and 8 nM  
 Area with  $Zn < 2$  nM hatched horizontally  
 Area with  $Zn > 6$  nM hatched vertically

While the distribution of salinity is mainly determined by mixing of Mediterranean deep water and fresher Atlantic water, Zn reflects the advection of two components within the inflow: surface Atlantic water and Spanish shelf water. This is due to Zn enrichments in Spanish shelf water by more than order of magnitude relative to surface Atlantic water (Chapter 3). Surface transects in April'86 showed that Spanish shelf water was restricted to the northern half of the Strait of Gibraltar (Chapter 4). The separation between Atlantic surface water and Spanish shelf water is clearly preserved in April'86 over a distance of 30 n.mi. into the Alboran Sea (Fig. 5.2). The Zn enriched plume (5 nM at 4°30' W) is sharply bordered by a Zn-depleted portion of the inflow ( $\leq 2$ nM). In June'82 (Fig. 5.2), there is an additional extension of the Zn enriched plume to the north and metal enrichments penetrate further east into the Alboran Sea. In contrast, the Zn enriched portion of plume is weaker in October'86 and appears to veer to the southeast. Another difference between October'86 and other sampling periods are low Zn concentrations ( $< 2$ nM) found north of the zone directly influenced by Spanish shelf water. Such Zn levels are only found at two station northwest of Alboran Island in April'86 and over a wider area southeast of the Strait in June'82. Since Zn concentrations generally increase in surface waters of the Mediterranean east of the Alboran Sea (Sherrell and Boyle, 1985), low concentrations of this element most likely indicate patches of surface Atlantic water.

## DISCUSSION

The composition of the three Atlantic contributors to the inflow (surface Atlantic water, NACW and Spanish shelf water, Table 5.4) is based on surveys of the Gulf of Cadiz in April and October'86 (Chapter 3). Cu and Cd concentrations in shelf water were found to increase linearly as a function of Zn concentrations on both occasions. The slope of this relation for Cu and Cd, however, was approximately 30% higher in the Fall than in the Spring. Another difference between the two seasons is that absolute Zn concentrations decreased by approximately a factor of two over the Spanish shelf from April to October when comparing similar locations. Despite such variations in the magnitude of metal enrichments west of the Strait of Gibraltar, Cu and Cd concentrations for this metal enriched end-member were defined relative to a constant Zn concentration of 21 nM. Since our main interest at this point is the trace metal mass-balance through the Strait, a common basis in terms of the most sensitive indicator of Spanish shelf water (which dominates advective metal fluxes) simplifies comparison of the different data sets. The composition of the June'82 Spanish shelf end-member was simply linearly interpolated with respect to time, assuming changes in inter-element ratios are seasonal. A gradual increase in the Cu/Zn ratio over the course of a year observed for enriched plume samples of the Alboran Sea (Fig. 5.3) supports this assumption. Seasonal variations in shelf water Cd concentrations relative to Zn, on the other hand, are too small to be detected against natural background variability of the surface Alboran Sea (Fig. 5.4).

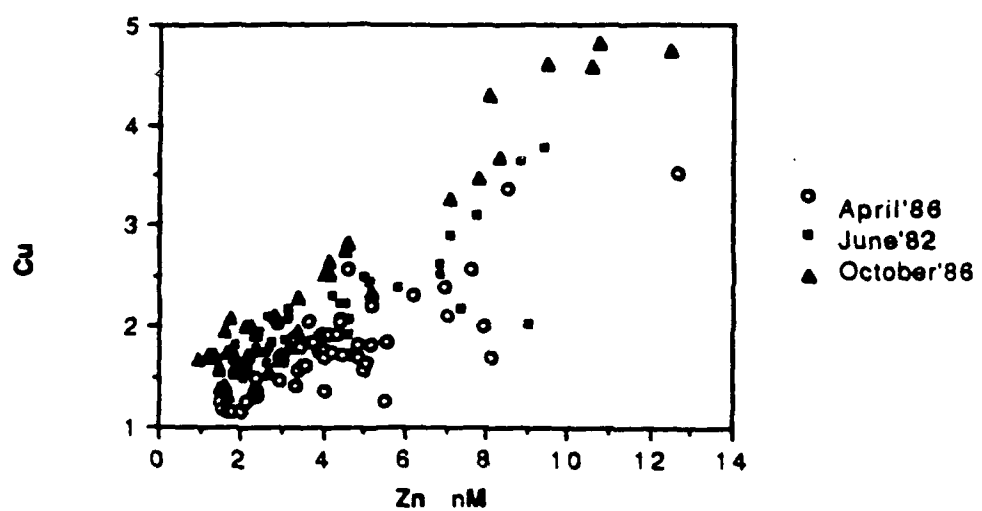


Fig. 5.3 Zn vs. Cu in Alboran Sea surface water, both in nM

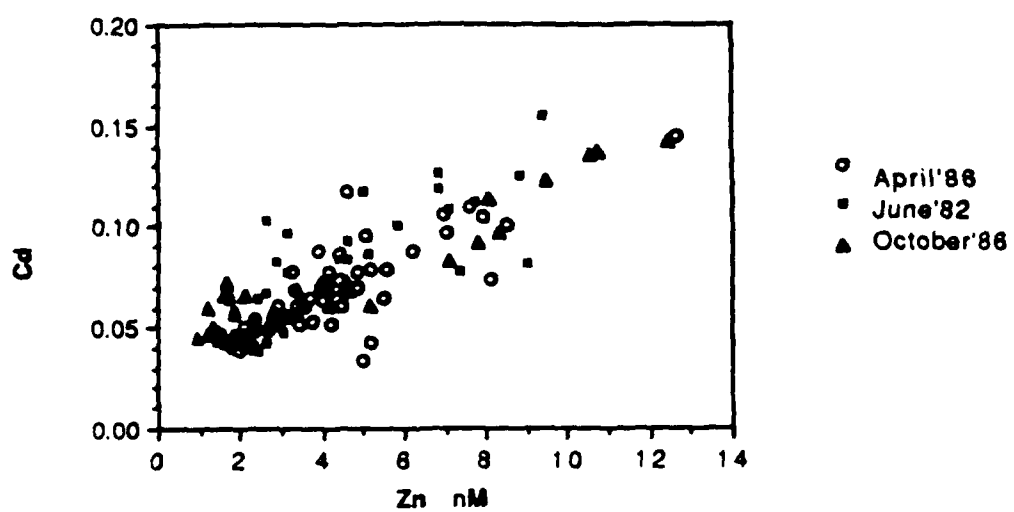


Fig. 5.4 Zn vs. Cd in Alboran Sea surface water, both in nM

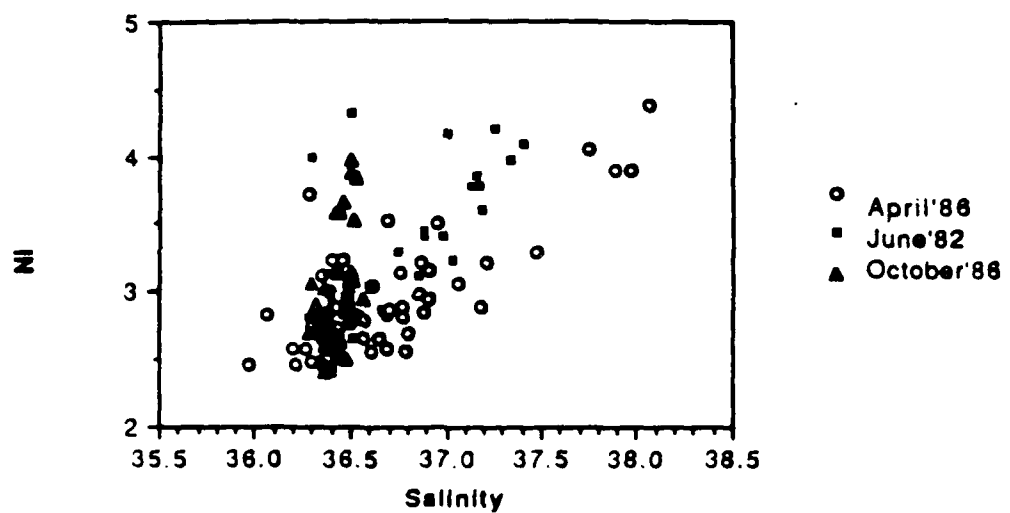


Fig. 5.5 Salinity ‰ vs. Ni (nM) in Alboran Sea surface water

Combining Zn and salinity with tracers Cu, Ni and Cd allows us to test to what extent the complex pattern of metal distributions is determined by the four end-members listed in Table 5.4. Assuming conservative mixing of salinity and trace metals, each surface sample can be described as a linear combination of four distinct end members. Following a more detailed description in Chapter 4, this relationship is expressed as:

$$(1) \quad A \cdot f = d$$

where A is the (6\*4) model matrix whose top five rows contain the tracer composition of each end-member (- Table 5.4) , (6\*1) vector d contains the composition of a specific sample and f is a (4\*1) vector whose four elements are the fractions of each contributing source which we want to estimate (Mackas et al., 1987). The fractions are constrained to be positive and to sum to unity. The system is over-determined since there are 4 unknowns (the end-member fractions) and 6 linear equations (one for each tracer and the closure condition). The best fit for the set of equations corresponding to each sample is obtained by minimizing the sum of the squared residuals (i.e. the  $L_2$  norm, Menke, 1985). Residuals are normalized with respect to each other by giving proper weights to each tracer equation: all tracer values are divided by their respective estimated standard errors, also listed in Table 5.4. The relative size of standard errors indicates the degree to which the model is required to fit the data for each tracer.

The least-squares solution to (1) for each surface sample is:

$$(2) \quad f = (A_w^T \cdot A_w)^{-1} \cdot A_w^T \cdot d_w.$$

In order to take the inequality constraints of positive end-member fractions into account, an iterative solution is determined using the Kuhn-Tucker theorem (Menke, 1984). Salinity dominates the estimate for the fraction of deep Mediterranean water, Zn and Cu dominate the estimate for the shelf end-member fraction, and Cd mainly resolves the deep Atlantic contribution after correction for Cd of shelf origin. Amplification of errors in the data as uncertainty in the model parameters is estimated from the unit covariance matrix:

$$(3) \quad \text{cov } f = (A_w^T \cdot A_w)^{-1}$$

The square root of the variance of each model parameter reflects errors due to uncertainty in the composition of a sample: 10% for surface Atlantic water, 4% for Spanish shelf water, 9% for NACW and 5% for Mediterranean deep water. When estimated standard errors in the composition of the end-members are included (Chapter 4), uncertainties for surface Atlantic, Spanish shelf, NACW and Mediterranean water contributions increase to 11, 5, 11 and 6%, respectively.

The conservative mixing model is applied to all April, June and October surface samples from the Alboran Sea (results listed in Tables 5.1, 2, 3). The difference between measured data and model derived data (residuals), can be evaluated graphically as deviations from a one to one correspondance (Fig. 5.6). As should be expected, measured and

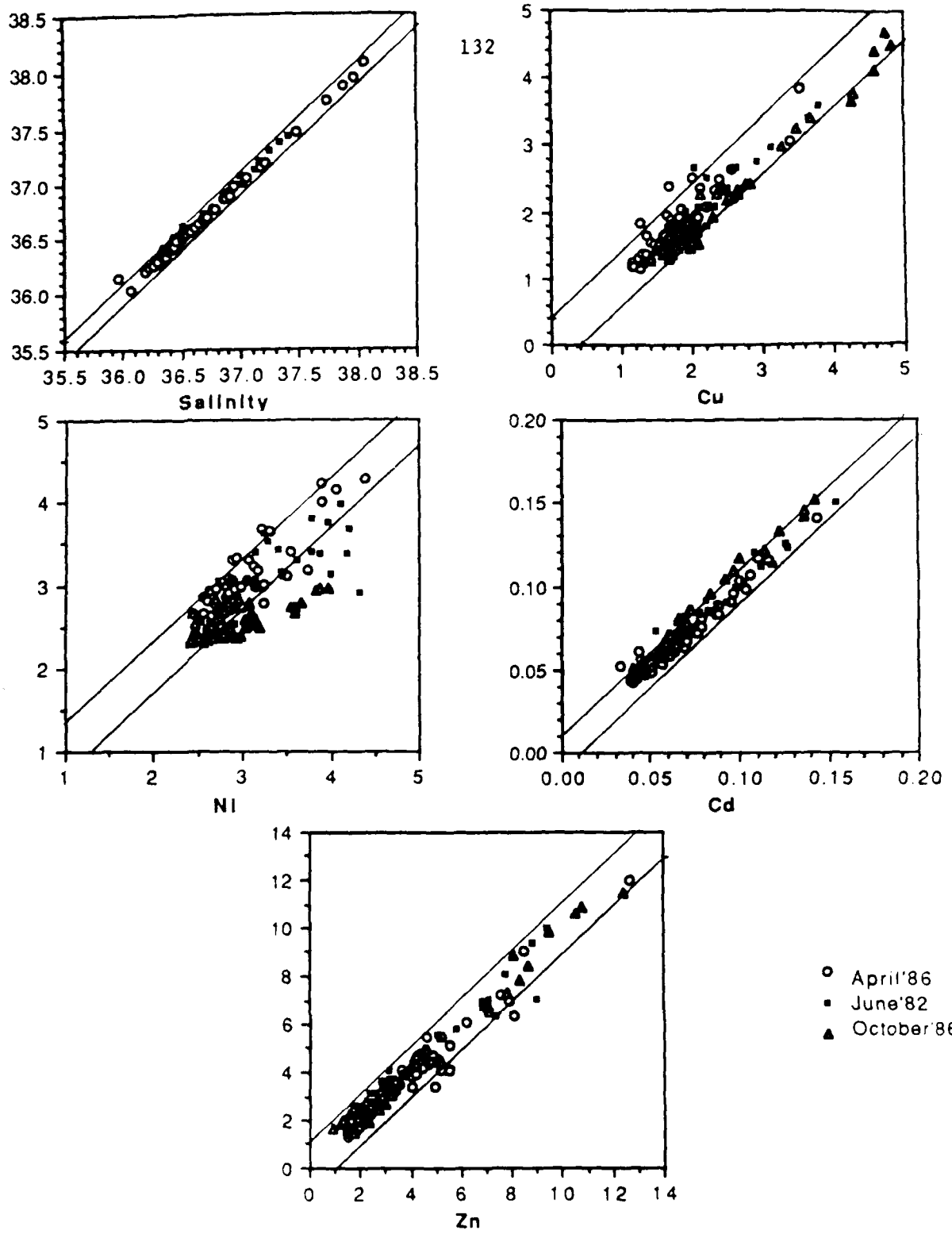


Fig. 5.6 Observed tracer data vs. model derived data  
All samples included, no corrections (see text)

model-derived salinity and Cd values agree with each other within the a priori error bands for most of the data. This reflects that both tracers (almost independently of other constraints) determine Mediterranean and NACW contributions, respectively, and therefore also control their own prediction (Chapter 4). In contrast, tracers that are redundant (e.g. Cu relative to Zn, or Ni relative to all other tracers) and therefore do not control their own prediction, provide a test for the assumptions of the mixing model: (1) conservative mixing and (2) the composition and choice of end-members. As shown in Fig. 5.6, there is also good agreement for most samples between observed and model-derived Zn and Cu concentrations. Surface enrichments in the Alboran Sea for these elements are indeed traceable to Spanish shelf water.

Since nutrients are not conservative in surface water and trace metals are removed by surface productivity, non-conservative mixing of metals can be examined by comparing both types of tracer. Potential non-conservative mixing, however, does not affect all tracers equally. Based on the composition of plankton determined by Collier and Edmond (1985), Cd should be much more sensitive to removal by phytoplankton than other metals of concern here. A 10 pM decrease in Cd concentration could be achieved by as little as a 0.015  $\mu\text{M}$  decrease in dissolved  $\text{PO}_4$  concentration, assuming stoichiometric uptake in proportion to the average metal/nutrient ratio of plankton. However, trace metals appear to be taken up in surface water less efficiently than nutrients in surface water (Boyle et al., 1985). In particular for the Gulf of Cadiz, uncoupling between nutrient and metal uptake was demonstrated: a

0.2  $\mu\text{M}$  decrease in  $\text{PO}_4$  concentration in shelf water advected to the open ocean was unaccompanied by detectable Cd, Cu or Zn removal (Chapter 3). Significant non-conservative behaviour for these elements therefore seems unlikely in the western Alboran Sea.

In contrast to Cu and Zn in the case of Spanish shelf water, there is no consistency check for the proportion of NACW dictated by Cd. Only an additional tracer significantly enriched in NACW could determine with greater certainty that the proportion of this end-member in surface water of the Alboran Sea is not, for instance, underestimated due to Cd removal. It is worth noting that NACW is required to explain surface Cd data because the sum of squared residuals increases sharply when neglecting this end-member in the regression (eg. from 0.3 to 6.1 for April sample # 180).

Agreement between observed and model-derived Ni concentrations is not as good as for the other four tracers (Fig. 5.6). Ni residuals are greater than one standard error unit (0.33 nM) for 1 sample out of a total of 55 in April'86, 2 out of 42 in June'82 and, 19 out 44 in October '86. Such deviations cannot be solely due to the small dynamic range between end-members with respect to Ni concentrations which reduces the weight of this element in its own prediction. In fact, a systematic error is suggested by observed concentrations greater than predicted values for all samples with large Ni residuals. The salinity-Ni relation of these samples (Fig. 5.5) shows how the two tracers conflict in their prediction of the proportion of Mediterranean deep water. Based on end-member compositions listed in Table 5.4, Ni concentrations in

October '86 correspond to as much as 50% more Mediterranean deep water than is dictated by salinity for samples in the northern half of the Alboran Sea. Rain input to the surface mixed layer diluting salinity by 1 °/oo (corresponding to the discrepancy with Ni) is unlikely: 135 cm of rain would be required for a mixed layer depth of 50 m. Therefore, Ni enrichments in October'86 (and an occasional sample in April'86 and June'82) suggest an additional, as yet unidentified, source for this element.

Keeping the limitations of the mixing model in mind, the distributions of water masses in April'86, June'82 and October'86 can be compared for samples in the region most directly reflecting the composition of the Atlantic inflow (Fig. 5.7-10). The regression for each sample in this region was done without considering Ni for all October'86 samples, April '86 sample # 181, and June'82 sample # 4. As indicated in Tables 5.1, 2, and 3, Cu or Zn constraints were neglected for 6 additional samples. After these corrections, the sum of squared residuals for each sample within Fig. 5.7 amounts to less than 3 standard error units. This indicates that the following main model results (Fig. 5.4) are consistent with the data: (1) penetration of Spanish shelf water into the Alboran Sea is greatest in June'86 and, as indicated by the 20% contribution contour, to the north of the shelf water core observed in April and October'86; (2) NACW is present in greater proportion in June'82 (up to 40%) than at other times (maximum of 23% and 21% in April and October '86, respectively) and closely follows the distribution of

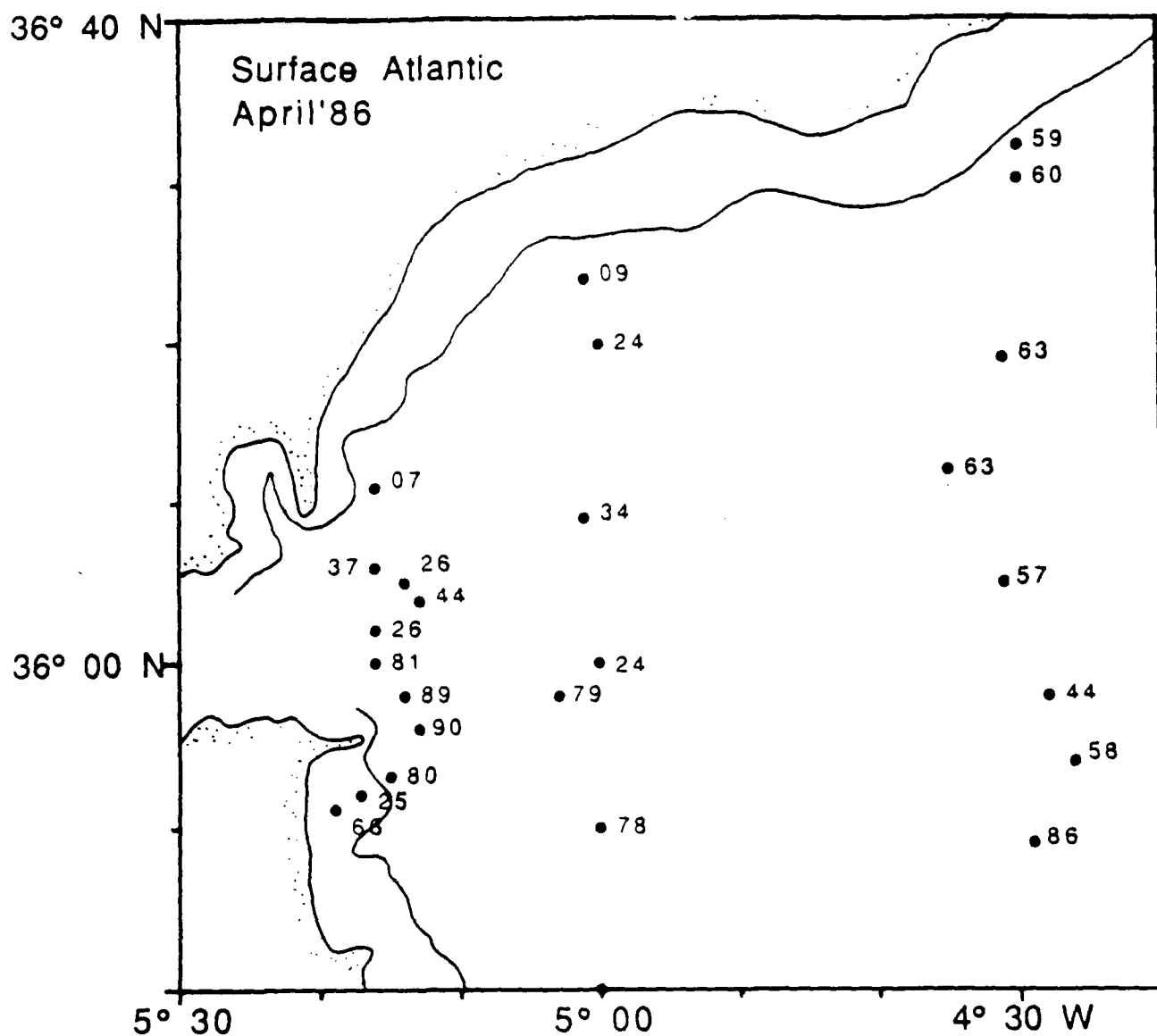


Fig. 5.7a Surface Atlantic end-member (%) distribution in the surface Alboran Sea water in April'86.

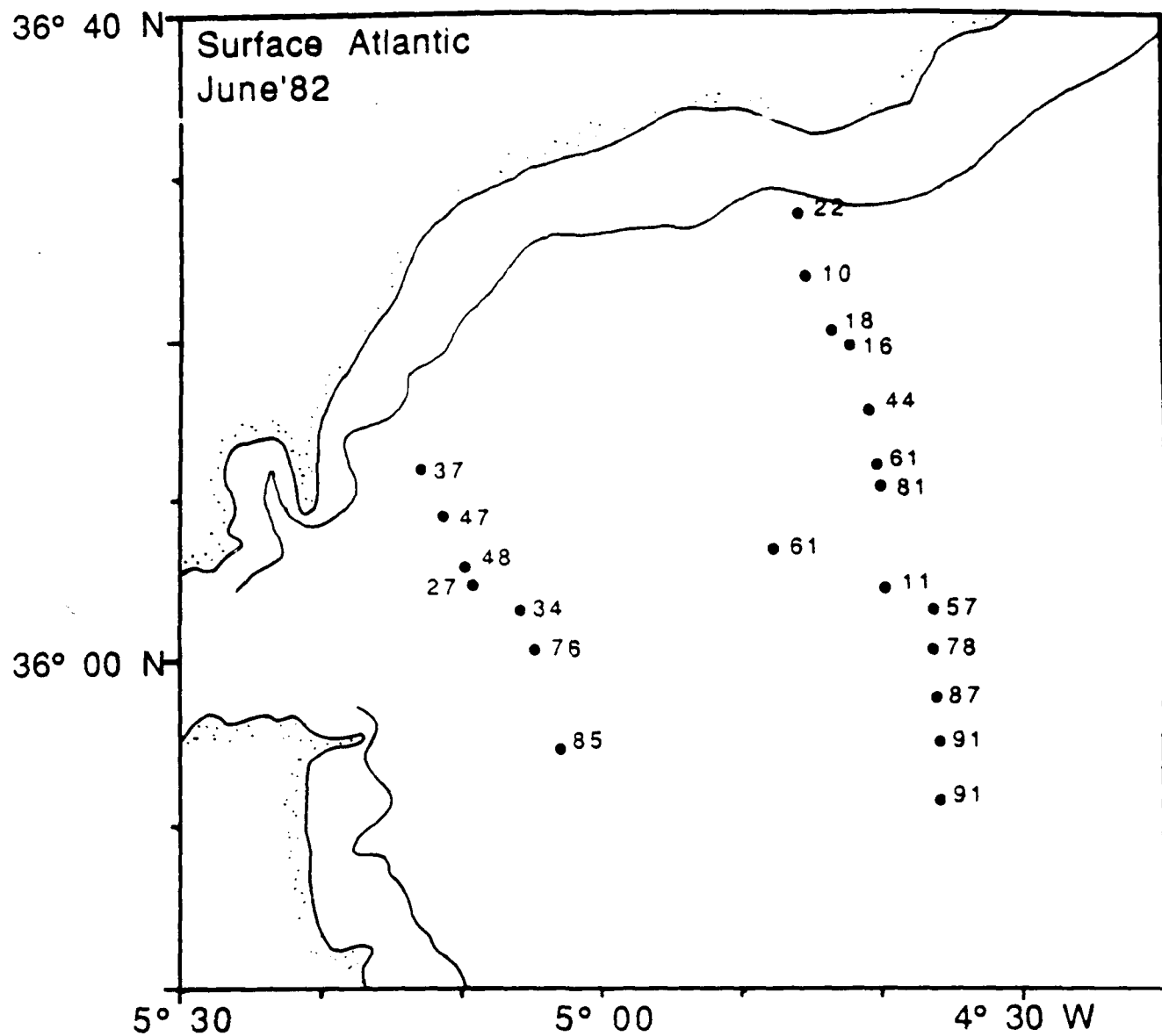


Fig. 5.7b Surface Atlantic end-member (%) distribution in the surface Alboran Sea water in June'82.

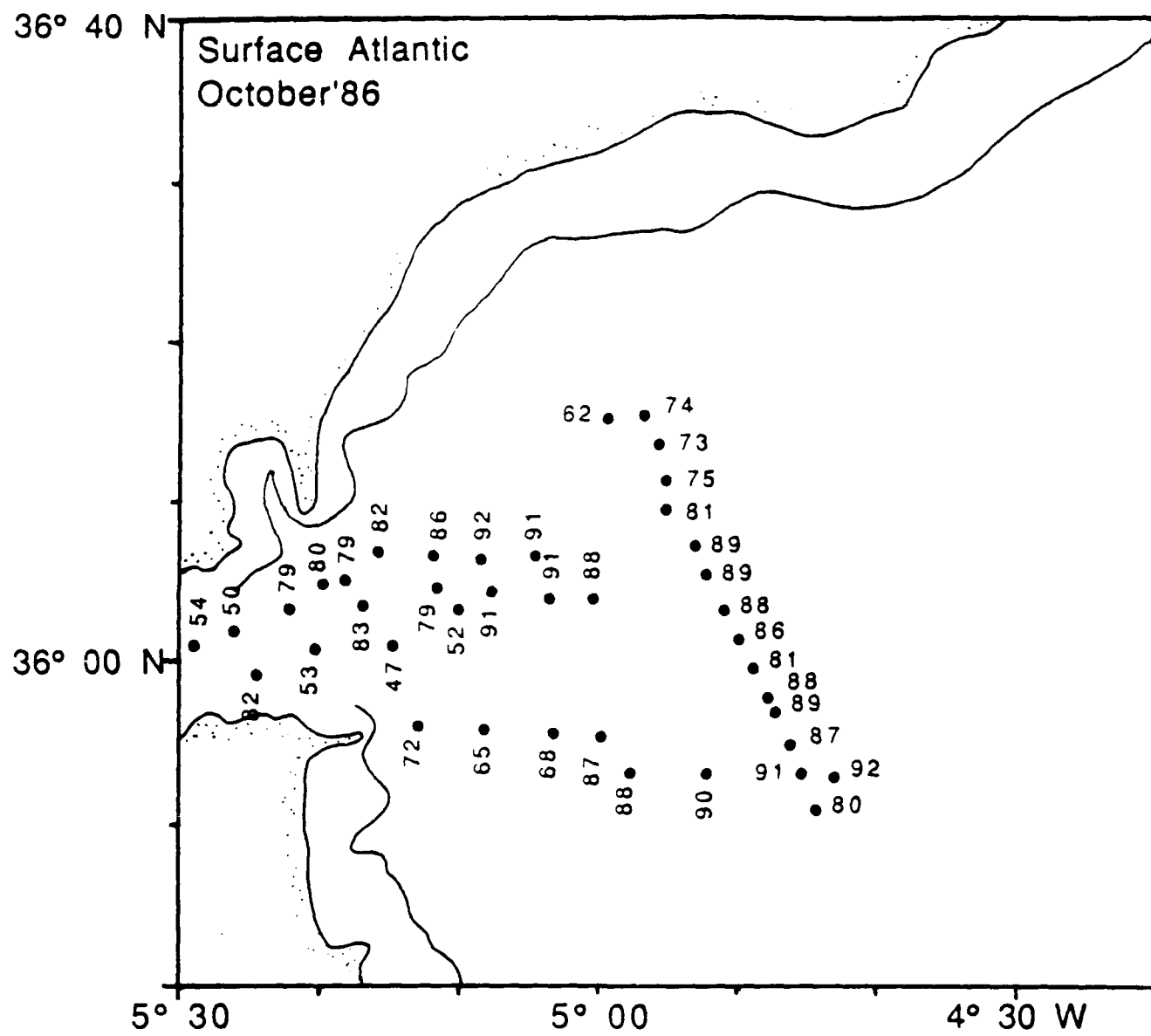


Fig. 5.7c Surface Atlantic end-member (%) distribution in the surface Alboran Sea water in October'86.

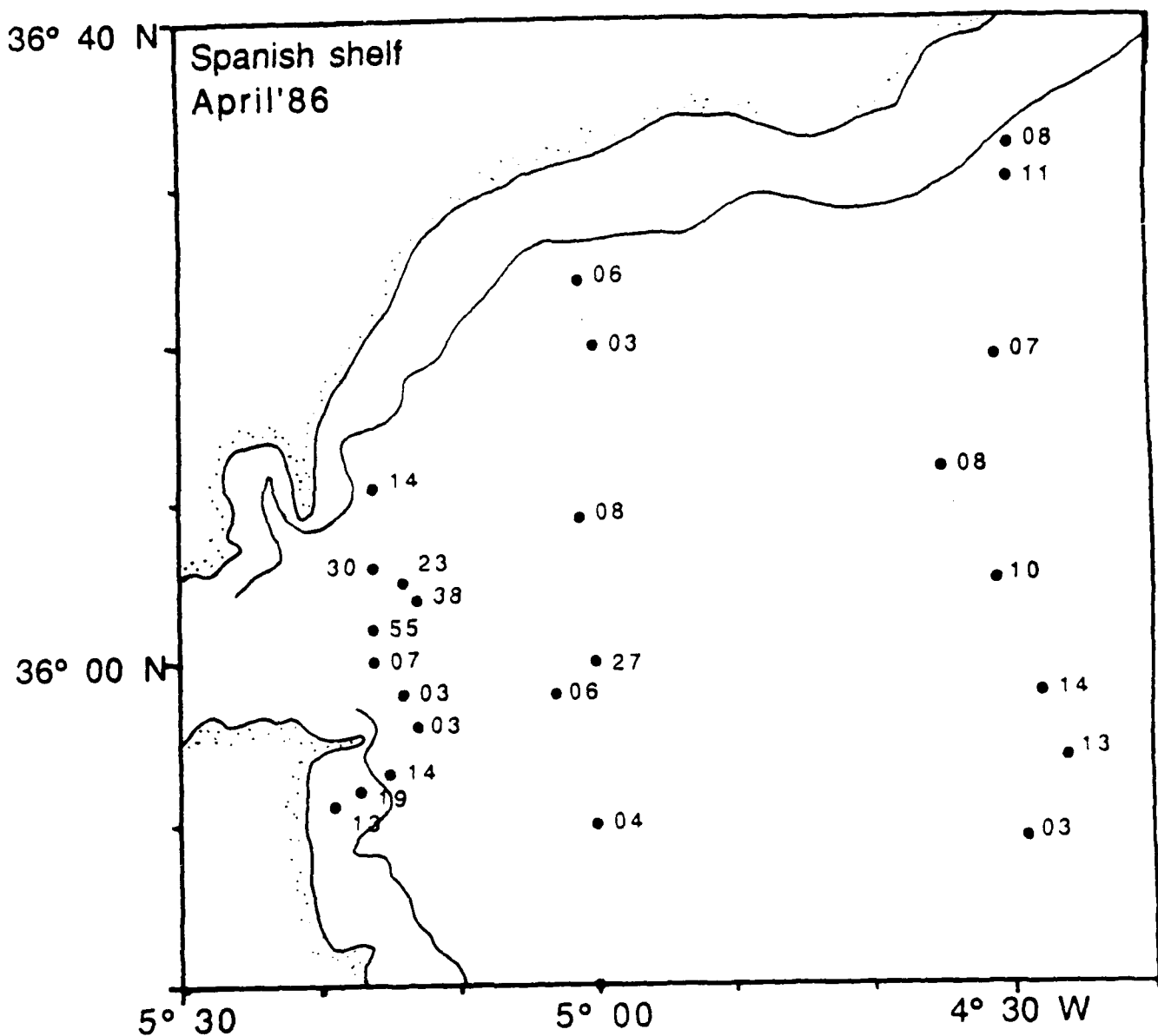


Fig. 5.8a Spanish shelf end-member (%) distribution in the surface  
Alboran Sea water in April'86

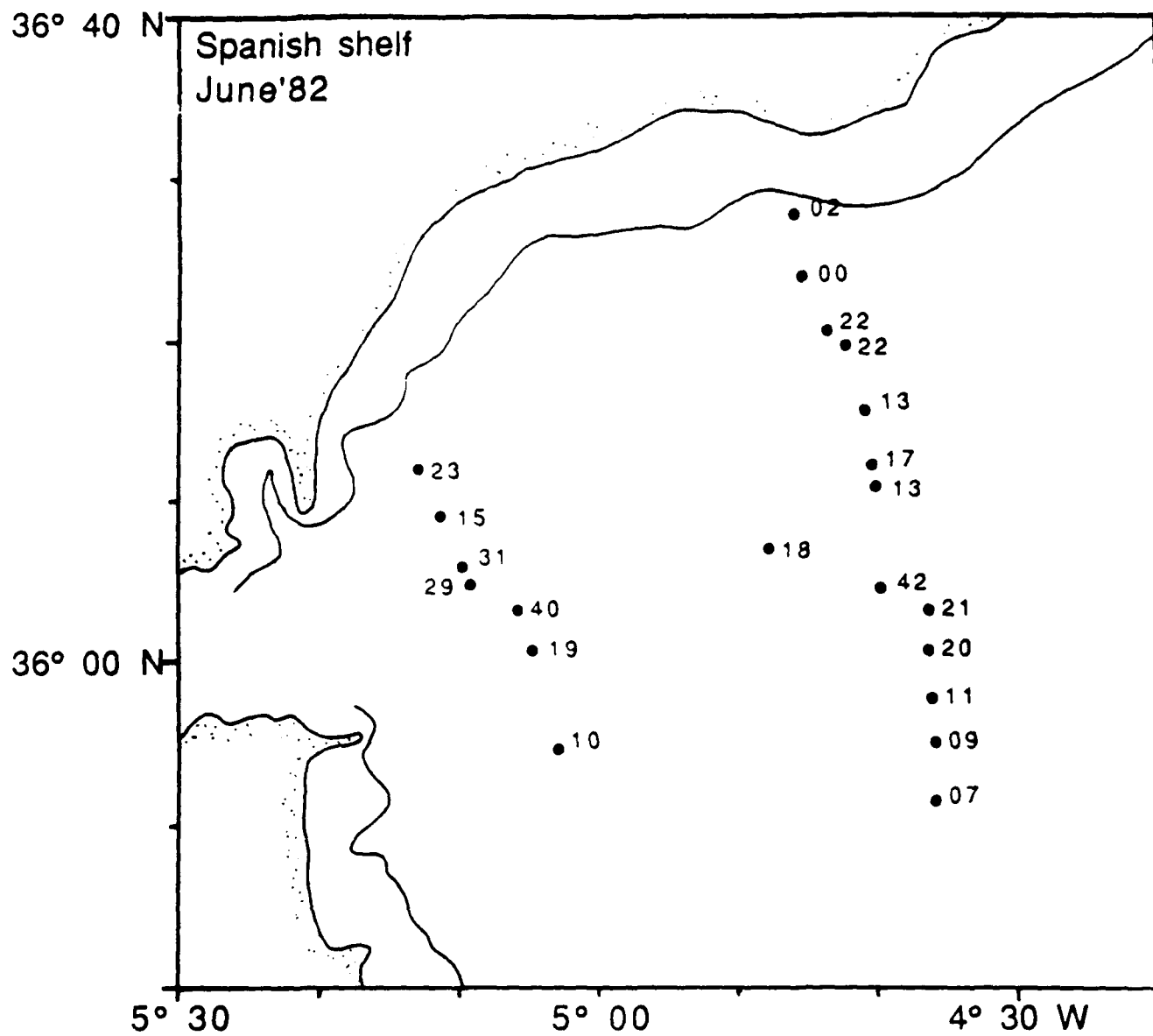


Fig. 5.8b Spanish shelf end-member (‰) distribution in the surface  
Alboran Sea water in June'82

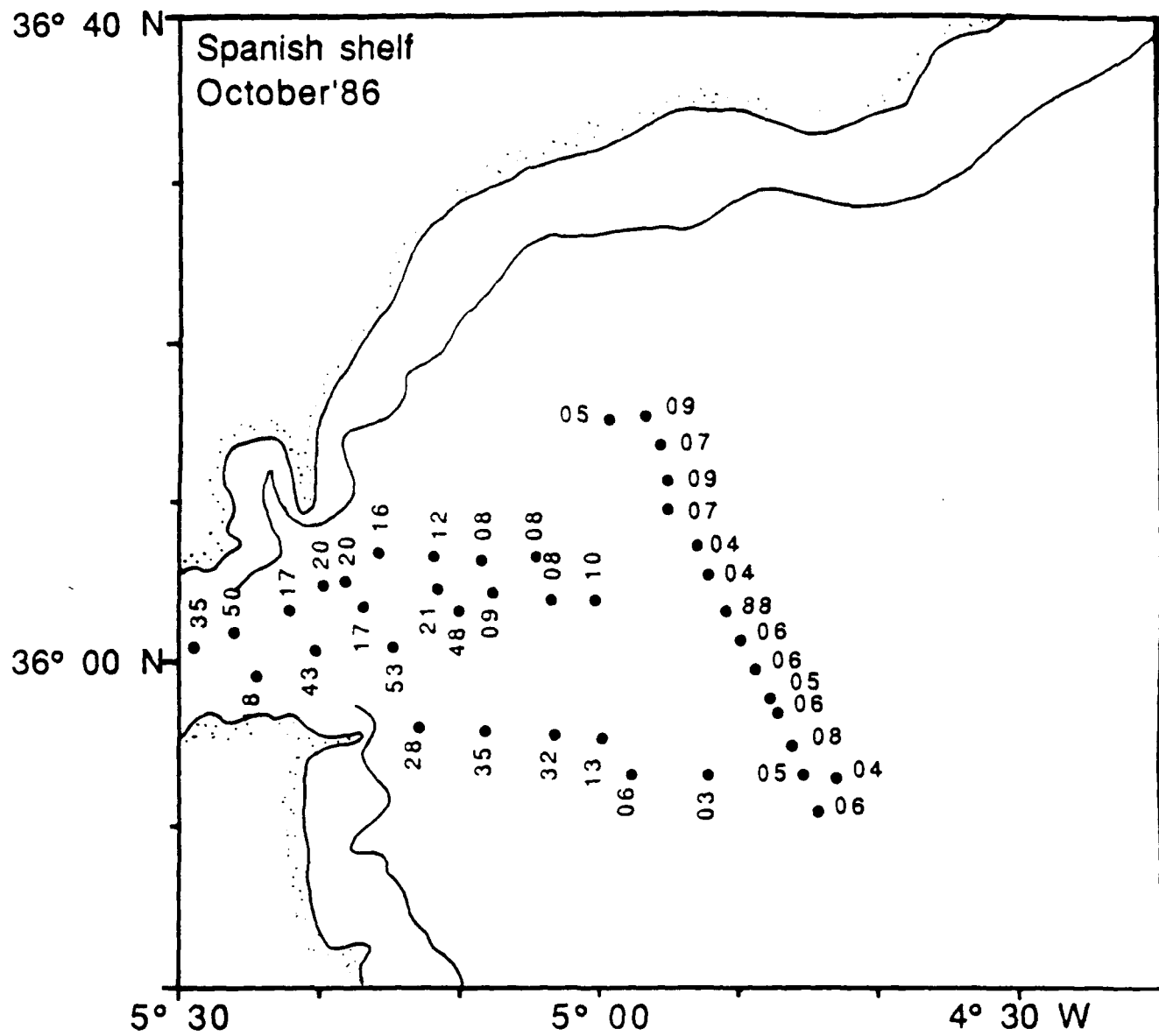


Fig. 5.8c Spanish shelf end-member (%) distribution in the surface  
Alboran Sea water in October'86.

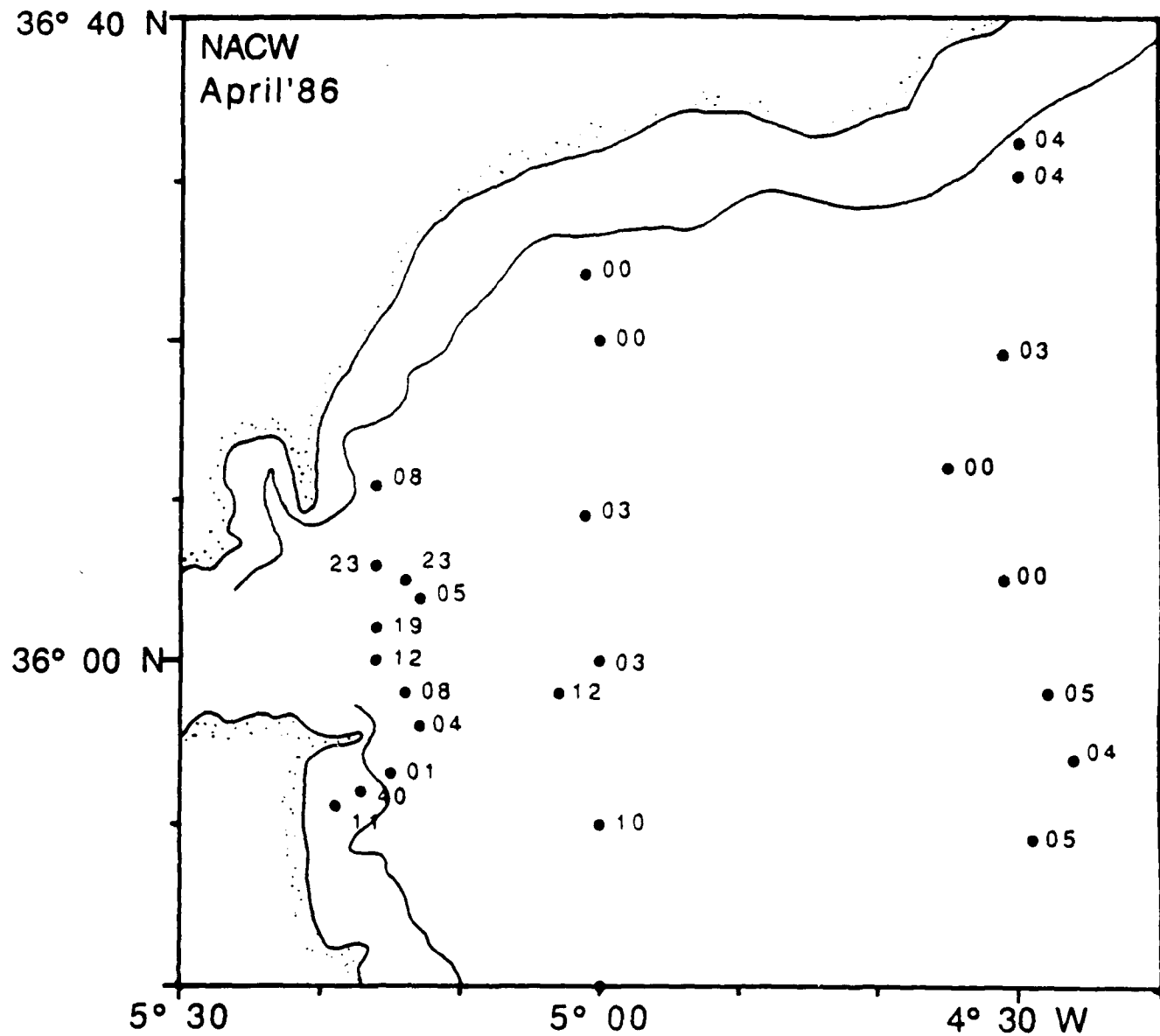


Fig. 5.9a NACW (%) distribution in the surface  
Alboran Sea water in April'86.

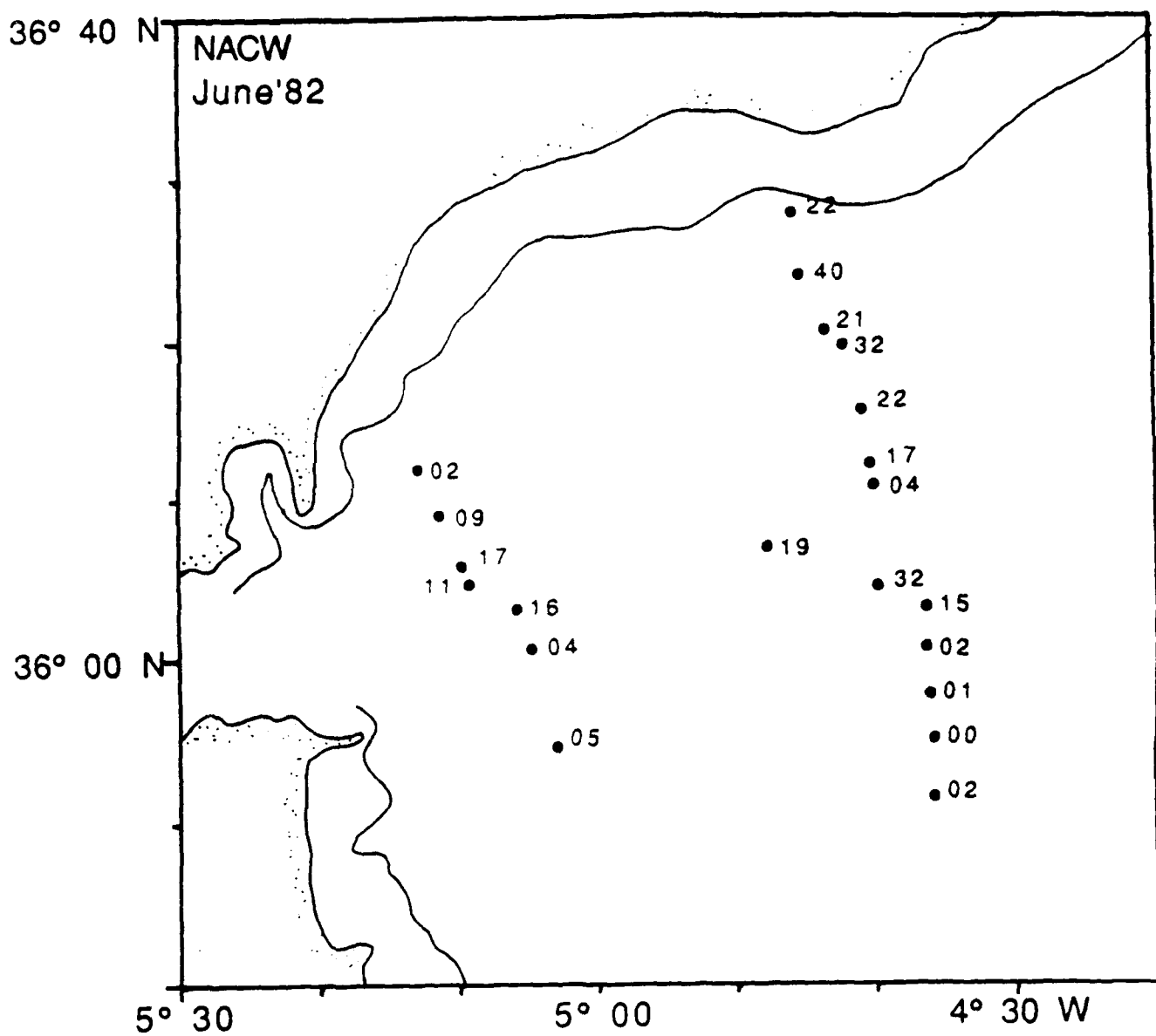


Fig. 5.9b NACW (%) distribution in the surface  
Alboran Sea water in June'82.

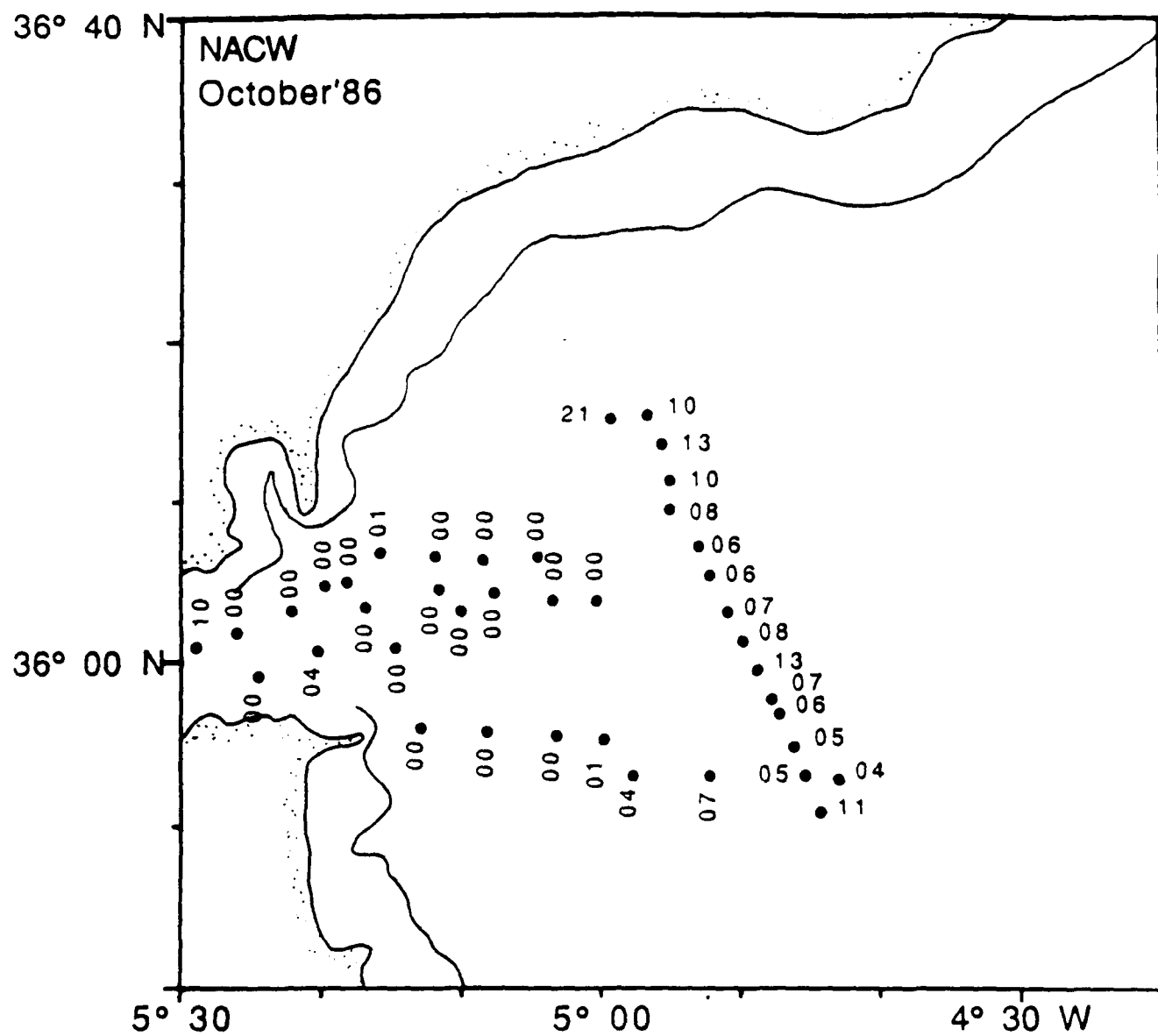


Fig. 5.9c NACW (%) distribution in the surface  
Alboran Sea water in October'86.

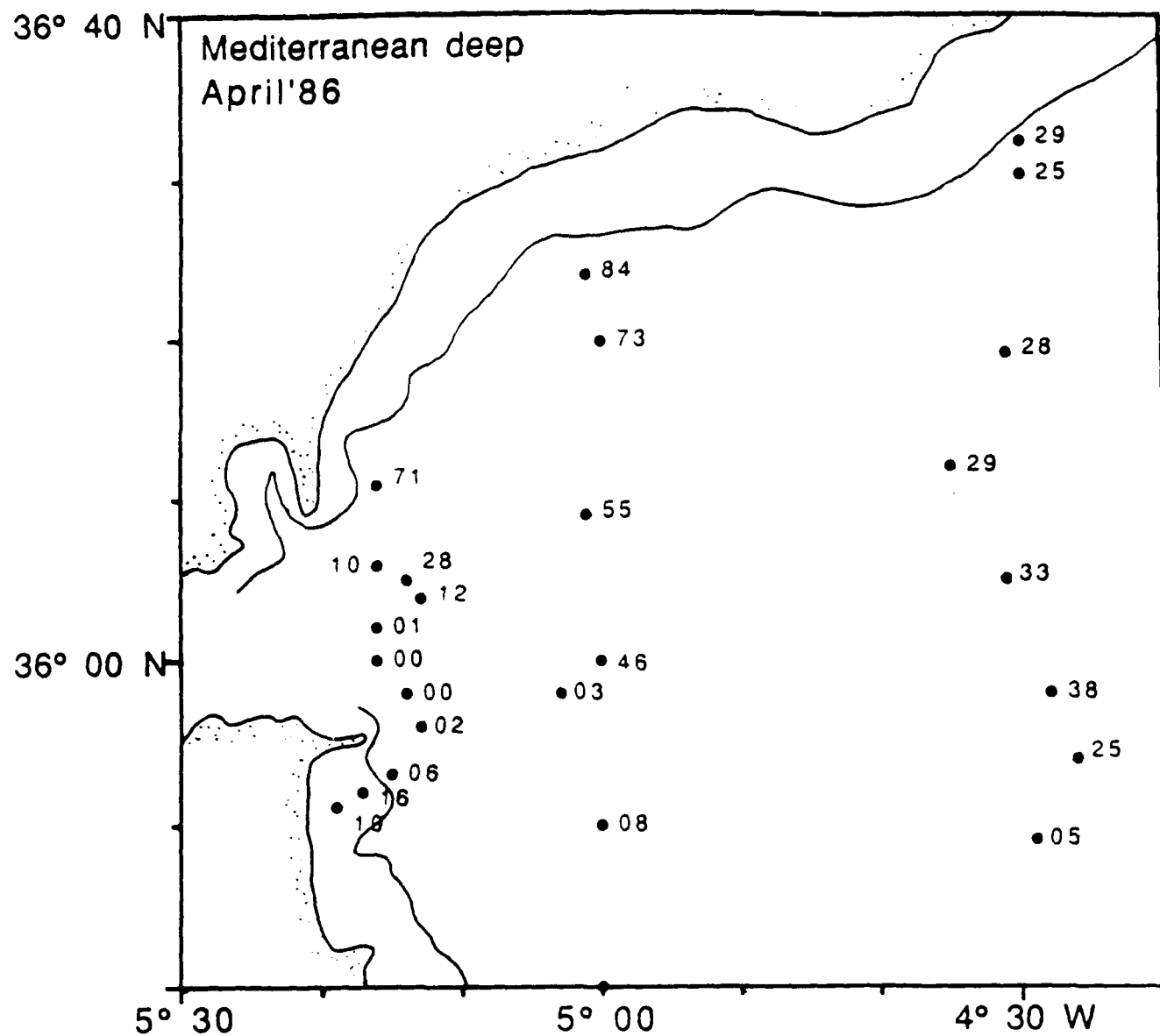


Fig. 5.10a Mediterranean deep end-member (%) distribution in the surface Alboran Sea water in April'86.

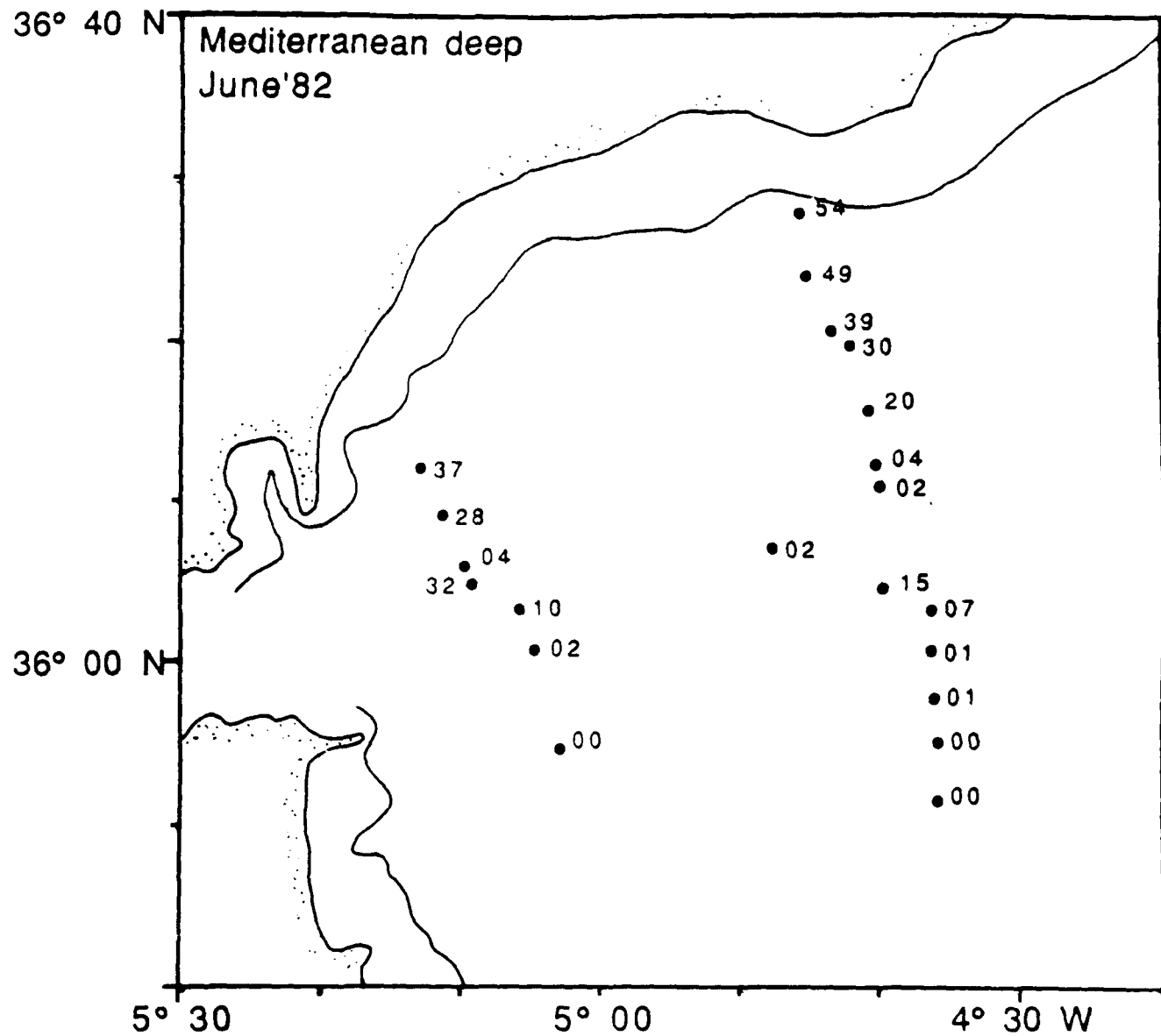


Fig. 5.10b Mediterranean deep end-member (%) distribution in the surface Alboran Sea water in June '82.

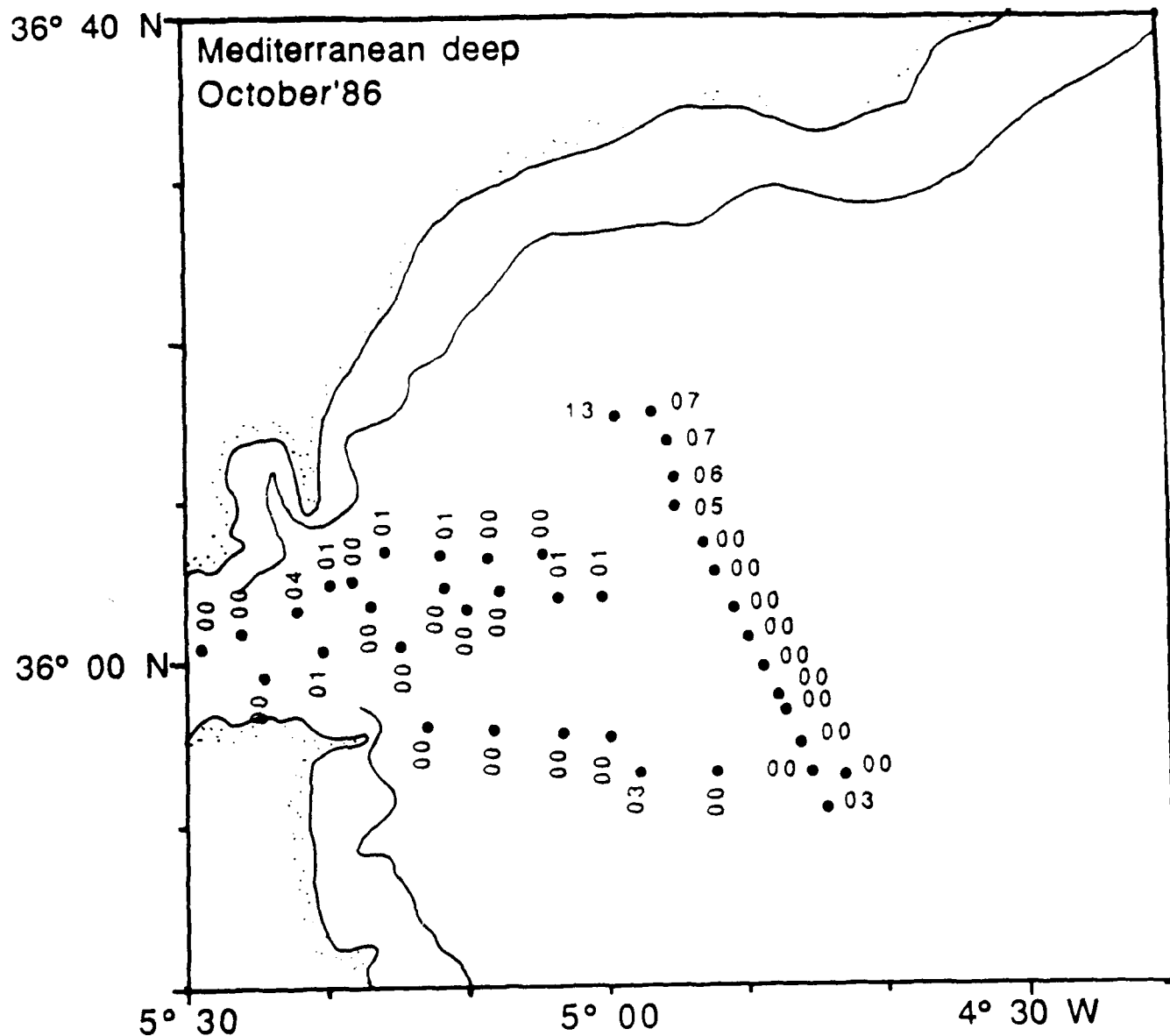


Fig. 5.10c Mediterranean deep end-member (%) distribution in the surface Alboran Sea water in October'86.

Spanish shelf water at that time, (3) the distribution of metal depleted surface Atlantic water varies considerably from one cruise to the other.

Interpreting temporal variations in the distribution of Atlantic end-members is complicated by the dynamic nature of surface circulation in the Alboran Sea. Current variations occur on times scale of hours (tides), weeks (spring vs. neap tides) and months (Ochoa and Bray, manuscript). In particular, the proportion of Spanish shelf water was shown to vary between 20 and 70% at the same location in the northern Strait of Gibraltar for samples taken one week apart (Chapter 4). High frequency variations in inflow composition should, however, be buffered by mixing in the western Alboran Sea since the residence time of water in the surface layer is approximately three weeks relative to the inflow. We believe that variations in the proportion of Spanish shelf water reflect seasonal changes in the composition of the inflow. However, the present data set cannot rule out modulation by the spring-neap cycle. Detailed time-series would be necessary to evaluate a potential link between surface distributions of end-members and spring tides at Gibraltar (June 22 '82, April 11 '86 and October xx '86, respectively).

An earlier attempt to determine the mass balance of Cu, Ni, Cd and Zn at the Strait of Gibraltar based on June '82 data (van Geen et al., 1988) can be revised based on the 1986 results. The composition of the Mediterranean outflow is well constrained, but a representative inflow composition appears much more difficult to determine due to variability in the proportion and/or composition of Spanish shelf water entering the

Alboran Sea. Trace metal concentration were on average lower in April and October'86 than in June'82 over the western Alboran Sea. Our previous calculation for the flow weighted composition of the Atlantic inflow may have overestimated average Cu, Cd and Zn concentrations over the course of a year.

Since the data is dominated by surface samples, overestimating the Spanish shelf water contribution could also be due to vertical stratification of the inflow. Tracer distributions for Station 4 collected in June'82 at 36°06'N, 5°10'W (5 km south-east of Gibraltar) provide a test for this possibility. Close to linear salinity-tracer relationships (Fig. 5.11, data in Table 5.5) indicate that the vertical distribution of Atlantic end-members is homogeneous as the inflow enters the Alboran Sea. In particular, Cu and Zn concentrations at 20 m depth which are not significantly lower than at the surface indicate Spanish shelf water is not restricted to a thin surface layer. Elevated Cd concentrations at 20m depth, on the other hand, indicate that the contribution of NACW to the inflow may be underestimated by surface samples.

Seasonal differences between metal distributions are reduced when considering samples closest to the Strait of Gibraltar only. Based on a simple average of samples across the eastern end of the Strait, the following end-member composition is obtained for the Atlantic inflow (1) April'86: 57, 27, and 16% for surface Atlantic, Spanish shelf and NACW respectively, (2) June'82: 58, 30, and 11%, (3) October'86: 74, 25 and 0%. Multiplying these contributions by the respective end-member metal

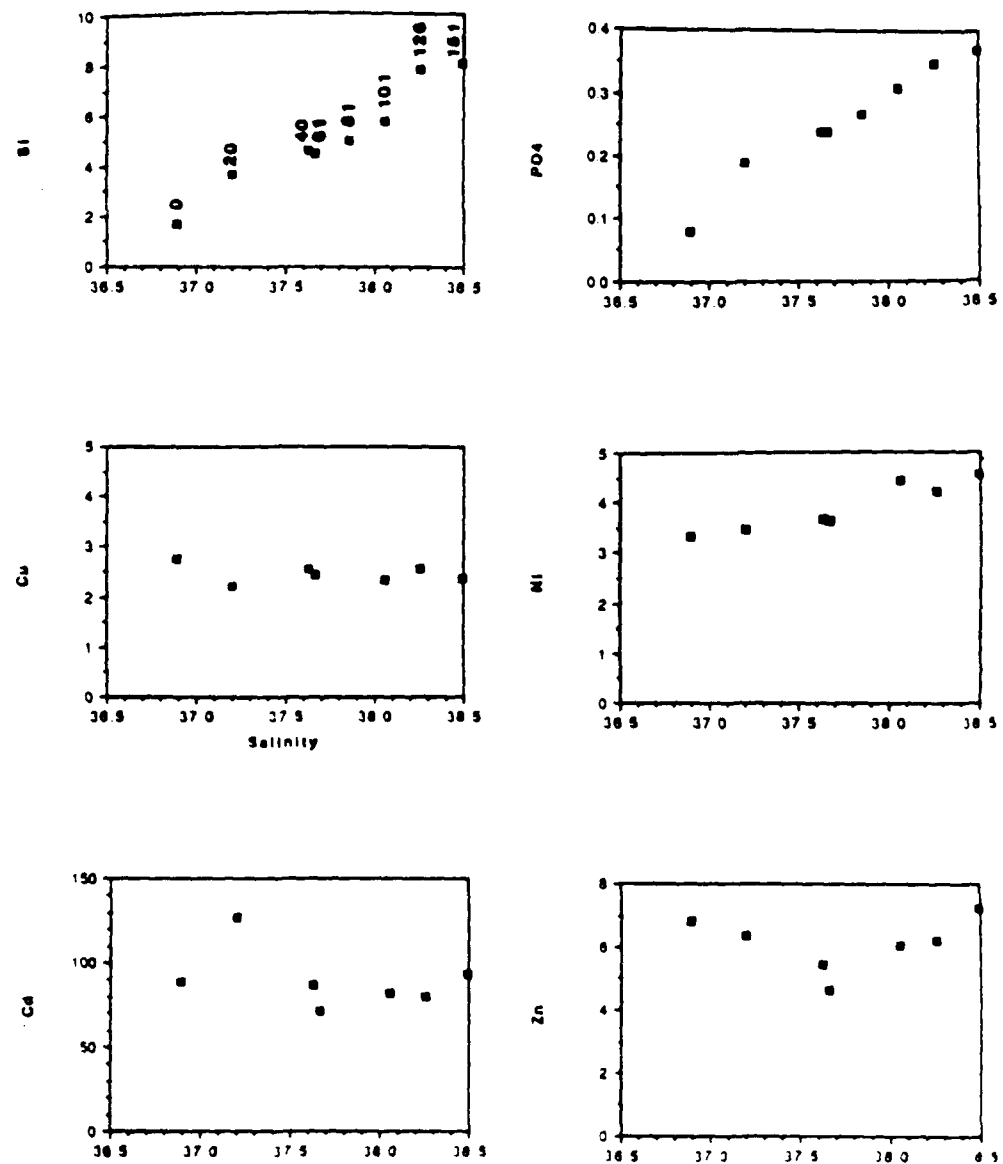


Fig. 5.11 Salinity ‰ vs. Si  $\mu\text{M}$ ,  $\text{PO}_4$   $\mu\text{M}$ ,  
 Cu, Ni, Cd and Zn (nM) at Station 4 (June '82).  
 Sample depths indicated in meters.

concentrations (Table 5.4), and finally averaging the resulting compositions for the three sampling times, yields the following estimate of the inflow composition: Cu: 2.6 nM, Ni: 2.6 nM, Cd: 92 pM and Zn: 6.2 nM. It should be noted that if velocities into the Alboran Sea are higher in the core of the Spanish shelf water plume, the contribution of this end-member is underestimated by this approach. These results confirm that no net source within the Mediterranean basin is required to explain Cu, Cd and Zn enrichments in the saline outflow relative to nutrient depleted surface Atlantic water. Some of the enrichment, however, must be internal to the basin since Cu, Cd, Zn, and especially, Ni concentrations, increase to the east in surface waters of the Mediterranean (Spivack et al., 1983).

#### CONCLUSION

We have shown that trace metals are unique tracers of Spanish shelf water, surface Atlantic water, NACW and Mediterranean water in the surface waters Alboran Sea. The complex distributions of Cu, Ni, Cd, Ni and salinity can be explained by conservative mixing of these four end-members in most cases. Such tracers may eventually contribute to quantitative modelling of surface circulation from the Gulf of Cadiz to the Alboran Sea when combined with the extensive CTD coverage obtained at the time of chemical sampling in June'82 and April'86, and within a few weeks in October'86.

Repeated sampling of a metal enriched plume in the Alboran Sea confirms the important role of Spanish shelf water in influencing the composition

of a basin as large as the Mediterranean. Inflow and outflow fluxes of Cu, Cd and Zn through the Strait of Gibraltar are close to balanced, given the uncertainty in the inflow estimate. A better constrained determination of contemporary metal fluxes through the Strait would require a sampling and analysis effort beyond current technology and resources.

#### ACKNOWLEDGEMENTS

Space and time were generously provided during the Gibraltar Experiment by Tom Kinder and Nan Bray on board USNS Lynch. We thank E. Callahan, C. Measures and H. Yee for help in collecting samples.

Station	Latitude	Longitude	Salinity	Si	POA	Qu	W	Cu	Na	All	Sp Shell	NaCl	Residual Sq
113	36.000	-3.500	36.565	0.53	0.08	2.0	2.6	0.052	2.9	0.75	0.11	0.00	0.14
114	36.183	-3.483	36.570	0.45	0.06	1.2	2.6	0.047	1.5	0.77	0.00	0.09	0.15
115	36.333	-3.517	35.989	0.55	0.06	1.3	2.5	0.045	1.5	0.79	0.02	0.19	0.00
116	36.417	-3.483	36.898	0.53	0.07	1.5	2.6	0.050	2.4	0.77	0.06	0.02	0.17
119	36.500	-3.500	36.794	0.42	0.07	1.5	2.6	0.057	2.9	0.68	0.06	0.02	1.02
120	36.583	-3.500	37.179	2.32	0.14	1.4	2.9	0.069	3.3	0.48	0.03	0.07	0.42
123	36.667	-3.517	37.982	3.83	0.19	2.1	3.9	0.087	4.4	0.09	0.04	0.08	0.79
171	35.850	-5.317	36.409	1.17	0.09	1.7	2.9	0.086	4.0	0.68	0.13	0.11	0.10
172	35.867	-5.283	36.354	1.09	0.08	2.6	3.1	0.117	4.6	0.25	0.18	0.40	0.16
173	35.877	-5.245	36.358	1.19	0.10	1.7	2.6	0.052	4.2	0.80	0.14	0.00	0.05
174	35.888	-5.250	36.383	1.22	0.09	1.8	2.7	0.053	3.8	0.80	0.14	0.01	0.06
175	35.933	-5.217	36.289	1.22	0.12	1.1	2.5	0.040	1.8	0.90	0.03	0.04	0.02
176	35.967	-5.233	36.218	1.09	0.12	1.2	2.5	0.042	1.6	0.89	0.03	0.00	0.34
177	36.000	-5.267	36.193	1.27	0.12	1.4	2.6	0.053	2.4	0.81	0.07	0.12	0.00
178	36.033	-5.267	36.083	1.41	0.20	3.5	2.8	0.144	12.7	0.26	0.55	0.19	2.18
179	36.067	-5.217	36.400	2.11	0.19	3.4	3.2	0.100	8.5	0.44	0.38	0.05	0.62
180	36.083	-5.233	36.693	2.41	0.22	2.4	3.5	0.106	7.0	0.26	0.23	0.23	0.27
181	36.100	-5.267	36.284	3.18	0.22	2.6	3.7	0.110	7.6	0.37	0.30	0.23	0.10
184	36.183	-5.267	37.792	3.20	0.17	2.1	4.0	0.097	7.1	0.07	0.14	0.08	0.71
185	36.400	-5.017	38.986	3.45	0.17	2.2	4.4	0.079	5.2	0.09	0.06	0.00	0.30
186	36.333	-5.000	37.881	2.33	0.12	1.7	3.9	0.068	4.7	0.24	0.03	0.00	0.73
187	36.150	-5.017	37.475	1.39	0.07	1.8	3.3	0.077	4.8	0.34	0.08	0.03	0.55
188	36.000	-5.000	37.219	2.23	0.21	2.0	3.2	0.104	7.9	0.24	0.27	0.09	0.46
189	35.987	-5.050	36.262	1.04	0.10	1.3	2.6	0.054	2.3	0.79	0.08	0.12	0.03
190	35.833	-5.000	36.391	1.46	0.12	1.2	2.7	0.050	2.1	0.78	0.04	0.10	0.08
191	35.687	-5.000	36.454	1.60	0.19	1.3	3.2	0.084	5.5	0.83	0.13	0.10	0.14
192	35.483	-5.000	36.426	1.36	0.13	1.4	2.9	0.071	4.0	0.81	0.10	0.17	0.12
193	35.350	-4.733	36.395	1.18	0.16	1.9	3.0	0.066	4.0	0.84	0.14	0.12	0.11
194	35.217	-4.483	36.381	1.50	0.10	1.7	2.6	0.050	4.5	0.78	0.15	0.03	0.21
195	35.333	-4.500	36.384	0.78	0.09	1.7	2.4	0.074	6.1	0.68	0.26	0.00	0.28
196	35.500	-4.533	36.387	0.75	0.08	1.6	2.7	0.033	5.0	0.83	0.12	0.00	0.36
197	35.650	-4.450	36.370	1.28	0.10	1.6	2.6	0.095	5.0	0.47	0.15	0.26	1.34
198	35.817	-4.483	36.325	1.04	0.10	1.2	2.8	0.038	2.0	0.86	0.03	0.05	1.97
199	35.900	-4.433	36.782	1.71	0.12	1.9	3.1	0.035	4.3	0.58	0.13	0.04	0.27
200	35.867	-4.487	37.057	2.62	0.28	1.6	3.1	0.079	5.5	0.44	0.14	0.05	0.38
201	36.083	-4.517	36.950	2.41	0.22	1.8	3.5	0.043	5.2	0.57	0.10	0.00	0.33
202	36.200	-4.583	36.873	0.59	0.19	1.8	3.2	0.052	3.4	0.63	0.08	0.00	0.29
203	36.317	-4.517	36.858	0.43	0.06	1.7	3.0	0.057	3.0	0.63	0.07	0.03	0.28
204	36.500	-4.500	36.797	0.72	0.06	1.8	2.7	0.068	4.0	0.60	0.11	0.04	0.22
205	36.533	-4.500	36.852	0.80	0.12	1.6	2.8	0.063	3.5	0.59	0.08	0.04	0.25
206	36.633	-4.217	36.773	0.67	0.04	1.9	2.8	0.055	3.7	0.60	0.10	0.05	0.15
207	36.667	-3.983	36.913	1.02	0.06	2.1	3.2	0.073	4.4	0.49	0.13	0.06	0.32
208	36.500	-4.000	36.869	0.83	0.04	1.7	2.8	0.060	3.0	0.65	0.07	0.03	0.21
209	36.333	-4.000	36.848	0.70	0.04	1.6	2.7	0.060	3.6	0.69	0.10	0.04	0.21
210	36.167	-4.000	36.686	0.53	0.03	1.6	2.6	0.061	3.4	0.68	0.08	0.04	0.19
211	36.000	-4.000	36.712	0.51	0.04	1.9	2.9	0.077	3.3	0.51	0.09	0.16	0.24
212	35.833	-4.000	36.542	1.23	0.06	1.9	2.8	0.072	4.0	0.60	0.13	0.11	0.16
213	35.887	-4.000	36.804	2.08	0.17	2.3	3.0	0.088	6.2	0.47	0.22	0.11	0.20
214	35.533	-4.000	36.388	1.63	0.09	0.9	2.2	0.041	2.2	0.00	0.00	0.00	0.00
215	35.387	-3.983	36.395	1.71	0.09	1.1	2.0	0.040	2.0	0.00	0.00	0.00	0.00
216	35.387	-3.700	36.433	1.58	0.10	2.0	2.7	0.063	3.6	0.70	0.14	0.06	0.10
217	35.350	-3.500	36.513	2.19	0.13	1.9	2.8	0.076	4.2	0.56	0.14	0.16	0.10
218	35.483	-3.500	36.518	1.71	0.12	1.7	2.8	0.063	4.0	0.68	0.12	0.06	0.11
219	35.667	-3.500	36.914	0.84	0.07	1.6	2.9	0.088	3.8	0.38	0.08	0.20	0.34
220	35.633	-3.483	36.772	1.55	0.12	1.7	2.8	0.070	4.6	0.54	0.13	0.04	0.24

Table 5.1 April surface sample composition, & end-members and sum of squared residuals.

Station	Latitude	Longitude	Salinity	Si	PO4	Cl	Ni	Cr	Zn	Surf All	Sp Shell	MACW	Med	Residual Sq
39	35.848	-4.738	36.438	0.03	1.54	2.6	0.1	1.870	0.8	0.06	0.11	0.03	0.13	0.38
40	35.882	-4.713	36.447	0.03	1.40	2.6	0.0	1.500	0.9	0.04	0.04	0.00	0.11	0.92
41	35.883	-4.755	36.422	0.04	1.41	2.6	0.0	1.610	0.9	0.05	0.05	0.00	0.13	0.81
43	35.883	-4.868	36.382	0.02	1.30	2.6	0.0	1.690	0.9	0.03	0.07	0.00	0.35	0.99
44	35.885	-4.962	36.498	0.05	1.40	2.6	0.0	2.280	0.9	0.06	0.04	0.03	0.05	3.92
45	35.922	-4.997	36.399	0.05	1.95	2.7	0.1	3.360	0.9	0.13	0.01	0.00	0.29	1.07
46	35.925	-5.053	36.328	0.09	3.48	2.7	0.1	7.820	0.7	0.32	0.00	0.00	2.34	2.46
47	35.928	-5.137	36.357	0.12	3.69	2.7	0.1	8.310	0.7	0.35	0.00	0.00	2.50	2.62
48	35.935	-5.217	36.368	0.12	3.26	2.5	0.1	7.110	0.7	0.28	0.00	0.00	2.54	2.59
65	35.987	-5.410	36.329	0.05	2.34	2.5	0.1	5.160	0.8	0.18	0.00	0.00	0.05	2.58
67	36.013	-5.337	36.318	0.14	4.60	2.9	0.1	9.460	0.5	0.43	0.04	0.01	0.00	3.57
69	36.015	-5.247	36.284	0.20	4.73	2.7	0.1	12.450	0.5	0.53	0.00	0.00	1.87	2.06
72	36.055	-5.187	36.288	0.15	4.59	3.1	0.1	10.520	0.5	0.48	0.00	0.00	0.68	1.37
74	36.057	-5.280	36.436	0.08	2.52	3.2	0.1	4.170	0.8	0.17	0.00	0.00	1.81	6.81
75	36.083	-5.302	36.437	0.08	2.75	3.1	0.1	4.570	0.8	0.20	0.00	0.00	1.55	5.30
77	36.077	-5.192	36.420	0.05	2.82	3.6	0.1	6.620	0.8	0.21	0.00	0.00	1.68	11.60
78	36.072	-5.127	36.471	0.04	2.00	2.9	0.0	2.240	0.9	0.09	0.00	0.00	1.83	4.83
79	36.067	-5.057	36.489	0.02	1.72	3.0	0.0	2.190	0.9	0.08	0.00	0.01	0.35	4.07
80	36.067	-5.003	36.479	0.02	1.68	2.9	0.1	2.970	0.9	0.10	0.00	0.01	0.02	1.60
81	36.093	-5.993	36.481	0.02	1.80	2.8	0.1	3.220	0.9	0.11	0.00	0.01	0.01	1.17
82	36.110	-5.077	36.470	0.03	1.54	2.5	0.1	4.620	0.8	0.21	0.00	0.00	0.00	1.60
83	36.108	-5.140	36.481	0.03	1.93	3.0	0.0	2.380	0.9	0.08	0.00	0.00	1.95	5.57
84	36.110	-5.198	36.484	0.01	2.10	3.1	0.1	2.810	0.9	0.12	0.00	0.01	0.75	4.20
85	36.113	-5.265	36.455	0.06	2.29	3.7	0.1	3.400	0.8	0.16	0.01	0.01	0.67	10.56
86	36.080	-5.330	36.446	0.05	2.68	3.6	0.1	4.150	0.8	0.20	0.00	0.01	1.19	10.02
87	36.053	-5.370	36.520	0.06	2.51	3.5	0.1	4.030	0.8	0.17	0.00	0.04	0.95	8.56
88	36.032	-5.433	36.288	0.22	4.82	2.8	0.1	10.750	0.5	0.50	0.00	0.00	1.60	1.80
89	36.015	-5.482	36.290	0.13	4.30	2.8	0.1	8.030	0.5	0.35	10.00	0.00	0.00	3.92
108	35.917	-4.767	36.356	0.03	1.77	2.8	0.1	2.360	0.9	0.08	0.05	0.00	1.00	2.84
109	35.950	-4.785	36.366	0.03	1.59	2.6	0.0	1.860	0.9	0.06	0.00	0.00	1.44	3.64
110	35.983	-4.792	36.385	0.03	1.58	2.8	0.0	1.500	0.9	0.05	0.07	0.00	0.68	2.43
111	35.993	-4.812	36.368	0.03	1.72	3.0	0.1	1.230	0.8	0.08	0.13	0.00	1.37	3.95
112	36.025	-4.830	36.375	0.03	1.72	2.8	0.1	1.340	0.9	0.06	0.08	0.00	1.44	3.03
113	36.055	-4.848	36.374	0.04	1.69	2.9	0.0	1.210	0.9	0.05	0.07	0.00	1.64	3.84
114	36.080	-4.868	36.387	0.02	1.67	2.6	0.0	0.930	0.9	0.04	0.06	0.00	1.98	3.64
115	36.122	-4.883	36.359	0.03	1.59	2.4	0.0	1.490	0.9	0.05	0.07	0.00	1.26	1.32
116	36.158	-4.917	36.507	0.02	1.70	3.1	0.1	1.970	0.8	0.07	0.08	0.05	0.52	2.93
117	36.188	-4.915	36.506	0.03	2.00	4.0	0.1	2.100	0.8	0.09	0.10	0.06	1.42	14.17
118	36.227	-4.925	36.523	0.02	1.98	3.9	0.1	1.590	0.7	0.07	0.13	0.07	2.20	12.70
119	36.258	-4.942	36.523	0.02	2.08	3.8	0.1	1.700	0.7	0.09	0.10	0.07	2.74	12.77
120	36.253	-4.988	36.568	0.02	1.75	3.0	0.1	1.670	0.6	0.05	0.21	0.13	1.08	1.25

Table 5.2 October surface sample composition, % end-members and sum of squared residuals.

Station	Latitude	Longitude	Salinity	Si	PO <sub>4</sub>	Ni	Cr	Zn	Surf All	Sp Shell	NACW	Med	Residual Sq
1	35.910	-5.050	36.400	0.55	0.00	1.8	2.6	0.051	2.4	0.85	0.10	0.05	0.00
2	36.012	-5.078	36.400	0.91	0.01	2.3	2.7	0.087	4.2	0.76	0.19	0.04	0.02
3	36.055	-5.098	36.370	1.74	0.13	3.6	3.1	0.125	6.8	0.34	0.40	0.16	0.10
4	36.100	-5.160	36.290	3.26	0.15	2.9	4.0	0.108	7.1	0.48	0.31	0.17	0.04
5	36.150	-5.187	36.880	2.05	0.00	2.2	3.4	0.077	7.3	0.47	0.15	0.09	0.28
6	36.200	-5.217	37.000	0.49	0.01	2.0	4.2	0.081	9.0	0.37	0.23	0.02	0.37
7	36.080	-5.153	36.890	1.67	0.08	3.1	3.4	0.112	7.7	0.27	0.29	0.11	0.32
8	36.117	-4.792	36.280	1.51	0.21	2.2	2.8	0.084	4.4	0.61	0.18	0.19	0.02
10	36.180	-4.665	36.430	0.22	0.06	2.1	2.7	0.056	2.9	0.81	0.13	0.04	0.02
11	36.078	-4.660	36.370	1.34	0.38	3.8	3.1	0.155	9.4	0.11	0.42	0.32	0.15
12	36.052	-4.607	36.400	1.34	0.12	2.4	3.0	0.087	5.1	0.57	0.21	0.15	0.07
13	36.012	-4.607	36.390	0.64	0.18	2.2	2.6	0.065	4.5	0.78	0.20	0.02	0.01
14	35.962	-4.602	36.430	0.18	0.10	1.6	2.6	0.048	3.1	0.87	0.11	0.01	0.63
15	35.920	-4.597	36.430	0.25	0.02	1.8	2.6	0.039	2.4	0.91	0.09	0.00	0.00
16	35.858	-4.597	36.410	0.25	0.04	1.5	2.4	0.041	2.0	0.91	0.07	0.02	0.00
17	36.205	-4.673	36.350	1.26	0.14	2.1	2.7	0.084	4.6	0.61	0.17	0.17	0.00
18	36.262	-4.680	36.670	3.07	0.26	1.9	2.9	0.093	4.6	0.44	0.13	0.22	0.81
19	36.327	-4.703	36.740	2.51	0.25	2.5	3.3	0.127	6.9	0.16	0.22	0.32	0.30
20	36.345	-4.723	37.030	1.64	0.27	2.6	3.2	0.119	6.8	0.18	0.22	0.21	1.88
21	36.400	-4.752	37.130	0.05	0.12	1.8	3.8	0.103	2.6	0.10	0.00	0.40	0.51
22	36.483	-4.762	37.340	0.13	0.10	2.0	4.0	0.083	2.9	0.22	0.02	0.22	0.54
23	36.683	-4.280	37.410	0.77	0.06	2.2	4.1	0.097	3.1	0.08	0.03	0.29	0.60
24	36.630	-4.292	37.180	1.21	0.08	1.8	3.6	0.059	1.9	0.48	0.01	0.11	0.41
25	36.578	-4.297	37.160	0.02	0.04	2.0	3.9	0.064	2.4	0.42	0.03	0.14	4.52
26	36.528	-4.303	36.980	0.05	0.05	1.8	3.4	0.063	1.8	0.51	0.01	0.15	0.32
27	36.453	-4.312	37.250	0.04	0.06	2.1	4.2	0.077	3.1	0.26	0.04	0.20	0.50
28	36.408	-4.270	37.170	0.04	0.06	1.9	3.8	0.069	3.9	0.41	0.07	0.10	1.78
29	36.373	-4.258	36.600	1.70	0.09	2.4	3.0	0.100	5.8	0.42	0.21	0.19	0.04
30	36.395	-4.253	36.350	0.85	0.09	2.5	2.7	0.117	5.0	0.36	0.20	0.34	1.80
31	36.285	-4.253	36.420	0.15	0.02	1.8	2.6	0.048	2.3	0.87	0.10	0.03	1.22
32	36.213	-4.242	36.410	0.17	0.03	1.9	2.7	0.057	3.0	0.79	0.12	0.07	0.02
33	36.133	-4.153	36.440	0.33	0.01	1.7	2.6	0.040	1.8	0.92	0.07	0.00	1.87
34	36.053	-4.128	36.450	0.20	0.08	2.1	2.7	0.043	2.6	0.87	0.11	0.00	0.02
35	35.870	-4.150	36.430	0.24	0.08	1.6	2.6	0.040	2.1	0.92	0.08	0.00	1.12
36	35.878	-4.040	36.430	0.25	0.02	1.5	2.5	0.048	2.0	0.86	0.07	0.08	0.40
37	35.845	-3.888	36.430	0.23	0.00	1.6	2.6	0.043	2.2	0.89	0.07	0.03	0.01
38	35.858	-3.835	36.410	0.29	0.01	1.6	2.5	0.047	2.2	0.88	0.08	0.04	0.00
39	35.900	-3.862	36.420	0.06	1.6	2.5	2.5	0.067	2.6	0.72	0.09	0.15	0.04
40	35.803	-3.520	36.850	0.01	1.9	3.1	0.067	3.3	0.58	0.08	0.09	0.24	0.57
41	35.897	-3.392	36.500	0.02	1.9	4.3	0.053	2.7	0.56	0.08	0.21	0.17	24.35
42	35.920	-3.257	36.510	0.02	1.6	2.7	0.048	2.7	0.95	0.10	0.01	0.04	1.05
43	35.922	-3.115	36.500	0.02	1.9	2.9	0.055	3.2	0.77	0.11	0.05	0.07	1.75

Table 5.3 June surface sample composition, % end-members and sum of squared residuals.

Table 5.4 End-member composition for April, June and October.

	Surface Atlantic	Shelf Apr.'86	Shelf June'82	Shelf Oct.'86	NACW	Mediter.	Error
Salinity 0.1 ‰	36.3	36.0	36.0	36.1	35.7	38.45	
Cu	1.0	6.1	6.7	8.0	1.3	1.9	.33 nM
Ni	2.2	3.4	3.4	3.4	3.3	4.6	.33 nM
Cd	30	190	211	260	150	77	10 pM
Zn	0.8	21	21	21	1.5	4.8	1 nM

Layer	Salinity	Si	PO <sub>4</sub>	Cu	Ni	Cd	Zn	Sulf. AII	Sph. Sulf.	NACW	Deep Med	E (residual)2
0	36.890	1.67	0.08	2.17	3.34	88	6.80	0.46	0.25	0.02	0.28	0.4
2.0	37.198	3.64	0.19	2.20	3.47	127	6.35	0.02	0.15	0.33	0.51	3.2
4.0	37.623	4.63	0.24	2.55	3.64	87	5.46	0.25	0.14	0.00	0.60	1.1
6.1	37.667	4.47	0.24	2.43	3.62	71	4.59	0.30	0.09	0.00	0.61	1.6
8.1	37.859	4.98	0.27									
10.1	38.037	5.76	0.31	2.33	4.43	62	6.06	0.08	0.09	0.00	0.63	0.3
12.6	38.254	7.92	0.35	2.56	4.21	80	6.19	0.02	0.08	0.00	0.90	1.9
15.1	38.492	8.05	0.37	2.39	4.55	93	7.23	0.00	0.06	0.00	0.94	6.2

Table 5.5 Salinity %, Si  $\mu\text{M}$ , PO<sub>4</sub>  $\mu\text{M}$ , Cu, Ni, Cd and Zn ( $\text{nM}$ ) at Station 4 (June '82).

## REFERENCES

Bormans, M., Garrett, C., Thompson, K. (1986) Seasonal variability of the surface inflow through the Strait of Gibraltar. *Oceanol. Acta* 9,4, 403-414.

Boyle, E.A., Chapnick, S.D., Bai, X.X. & Spivack, A.J. (1985) Trace metal enrichments in the Mediterranean Sea. *Earth Planet. Sci. Lett.* 74, 405-419.

Bray, N. (1986) Gibraltar Experiment CTD data report, SIO Reference series #86-21, Scripps Institution of Oceanography

Gascard, J.C. and C. Richez (1985) Water masses and circulation in the Western Alboran Sea and in the Strait of Gibraltar, *Prog. Oceanog.* 15, 157-216.

Kinder, T.H., Z.R. Hallock, D.A. Burns and M. Stirgus (1983) *Donde Va?*, Hydrographic measurements in the Western Alboran Sea, June 1982, NORDA Technical Note 202.

Kinder, T.H. and H.L. Bryden (1987) The 1985-86 Gibraltar Experiment: Data collection and preliminary results. *EOS, Transactions, American Geophysical Union*, 68, 786-787, 793-795.

Mackas, D.L., Denman, K.L. & Bennett, A.F. (1987) Least squares multiple tracer analysis of water mass composition. *J. Geophys. Res.* 92, 2907-2918.

Menke, W. (1985) *Geophysical data analysis-Discrete inverse theory*, Academic Press, Orlando Ca.

Ochoa, J.L. and N.A. Bray (198x) Exchange of Mediterranean and Atlantic water masses in the Gulf of Cadiz, submitted to *Deep Sea Res.*

Parilla, G. and T. H. Kinder XXX In: *Proc. NATO Advanced Research Workshop on the Physical Oceanography of the Mediterranean*, La Spezia, 1983, in press.

Sherrell, R.M. and E.A. Boyle (1988) Zinc, chromium, vanadium and iron in the Mediterranean Sea. *Deep-Sea Res.* 35 1319-1334.

Spivack, A. J., S. S. Huested & E. A. Boyle (1983) Copper, Nickel and Cd in surface waters of the Mediterranean, In: *Trace Metals in Seawater*, C. S. Wong, E. Goldberg, K. Bruland and E. Boyle, eds., pp 505-512, Plenum Press, New York, NY.

Strickland, J.D.H., and T.R. Parsons (1968) *A practical handbook of seawater analysis*, Fisheries Research Board of Canada.

Tchernia, P. (1980) *Descriptive Regional Oceanography*, Pergamon, Oxford.

van Geen, A., P. Rosener and E. Boyle (1988) Entrainment of trace metal-enriched Atlantic shelf-water in the inflow to the Mediterranean Sea. Nature 331, 423-426.

CHAPTER SIX

CONCLUSIONS

Three questions were posed at the onset of this work:

- (1) What portion of Cu, Ni, Cd and Zn enrichments observed in the Mediterranean Sea originates in the Atlantic ?
- (2) Are metal enrichment patterns in the surface Alboran Sea systematically related to contributing Atlantic and Mediterranean water masses ?
- (3) Do anthropogenic metal inputs influence trace metal concentrations in the Mediterranean ?

As shown in the preceding chapters, the answer to the second question is affirmative since the composition of surface Alboran Sea water is consistent with conservative mixing of the four end-members contributing to the region. While the results do not provide definitive answers to questions (1) and (3), certain constraints can be placed on the nature of Cu, Ni, Cd and Zn fluxes to the Mediterranean. As was mentioned in Chapter 1, one of the ideas behind studying the Mediterranean is that the two-layered circulation pattern through the Strait of Gibraltar integrates the net effect of metal input and removal over the residence of water time within the basin (on the order of a century). Potential sources of metals (natural or anthropogenic) are rivers, rain and aerosols, and sediment diagenesis. A sink which could offset these inputs to the water column is scavenging of metals dissolved in the water column onto sinking particles.

The budget approach for determining metal fluxes to the Mediterranean basin, i.e. the comparison of fluxes through the Strait of Gibraltar, has recently been applied to another element: Al. Measures and Edmond (1988) found inflow/outflow concentrations of 16 and 86 nM, respectively, indicative of a strong source within the basin. When compared with the total dust input to the basin ( $24.10^9$  kg/year, mainly from the Sahara desert) and taking into account that dust contains 10% by weight Al, the exchange through the Strait can be supported by as little as 5% dissolution of Al from dust input to the Mediterranean. The situation is simplified for this particular element because anthropogenic or riverine inputs are negligible. One limitation to this comparison is that it is not clear whether Al scavenging from the water column could be significant over the residence time of water in the basin. On the other hand, a 5% dissolution fraction was in fact observed directly with sea water suspensions of aerosols collected over the central Pacific by Maring and Duce (1987). The setting for these calculations is most favorable in the case of Al due to (1) relatively low concentrations in the inflow and (2) the very high fraction of Al in airborne dust.

The situation is not as clear-cut for Cu, Ni, Cd and Zn as it is for Al. First of all, the apparent difference between inflow and outflow trace metal concentrations initially calculated by Spivack et al. (1983) only holds for Ni after the Atlantic inflow composition is corrected for entrainment of metal enriched Spanish shelf water and NACW (Table 6.1). If Cu, Cd and Zn input and removal fluxes within the basin are

significant, they must be roughly in balance. For comparison, input fluxes from rivers and aerosol dissolution are estimated in the following way:

(1) River concentrations of two essentially pristine rivers (Amazon and Orinoco) and two rivers draining industrially developed regions (Mississippi and Guadalquivir) are listed (Table 6.2). Interestingly, the effect of anthropogenic activity appears minimal, except perhaps in the case of Ni which is enriched in both the Mississippi and the Guadalquivir. The integrated effect of riverine input ( $500 \text{ km}^3/\text{year}$ , Sarmiento and Toggweiler, 1988) on water column Cu, Ni, Cd and Zn concentrations is estimated on the basis of the highest river concentration for each element listed in Table 6.2. To account for Cd desorption, the Mississippi river concentration is increased by a factor of ten. Riverine input is integrated over the volume of the basin ( $3.8 \cdot 10^6 \text{ km}^3$ , Sverdrup et al., 1942) taking into account the 170 year residence time of water relative to the Atlantic inflow ( $22,000 \text{ km}^3/\text{year}$ , from Sarmiento and Toggweiler (1988) based on data from Bryden and Pillsbury, 1988)). Table 6.1 expresses the impact of riverine dissolved metal input in terms of an estimated change in water column concentrations between inflow and outflow through the Strait of Gibraltar due to this source. The net effect of input from the Black Sea ( $200 \text{ km}^3/\text{year}$ ) corrected for the deep Mediterranean outflow through the Bosphorus ( $100 \text{ km}^3/\text{year}$ ) is negligible.

(2) The effect of atmospheric input on Cu, Ni, Cd and Zn concentrations is normalized with respect to the observed Al increase of 70 nM in the water column. The main difficulty lies in determining concentrations of other soluble metals in dust relative to Al. Enrichment factors (EF) relative to crustal metal/Al ratios of Cu, Ni, Cd and Zn determined for aerosols over the remote Pacific ocean (Arimoto et al., 1985) are listed in Table 6.2. While enrichment factors over the North Atlantic and the Mediterranean higher by a factor of 10 have been reported for Cd and Zn (Buat-Menard et al., 1979 and Arnold et al., 1985), such differences will only reinforce the argument that follows. The impact of dust input to the Mediterranean with respect to water column concentrations is calculated for two scenarios: Estimate (1) assumes an aerosol composition reflecting crustal metal/Al ratios (EF=1) and 100% dissolution of Cu, Ni, Cd and Zn, Estimate (2) assumes dust input according to enrichment factors listed in Table 6.2 and again total dissolution of metals other than Al.

Distributions of Cu, Ni, Cd and Zn concentrations in Mediterranean surface waters from the Strait of Gibraltar to Greece (Fig. 6.1 from Spivack et al., 1983 and Sherrell and Boyle, 1988) can now be compared to the relative strengths of the three metal sources which have been estimated: (1) the Atlantic inflow, (2) rivers, and (3) atmospheric input (highly uncertain). From the eastern Alboran Sea to the center of the Western Mediterranean basin, Cu, Ni, Cd and Zn concentrations remain essentially constant (with some scatter) at the level of the average composition of the inflow. Apparently, the influence of Spanish

Table 6.1 Metal balance through the Strait and internal source estimates  
 $\Delta C$ : change in concentration in basin over residence time of water

		$C_{atl.in}$	$\Delta C_{rivers}$	$\Delta C_{aerosol}$ crustal	$\Delta C_{aerosol}$ EF	$C_{med.out}$
Cu	nM	2.6 ± .3	+ .5	+ .9	+ 4.8	1.9 ± .2
Ni	nM	2.6 ± .3	+ 1.4	+ 1.3	+ 3.9	4.6 ± .2
Cd	nM	.092 ± .01	+ .027	+ .003	+ .700	.077 ± .005
Zn	nM	6.2 ± 1	+ .7	+ 1.1	+24.0	4.8 ± .5

-----INFLOW----|-----INPUTS-----|-----OUTFLOW-----

Inflow and outflow concentration uncertainties based on spatial and temporal variability.

$\Delta C$  rivers assumes: river input of 500 km<sup>3</sup>/year and inflow of 22,000 km<sup>3</sup>/year, highest river concentration chosen for each element from Table 1, desorption estimated to cause ten-fold increase in Cd river concentration,  $\Delta C = (C_{river} \cdot Q_{river}) / Q_{inflow}$ .

$\Delta C$  aerosols normalized to 70 nM Al, corresponding to 5 % dissolution of aerosol, 100 % dissolution for Cu, Ni, Cd and Zn with crustal ratios (EF=1, crustal concentrations listed in Table 6.2))

$\Delta C$  aerosols assuming enrichment factors listed in Table 6.2 and total dissolution, (EF from Table 6.2)

Table 6.2 River and aerosol input characterization

		Amazon	Orinoco	Mississippi	Guadalquivir	Black Sea	Crustal ppm	EF
Cu	nM	24	19	23	16	2	55	5
Ni	nM	5	38	23	64	10	75	3
Cd	nM	.060	.030	.120	.100	.070	.2	200
Zn	nM	4	2	3	33	3	70	20

River data other than Guadalquivir (this work), Shiller and Boyle (1987)  
 Black Sea surface water, W. Landing (pers. comm.)  
 Crustal metal concentrations, Taylor (1964)  
 Enrichment factors from Arimoto et al., 1985

shelf water extends over at least 2000 km from the Strait of Gibraltar at the time this survey was made (September '80). Further east, an increase in surface water concentrations (about 1 nM for Cu, Ni and Zn, 20 pM for Cd) is comparable to the predicted effect of river input or aerosol input at crustal metal/Al ratios. There is a limit to this comparison since atmospheric and riverine inputs affect mainly surface waters at first; gradients in surface water metal concentrations amplify the impact of these sources. For this reason, it is clear that aerosol input according to the reported open ocean (Pacific) enrichment factors (and a fortiori Mediterranean EF) would be considerably greater than the east-west change observed in surface waters: higher by factors of at least 5, 4, 35 and 20 for Cu, Ni, Cd and Zn, respectively.

There may be two explanations for the difference between the observed and predicted magnitude in concentration changes in surface water due to aerosol input. One possibility is that Cu, Ni, Cd and Zn removal from surface water is sufficient to compensate for a strong atmospheric source. However, this is unlikely given the low productivity in surface waters of the basin. Little vertical metal redistribution by plankton uptake from surface water (followed by regeneration at depth) is also indicated by the similarity between surface and deep water metal concentration. A more likely explanation is that aerosols with  $EF >> 1$  do not reflect the composition of the dominating dust input to this region. Indeed, during the 3 to 4 major Saharan dust storms each year, atmospheric Al concentrations in the air increase by more than two orders of magnitude (Dulac et al., 1987). According to measurements

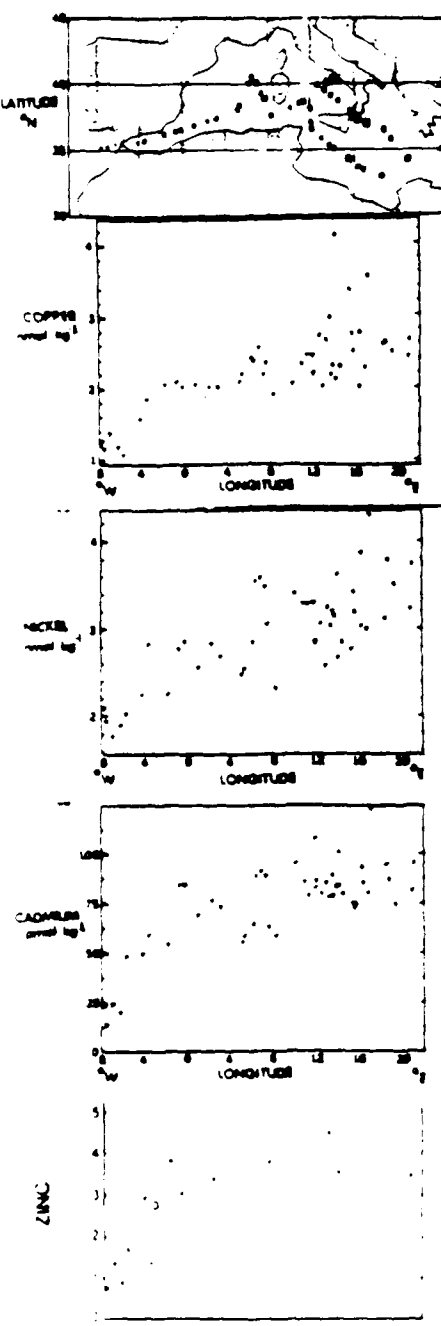


Fig. 6.1 Cu, Ni, Cd and Zn in Mediterranean surface water,  
September '80.

from Bermuda by Duce et al. (1976) , Cu, Ni, Cd and Zn levels in aerosols approach crustal ratios relative to Al during these events. In addition, Maring and Duce (1989) found that only a small fraction of the aluminosilicate Cu fraction in aerosols dissolves in seawater. A combination of these factors could explain why metal/Al ratios measured in aerosols off Corsica do not seem representative of the flux weighted composition input to the Mediterranean.

Summarizing the answer to the first question, surface concentrations of Cu, Ni, Cd and Zn in the Western Mediterranean reflect mainly the composition of the Atlantic inflow. Further east, metal concentrations increase due to a combination of atmospheric and riverine input. Unless trace metal scavenging from Mediterranean surface waters is significant, aerosols enriched relative to the crust in Cu, Ni, Cd and Zn do not seem to dominate the dust input to the basin. With regard to the final question concerning the effect of anthropogenic inputs, Cu and Cd do not appear significantly enriched in rivers draining industrialized regions. While Zn may be enriched in certain polluted rivers (Shiller and Boyle, 1987 and Chapter 3), the effect on the Mediterranean as a whole relative to enrichment by Spanish shelf water entrained with the inflow is limited (Table 6.1). In the case of Ni, on the other hand, riverine input (perhaps raised by anthropogenic inputs) seems to be the main cause for elevated Mediterranean outflow concentrations relative to the Atlantic inflow.

## REFERENCES

Arimoto, R., R.A. Duce, B.J. Ray, and C.K. Unni (1985) Atmospheric trace elements at Enewetak Atoll 2, Transport to the oceans by wet and dry deposition, *J. Geophys. Res.* 90, 2391-2408.

Arnold, M., A Seghaier, D. Martin, P. Buat-Menard and R. Chesselet (1982) *Geochimie de l'aerosol marin au-dessus de la Méditerranée Occidentale, Contribution to workshop on Marine Pollution of the Mediterranean*, Cannes, December 1982.

Buat-Menard, P. and R. Chesselet (1979) Variable influence of the atmospheric flux on the trace metal chemistry of oceanic suspended matter, *Earth Planet. Sci. Lett.* 42, 399-411.

Duce, R.A., B.J. Ray, G.L. Hoffman, and R.P. Walsh (1976) Trace metal concentration as a function of particle size in marine aerosols from Bermuda, *Geophys. Res. Lett.* 3, 339.

Dulac, F., P. Buat-Menard, M. Arnold and U. Ezat (1987) Atmospheric input of trace metals to the western Mediterranean Sea: 1. Factors controlling the variability of atmospheric concentrations, *J. Geophys. Res.* 92, 8437.

Jickells, T.D., T.M. Church and W.G. Deuser (1987) A comparison of atmospheric inputs and deep-ocean particle fluxes for the Sargasso Sea, *Global Biogeochem. Cycles* 1, 117-130.

Maring, H.B. and R.A. Duce (1987) The impact of atmospheric aerosols on trace metal chemistry in open ocean surface seawater, *Earth Planet. Sci. Lett.* 84, 381.

Maring, H.B. and R. A. Duce (1989) The impact of atmospheric aerosols on trace metal chemistry in open ocean surface seawater 2. Copper, *J. Geophys. Res.* 94, 1039-1045.

Measures, C.I. and J. M. Edmond (1988) Aluminium as a tracer of the deep outflow from the Mediterranean, *J. Geophys. Res.* 93, 591-595.

Sherrell, R.M. and E.A. Boyle (1988) Zinc, chromium, vanadium and iron in the Mediterranean Sea, *Deep-Sea Res.* 35, 1319.

Shiller, A.M., and E.A. Boyle (1987) Variability of dissolved trace metals in the Mississippi River. *Geochim. Cosmochim. Acta* 51 3273-3277.

Spivack, A. J., S. S. Huested & E. A. Boyle (1983) Copper, Nickel and Cd in surface waters of the Mediterranean, In: *Trace Metals in Seawater*, C. S. Wong, E. Goldberg, K. Bruland and E. Boyle, eds., pp 505-512, Plenum Press, New York, NY.

Sverdrup, H.U., M.W. Johnson and R.H. Fleming (1942) The oceans, their physics, chemistry and biology, Prentice-Hall, Englewood Cliffs, NJ.

Taylor, S.R. (1964) Abundance of chemical elements in the continental crust: a new table, Geochim. Cosmochim. Acta 28, 1273-1285.

APPENDIX

In this BASIC program written for the Tektronix 4052, the (overdetermined) system of linear equations  $A.f = d$ , is solved by weighted least-squares, subject to the constraint that elements of the solution  $f$  must be positive. Construction of the model matrix and the data vector is discussed in manuscript b. Convergence of the algorithm is assured by the Kuhn-Tucker theorem discussed by Lawson and Hanson in Solving least square problems, Prentice-Hall, Englewood Cliffs, NJ (1974).

#### Step 1. Initialization and data input.

Data for a total of  $r$  samples is read into ( $r$ , 11) matrix  $U_1$  in the order: sample #, latitude, longitude, salinity, Si, PO<sub>4</sub>, Cu, Ni, Cd, Zn, free.

After the number of tracers used in the inversion  $D_1$  is entered (and subsequently incremented to  $D_1+1$  to account for extra constraint on sum of fractions), a number of matrices are declared:

$A_5(8,4)$  contains the composition of the four end-members for all tracers  
 $U_7(D_1)$  contains ID# for each tracer retained for inversion

$A(D_1,4)$  is the reduced model matrix reflecting tracer choice

$U_8(8)$  contains weights for all tracers (inverse of standard error)

$U_2(D_1,D_1)$  is the diagonal matrix containing weights of the retained tracers.

Multiplied by  $U_2$ , the reduced model matrix  $A$  is modified to the weighted model matrix of the same name.

Starting the loop ( $U_3$ ) marking each sample, zero values for any of the retained tracers are checked. Vector  $B_9(D_1)$  is loaded with the composition of the sample plus one extra element equal to one, and multiplied by  $U_2$  to obtain the weighted data vector  $B(D_1)$ . Both model matrix and data vector are now in the same units and have matching dimensions. The initial guess for the model parameter is set to  $X=(0,0,0,0)$ . The end-members are separated in two groups: (1) those satisfying the inequality constraint ( $X_i > 0$ ) and (2) end-members satisfying  $X_i = 0$ . The index vector  $I_1(4)$  indicates whether if each model parameter is free ( $I_1=1$ ) or restricted to 0 ( $I_1=0$ ). Initially  $X=(0,0,0,0)$ , hence  $I_1=(0,0,0,0)$ .

#### Step. 2 Test on gradient vector

From the previous solution  $X$ , the gradient vector (also called dual of the problem)  $W = A^t(d - A \cdot X)$  is calculated to determine the change in total error when varying either of the model parameters. The highest positive element of  $W$  indicates which element of  $X$  to include next in the regression set in order to cause the largest decrease in total error. If at this stage there is no end-member left with  $I_1=0$ , or if  $W_i \leq 0$  for any end-member with  $I_1=0$ , then the solution has been found and the program exits to the next sample. At the solution, the gradient vector

$W$  is zero for end-members with  $I1=1$ , indicating a minimum in the total error. The solution does not correspond to the absolute minimum error ( $W_i < 0$ ) when a boundary is reached, i.e. when  $I1(i)$  and  $X_i$  equal zero.

If, on the other hand, one of the elements of  $W$  is positive and  $I1=0$  for that element, then this parameter is set free by changing  $I1$  to 1 and included in the regression.

### Step 3. Least squares solution

A new model matrix is calculated containing all the retained tracers and all model parameters with  $I1=1$ . The least square solution is:  

$$Y = (A2^T \cdot A2)^{-1} \cdot A2^T \cdot B$$
 The matrix inverse is calculated by a supplied subroutine based in Gauss-Jordan triangularization.

### Step 4. Test for negative model parameters and readjustment

If all model parameters are positive, the program returns to Step 2 in order to determine the new gradient vector.

If, on the other hand, any of the model parameters has become negative, the inequality condition is infringed. The index of the model parameter whith smallest  $X(i)/(X(i)-Z(i))$  is reset to  $I1=0$ . The program then returns to Step 3 where the least-square solution is calculated for the reduced set of end-members.

This version of the program allows a maximum of four end-members and 7 tracers. In practice, 5 or less tracers (Salinity, Cu, Ni, Cd and Zn) are used. If desired, the additional tracer options can be used to eliminate one or more of the end-members. This is simply done by setting the composition of that end-member for a fictitious tracer to, for instance, 1000 (zero for other end-members), and the corresponding sample composition to 1 (on data entry into  $U1$ ). Since for any end-member composition, the residual to this constraint ( $1000 \cdot X(i) = 1$ ) will be very large, the solution is forced to eliminate the corresponding end-member.

```

90 REM TM INVERSION 6-88
100 INIT
110 REM LOADING OF DATA MATRIX
120 PRINT "BINARY INPUT FILE = ?"
130 INPUT F
140 FIND F
150 READ Q33:R,C
160 DIM U1(R,11)
170 FOR M=1 TO R
180 FOR N=1 TO C
190 READ Q33:U1(M,N)
200 NEXT N
210 U1(M,11)=0
220 NEXT M
230 REM SETS # TRACERS. INITIALIZES OUTPUT FILE
240 PRINT "# OF TRACERS"
250 INPUT D1
260 D1=1+D1
270 DIM X(4),W(4),I1(4),Z(4),E8(1,1)
280 DIM A(D1,4),B(D1),E1(1,D1),S9(D1,4)
290 DIM P3(4,4),Y(1),U7(D1),U8(8)
300 DIM A1(4,D1),B1(D1,1),P1(D1,1),A2(D1,4),A4(4,D1),B5(4,D1)
310 DIM U2(D1,D1),B9(D1),B8(D1),B7(D1,1),U5(R,11),A5(8,4)
320 FOR I=1 TO R
330 FOR J=1 TO 11
340 U5(I,J)=0
350 NEXT J
360 NEXT I
370 REM LOADS MODEL MATRIX
380 READ A5
390 DATA 36.5,36.1,35.7,38.45
400 DATA 0.0.0.0
410 DATA 0.0.0.0
420 DATA 1.8.1.3.1.9
430 DATA 2.2.3.4.3.3.4.6
440 DATA 0.03.0.26.0.15.0.077
450 DATA 0.8.21.1.5.4.8
460 DATA 1.1.1.1
470 REM SELECTS TRACERS, UP TO 7
480 FOR I=1 TO D1-1
490 PRINT "TRACER ID = "
500 INPUT U7(I)
510 NEXT I
520 U7(D1)=8
530 REM REDUCES MODEL MATRIX TO CHOSEN TRACERS
540 FOR I=1 TO D1-1
550 FOR J=1 TO 4
560 A(I,J)=A5(U7(I),J)
570 A(D1,J)=1
580 NEXT J
590 NEXT I
600 REM LOADS WEIGHTS FOR ALL TRACERS
610 READ U8
620 DATA 10 0 02 0 1 0 3 100 1 1000
630 REM LISTS MODEL MATRIX AND WEIGHTS FOR CHECKING
640 PRINT A
650 PRINT U8

```

```

660 PRINT "WANT TO CHANGE END-MEMBERS OR ERRORS?"
670 PRINT " IF NOT RUN 690"
680 END
690 REM SETS UP DIAGONAL WEIGHT MATRIX
700 FOR I=1 TO O1
710 FOR J=1 TO O1
720 U2(I,J)=0
730 IF I<>J THEN 750
740 U2(I,J)=U8(U7(I))
750 NEXT J
760 NEXT I
770 REM TRANSFORMATION TO WEIGHTED MODEL MATRIX
780 S9=U2 MPY A
790 A=A\$9
800 REM START OF INDIVIDUAL SAMPLE LOOP
810 FOR U3=1 TO R
820 REM CHECKS FOR NULL DATA
830 IF U1(U3,4)=0 THEN 2040
840 IF U1(U3,7)=0 THEN 2040
850 IF U1(U3,8)=0 THEN 2040
860 IF U1(U3,9)=0 THEN 2040
870 IF U1(U3,10)=0 THEN 2040
880 REM LOADS DATA FOR CHOSEN TRACERS
890 FOR L1=1 TO O1-1
900 B9(L1)=U1(U3,3+U7(L1))
910 NEXT L1
920 B9(O1)=1
930 REM CONVERSION TO WEIGHTED SAMPLE DATA
940 B=U2 MPY B9
950 REM SETS INITIAL SOLUTION AND INDICES II TO ZERO
960 FOR N8=1 TO 4
970 DIM I1(4), X(4), Z(4)
980 I1(N8)=0
990 X(N8)=0
1000 Z(N8)=0
1010 NEXT N8
1020 REM CALCULATES ERROR GRADIENT OF CURRENT SOLUTION
1030 P1=A MPY X
1040 P1=B-P1
1050 A1=TRN(A)
1060 E1=TRN(P1)
1070 E8=E1 MPY P1
1080 W=A1 MPY P1
1090 REM SELECTS LARGEST POSITIVE GRADIENT FOR II=0
1100 W9=0
1110 I9=0
1120 FOR I=1 TO 4
1130 IF I1(I)=1 THEN 1170
1140 IF E1(I)<-W9 THEN 1170
1150 W9=W(I)
1160 I9=I
1170 NEXT I
1180 REM SOLUTION IF EITHER <0 FOR ALL II=0 OR NO II=0 IS LEFT
1190 IF -W9<0 THEN 1330
1200 REM ADDS END MEMBER WITH HIGHEST GRADIENT AND SETS II=1
1210 I1(I9)=1
1220 B1=B
1230 REM COUNTS # OF END MEMBERS WITH II=1
1240 N=0
1250 FOR I=1 TO 4

```

```

1260 IF II(I)=0 THEN 1400
1270 N=N+1
1280 REM RESETS MATRICES FOR MODIFIED II LIST
1290 DELETE P5,Y,P3,A4,A2,P6,P7
1300 DIM A2(D1,N),A4(N,D1),P3(N,N),Y(N),P5(N,D1),P6(N,N),P7(N,N)
1310 M=0
1320 FOR K=1 TO I
1330 IF II(K)=0 THEN 1390
1340 M=M+1
1350 FOR J=1 TO D1
1360 REM SKIPS COLUMN IF II=0
1370 A2(J,M)=A(J,K)
1380 NEXT J
1390 NEXT K
1400 NEXT I
1410 REM FINDS LEAST SQUARE SOLUTION
1420 A4=TRN(A2)
1430 P3=A4 MPY A2
1440 P6=P3
1450 P7=P3 MPY P6
1460 P3=INV(P3)
1470 P7=P3 MPY P6
1480 P5=P3 MPY A4
1490 Y=P5 MPY B
1500 M1=0
1510 REM SETS Z EQUAL TO SOLUTION UNLESS II=0, THEN Z=0
1520 FOR J=1 TO 4
1530 IF II(J)=0 THEN 1570
1540 M1=M1+1
1550 Z(J)=Y(M1)
1560 GO TO 1590
1570 Z(J)=0
1580 GO TO 1590
1590 NEXT J
1600 REM CHECKS FOR NEGATIVE END MEMBER
1610 A9=1
1620 FOR I=1 TO 4
1630 REM EXITS LOOP IF ANY Z<0
1640 IF Z(I)<0 THEN 1700
1650 X(I)=Z(I)
1660 NEXT I
1670 REM RETURNS TO CALCULATE NEW GRADIENT IF ALL Z>0
1680 GO TO 1330
1690 REM FINDS NEGATIVE EM WITH SMALLEST A9
1700 FOR I=1 TO 4
1710 IF II(I)=0 THEN 1770
1720 IF Z(I)>0 THEN 1770
1730 A8=X(I)/X(I)-Z(I)
1740 IF A8>A9 THEN 1770
1750 A9=A8
1760 A9=X(I)/X(I)-Z(I)
1770 NEXT I
1780 REM CALCULATES NEW ESTIMATE FOR X WITH EM<0 SET TO 0
1790 FOR I=1 TO 4
1800 X(I)=X(I)+A9*(Z(I)-X(I))
1810 IF ABS(X(I))>1.0E-3 THEN 1830
1820 IF I=4
1830 NEXT I
1840 REM RETURNS FOR NEW LEAST SQUARE SOLUTION
1850 GO TO 1240

```

```
1860 REM FINAL SOLUTION
1870 REM LOADS OUTPUT MATRIX
1880 US(U3,1)=U1(U3,1)
1890 US(U3,2)=X(1)
1900 US(U3,3)=X(2)
1910 US(U3,4)=X(3)
1920 US(U3,5)=X(4)
1930 US(U3,6)=E8(1,1)
1940 US(U3,7)=E1(1,1)
1950 US(U3,8)=E1(1,2)
1960 US(U3,9)=E1(1,3)
1970 US(U3,10)=E1(1,4)
1980 US(U3,11)=E1(1,5)
1990 IF E8(1,1)>50 THEN 2040
2000 IMAGE 7(IE )
2010 REM PRINTS OUTPUT. CHANGE FORMAT IF LESS THAN 5 TRACERS
2020 PRINT USING "5D.4 2D 2D .2X.2D.1D,   6(3D.1D)":U1(U3,1),X,E8,E1
2030 REM NEXT SAMPLE
2040 NEXT U3
2050 END
2060 REM VARIANCE AND COVARIANCE MATRIX
2070 DIM R9(6,4),P9(6,6),D9(3,3),A8(4,3),A7(3,4),A6(4,4)
2080 P9=A MPY P3
2090 P9=R9 MPY AL
2100 PRINT "OUTPUT FILE="
2110 INPUT F
2120 FIND F
2130 WRITE #33 R,11
2140 FOR J8=1 TO R
2150 FOR J9=1 TO 11
2160 WRITE #33 US(J8,J9)
2170 NEXT J9
2180 NEXT J8
2190 END
```

## BIOGRAPHICAL NOTE

The author was born in Utrecht (Netherlands) on June 17th, 1960. After living in various European countries while following the French school system, he received his Baccalaureat C in 1978 from the Lycee Franco-Japonais in Tokyo. In 1982, the author received a B.S. in Oceanography and a B.S. in Chemistry (Cum Laude) from the University of Washington. During the subsequent 18 months of military service, he was stationed on the Dutch Navy research/hydrographic ship H.Nl.M.S. "Tydeman". He left the service as sub-lieutenant certified for watch duty on the bridge. In January 1985, the author entered the MIT/WHOI Joint Program in Oceanography as a candidate for the degree of Doctor of Philosophy.

## PUBLICATIONS

J.H. Hedges and A. van Geen (1981) A comparison of lignin and stable carbon isotope compositions in Quaternary marine sediments, *Marine Chemistry*, 11, 43-54.

E. A. Boyle, B. Handy and A. van Geen (1987) Cobalt determination in natural waters using cation-exchange liquid chromatography with luminol chemiluminescence detection, *Analytical Chemistry*, 59, 1499-1503.

A. van Geen, E. Boyle and P. Rosener (1988) Entrainment of trace-metal-enriched Atlantic shelf-water in the inflow to the Mediterranean Sea, *Nature*, 331, 423-426.

A. van Geen and E. Boyle (1989) Automated pre-concentration of trace metals from seawater, submitted to *Analytical Chemistry*.

A. van Geen, W. S. Moore and E. Boyle (in preparation) Cu, Ni, Cd and Zn in the Gulf of Cadiz.

A. van Geen and E. Boyle (1989) Variability of trace metal fluxes through the Strait of Gibraltar, submitted to *Global Change*.

A. van Geen and E. Boyle (in preparation) Variability of trace metal distributions in the Alboran Sea.

A. van Geen, C. Measures and E. Boyle (in preparation) Trace metals and pH in lakes of the Adirondack State Park.

## DOCUMENT LIBRARY

July 5, 1989

### Distribution List for Technical Report Exchange

Attn: Stella Sanchez-Wade  
Documents Section  
Scripps Institution of Oceanography  
Library, Mail Code C-075C  
La Jolla, CA 92093

Hancock Library of Biology &  
Oceanography  
Alan Hancock Laboratory  
University of Southern California  
University Park  
Los Angeles, CA 90089-0371

Gifts & Exchanges  
Library  
Bedford Institute of Oceanography  
P.O. Box 1006  
Dartmouth, NS. B2Y 4A2, CANADA

Office of the International  
Ice Patrol  
c/o Coast Guard R & D Center  
Avery Point  
Groton, CT 06340

Library  
Physical Oceanographic Laboratory  
Nova University  
8000 N. Ocean Drive  
Dania, FL 33304

NOAA/NESDIS Miami Library Center  
4301 Rickenbacker Causeway  
Miami, FL 33149

Library  
Skidaway Institute of Oceanography  
P.O. Box 13687  
Savannah, GA 31416

Institute of Geophysics  
University of Hawaii  
Library Room 252  
2525 Correa Road  
Honolulu, HI 96822

Library  
Chesapeake Bay Institute  
4800 Atwell Road  
Shady Side, MD 20876

MIT Libraries  
Serial Journal Room 14E-210  
Cambridge, MA 02139

Director, Ralph M. Parsons Laboratory  
Room 48-311  
MIT  
Cambridge, MA 02139

Marine Resources Information Center  
Building E38-320  
MIT  
Cambridge, MA 02139

Library  
Lamont-Doherty Geological  
Observatory  
Colombia University  
Palisades, NY 10964

Library  
Serials Department  
Oregon State University  
Corvallis, OR 97331

Pell Marine Science Library  
University of Rhode Island  
Narragansett Bay Campus  
Narragansett, RI 02882

Working Collection  
Texas A&M University  
Dept. of Oceanography  
College Station, TX 77843

Library  
Virginia Institute of Marine Science  
Gloucester Point, VA 23062

Fisheries-Oceanography Library  
151 Oceanography Teaching Bldg.  
University of Washington  
Seattle, WA 98195

Library  
R.S.M.A.S.  
University of Miami  
4600 Rickenbacker Causeway  
Miami, FL 33149

Maury Oceanographic Library  
Naval Oceanographic Office  
Stennis Space Center  
NSTL, MS 39522-5001

Marine Sciences Collection  
Mayaguez Campus Library  
University of Puerto Rico  
Mayaguez, Puerto Rico 00708

<b>REPORT DOCUMENTATION PAGE</b>	<b>1. REPORT NO.</b> WHOI-89-17	<b>2.</b>	<b>3. Recipient's Accession No.</b>
<b>4. Title and Subtitle</b>  Trace Metal Sources for the Atlantic Inflow to the Mediterranean Sea		<b>5. Report Date</b> June 1989	<b>6.</b>
<b>7. Author(s)</b> Alexander F.M.J. van Geen		<b>8. Performing Organization Rept. No.</b> WHOI-89-17	
<b>9. Performing Organization Name and Address</b>  The Woods Hole Oceanographic Institution Woods Hole, Massachusetts 02543, and The Massachusetts Institute of Technology Cambridge, Massachusetts 02139		<b>10. Project/Task/Work Unit No.</b>	
<b>12. Sponsoring Organization Name and Address</b>  The Office of Naval Research through the Massachusetts Institute of Technology		<b>11. Contract(C) or Grant(G) No.</b> (C) N00014 - 86 - 0325 (G)	
		<b>13. Type of Report &amp; Period Covered</b> Ph.D. Thesis	
		<b>14.</b>	
<b>15. Supplementary Notes</b>  This thesis should be cited as: Alexander F.M.J. van Geen, 1989. Trace Metal Sources for the Atlantic Inflow to the Mediterranean Sea. Ph.D. Thesis, MIT/WHOI, WHOI-89-17.			
<b>16. Abstract (Limit: 200 words)</b>  Enrichments observed over the Spanish shelf are sufficient to influence the composition of the Mediterranean because Spanish coastal water is entrained in the inflow to the Alboran Sea. A shelf "metal-trap" mechanism is presented in order to reconcile the magnitude of observed metal enrichments with their geographical distribution and seasonal variability. Water masses originating in the Atlantic and entering the Alboran Sea through the Strait of Gibraltar are (1) Atlantic surface water, (2) North Atlantic Central Water and (3) Spanish shelf water, based on salinity and Cu, Ni, Cd and Zn concentrations. A conservative mixing model of these end-members is solved by weighted least-squares and shown to be consistent with tracer data for surface stations in the Strait of Gibraltar and the Alboran Sea. On three occasions (April '86, June '82 and October '86), a metal enriched plume originating from the Spanish shelf was present in the Alboran Sea. In- and outflow are roughly in balance for Cu, Cd and Zn. In contrast, Ni concentrations of the inflow are a factor of two lower than for the Mediterranean outflow. Estimates of metal sources within the basin indicate the difference may be due to river input. Estimates of atmospheric input of Cu, Cd, Ni and Zn are an order of magnitude higher than either the uncertainty in the difference between in- and outflow concentrations, or the east-west gradient in surface water concentrations of the basin.			
<b>17. Document Analysis</b> <b>a. Descriptors</b>			
1. trace metal 2. Mediterranean 3. Strait of Gibraltar			
<b>b. Identifiers/Open-Ended Terms</b>			
<b>c. COSATI Field/Group</b>			
<b>18. Availability Statement</b>  Approved for publication; distribution unlimited.		<b>19. Security Class (This Report)</b> UNCLASSIFIED	<b>21. No. of Pages</b> 179
		<b>20. Security Class (This Page)</b>	<b>22. Price</b>